Department of Chemical and Biomolecular Engineering
School of Engineering and Applied Science
University of Pennsylvania
220 S. 33rd Street Philadelphia, PA 19104
April 17, 2018

Dear Dr. Warren Seider and Prof. Bruce Vrana,

Our team set out to design a process where algae would be grown to convert carbon dioxide from flue gas into valuable biomass. The design would operate at a pilot scale and would be required to convert a large fraction of the carbon dioxide from an incoming concentrated flue gas stream. Little more was specified; creativity would be valued in this design, as algae cultivation for carbon conversion is a relatively new field and represents an industry in its infancy.

Algae production is a complex process with no shortage of technical challenges. Setting out with an ambitious carbon sequestration goal consistent with current industry targets, and the desire to create an innovative process that demonstrates significant technical capacity, we were met with many challenges along the way. The open-ended nature of the project requirements created space for applying unique and novel solutions to these challenges.

We began with a First Principles assessment of the overarching purpose of algae cultivation. How best can algae be a vehicle for rapidly closing the carbon cycle on earth? Given that fossil fuel use is expected to remain high for decades to come, increasing the need for commercially attractive carbon conversion technologies, how can algae play a role in moving our system of energy generation and use towards carbon neutrality? What else can the highly carbon-dense and nutrient-dense material that is algae biomass be put to use for besides as a source of biofuel?

Our goals were clear: focus on overcoming the significant biological and engineering challenges associated with developing an algae-based process that operates in the direction of carbon neutrality. Profitability was a desire, but not an expectation. Pilot scale facilities are are rarely profitable in any process, and the algae industry remains largely in a stage highly reliant on ongoing R&D, expectant technological leaps, strong public and private investment, and regulatory support for algae-based ventures. Given this, profitability was originally tepidly approached.

However, after many re-designs, we landed on a successful process design that met the most ambitious technical target we set for ourselves, and from there, the potential for profitability began to emerge. A final profitability analysis presents a 9-15% ROI over a 4-5 year period. We are excited to present what we believe is a novel and unique bioreactor design that provides a high level of flexibility,

tailorability, and capacity to harness the biosynthetic potential of microalgae for sustainable carbon emissions reduction and value-added product creation.

Thank you for your time, guidance, and reviewal of our work. Your contributions have been indispensable to the development of our project.

Regards,

_____	_____	_____
Casey Barkan	Kyle DeLuca	Mikaela Preston

Design of a Flexible, High-volume Direct Flue Gas-to-Algae Conversion Process for Value-added Bioproducts

Casey Barkan | Kyle DeLuca | Mikaela Preston

Faculty Adviser:
Warren D. Seider

Suggested by:
Mikaela Preston

Department of Chemical and Biomolecular Engineering
School of Engineering and Applied Science
University of Pennsylvania
April 17, 2018

Table of Contents

1 Abstract

Carbon conversion processes (where carbon dioxide is not only captured and stored, but converted to commercially-valuable products) have high barriers to sustained and large-scale commercial viability. Mass algae production as a means to carbon emissions reductions is considered to have great commercial potential, but the viability of deployment is going to rely on technological leaps supported by strong public and private investment. Presented in this Design Report is a novel pilot-scale microalgae cultivation system that successfully converts over 50% of the carbon dioxide (CO_2) present in a stream of flue gas from a coal-fired power plant into valuable biomass. The process operates at a carbon dioxide input rate of 200 kilograms per day from a 10% carbon dioxide by volume flue gas stream. A 9-15% Return on Investment over a 4-5 year period is reported. The project met a set of highly ambitious carbon conversion goals, and contributes to a positive outlook for the future of algae production for sustainable carbon emissions reduction and value-added product creation.

This presented design should encourage investment into pilot-scale and demonstration facilities in a move towards large-scale operation. The presented process can be used to convert high volumes of CO_2 to valuable biomass that can be sold for many applications ranging from feed to nutraceuticals to biofuels. The innovative "Hybrid Petal Reactor" design incorporates a central gas exchange column with a horizontal tubular photobioreactor system that harnesses sunlight during the day, and an internally-illuminated nighttime tank that involves innovative use of optics. The outdoor system was designed to scale with a series of tubes that branch out like "petals" from the central gas exchange column. The tube design is optimized for high productivity and low costs. An emphasis was placed on designing a process highly considerate of biological constraints. The presented final design offers great flexibility and opportunity for scale-up.

2 Introduction

2.1 Background

As atmospheric CO_2 levels continue to rise, it becomes increasingly important to find methods to efficiently and economically sequester large amounts of CO_2, and either store it (carbon capture and storage technologies), or convert it to value-added products (carbon conversion technologies). Combating climate change will be heavily dependent on the ability to not only reduce emissions but to bring processes like energy generation closer to carbon neutrality. Carbon sequestration, the process by which carbon dioxide is naturally or artificially removed from the atmosphere and stored in solid or liquid form, will play a large role in meeting global carbon goals in the coming decades (Williamson, 2016).

Algae, photosynthetic organisms that are found in both fresh and marine water, have the potential to contribute greatly to the carbon sequestration industry. Algae consume CO_2 and convert it into highly valuable biomass and lipids. The biomass has many applications such as nutraceuticals (Matos et al., 2017), and the lipids can be converted to a range of biofuels (Ghadiryanfar et al., 2017). Algae produce more fuel per area than any other biofuel; they are 12 times more productive than corn ethanol and over 70 times more productive than soybean biodiesel. As well, unlike deriving fuel from corn or ethanol, algae fuels do not compete with important staple food sources (WorldWatch). Furthermore, algae can utilize non-arable land and waste products, such as waste flue gas, to grow and produce these products. There is massive potential for industrial flue gases to be used as a source of CO_2 for large scale algae sequestration operations (Huang et al., 2015).

Flue gases from power and industry sectors account for over 60% of global CO_2 emissions (Gale et al., 2005). Not only could algae significantly contribute to keeping atmospheric CO_2 levels below currently dangerous (and rising) levels, but the value-added bioproducts containing sequestered carbon would have many profitable applications. However, there are challenges associated with flue gas usage that currently limit large scale success (Zhu et al., 2016). Most algae grow optimally with an input CO_2 concentration of around 5%, but flue gases can contain much higher concentrations of CO_2 that can inhibit growth, mainly due to the resulting drop in pH of the algae slurry (most algae maintain high growth in pH's between 6 and 9). Achieving adequate dissolution of CO_2 in solution is also a challenge, especially at the high input velocities of the flue gas, due to the low mass transfer rate between the gas and liquid solutions (Sadeghizadeh et al., 2017). High temperatures of flue gases also inhibit CO_2 dissolution and algae growth; algae grow optimally around 25-30C, but flue gases can reach much higher temperatures, often leading to the need to cool the gas before entry into the algae volume, or the need to cool the algae volume itself. Finally, the presence of NOx and SOx in flue gases can also cause a drop in pH and further inhibit grow. Successful commercialization of large scale algae carbon conversion operations will

require the use of flue gas as directly and efficiently as possible by overcoming these constraints in an economically viable manner.

2.2 Motivations and Goals

The design of this process was based off of carbon conversion goals that are biologically, technologically, and economically ambitious. The carbon sequestration industry as a whole struggles with creating processes that not only have the capacity for not only high volume throughput but are also able to utilize a high fraction of any input carbon dioxide. Furthermore, when designing a process that harnesses biological methods of carbon sequestration, the various complexities and constraints of the living system employed must be closely attended to. The presented design places an emphasis on adherence to reasonable biological boundaries, while simultaneously aiming to maximize the biosynthetic potential of the algae for carbon sequestration. This project aimed to tackle the sequestration fraction challenge by designing a pilot-scale complete flue gas-to-algae conversion facility that would utilize a stream of flue gas (10% CO_2 v/v) containing 200 kilograms of CO_2 per day. The baseline goal was to convert at least 30% of the input CO_2 to biomass, but the ideal goal was to convert over 50%. This goal was inspired by the currently ongoing $20 million NRG COSIA Carbon XPRIZE, the high-profile international competition that aims to find and accelerate the development of the world's most innovative CO_2 capture technologies. The competition is currently in Round 2 as of spring 2018, where leading businesses and engineers from a wide range of fields are competing to build pilot-scale demonstrations of various carbon conversion processes. According to the Competition Guidelines, the competitors' pilot operations must operate continuously 24 hours a day, taking in 200 kilograms per day of CO_2 from a simulated flue gas stream. To avoid immediate elimination from the competition, at least 30% of the CO_2 must be converted to product. To receive points after that, over 50% must be converted. Points are also awarded for the value and marketability of the carbon-based product. These requirements were chosen by the XPRIZE designers after a rigorous assessment of the carbon conversion landscape and market. They represent an aggressive step towards successful deployment of carbon conversion technologies. Basing the goals of this design project off of the Carbon XPRIZE criteria presented a technically and biologically challenging problem. If the project was successful, it would be on par with current high-reaching targets of the carbon conversion industry. Presented in this report is a novel highly versatile microalgae photobioreactor, the "Hybrid Petal Reactor", that uses primarily sunlight to convert over 50% of the CO_2 contained in a stream of flue gas from a coal-fired power plant. At the pilot-scale, over 200 kilograms of CO_2 per day is processed, and valuable biomass that can be sold for a wide range of applications is produced. Equipment and systems that were designed include a horizontal tubular outdoor reactor system, a closed internally-illuminated nighttime tank system, a CO_2/O_2 gas exchange column, tempera-

ture and pH balancing systems, nutrient delivery systems, and post-processing systems for the harvested biomass, including flocculation and drying. This design successfully overcomes key technical challenges while working under the limitations of biological constraints. In a push to improve the overall viability and attractiveness of the design, a profitability optimization was carried out to determine the optimal set of specific design parameters for the process. Finally, an overall economic analysis was performed to assess the long-term viability of the pilot process as well as the potential for scale-up.

2.3 Objective-Time Chart

Figure 2.1 shows the Objective-Time Chart under which the project timeline was carried out.

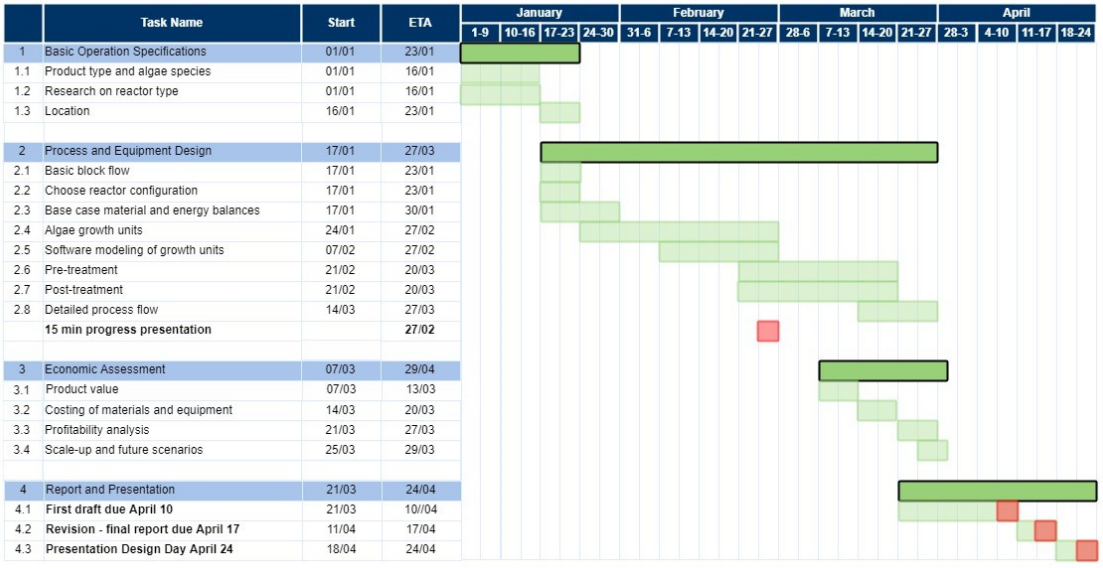

	Task Name	Start	ETA
1	Basic Operation Specifications	01/01	23/01
1.1	Product type and algae species	01/01	16/01
1.2	Research on reactor type	01/01	16/01
1.3	Location	16/01	23/01
2	Process and Equipment Design	17/01	27/03
2.1	Basic block flow	17/01	23/01
2.2	Choose reactor configuration	17/01	23/01
2.3	Base case material and energy balances	17/01	30/01
2.4	Algae growth units	24/01	27/02
2.5	Software modeling of growth units	07/02	27/02
2.6	Pre-treatment	21/02	20/03
2.7	Post-treatment	21/02	20/03
2.8	Detailed process flow	14/03	27/03
	15 min progress presentation		**27/02**
3	Economic Assessment	07/03	29/04
3.1	Product value	07/03	13/03
3.2	Costing of materials and equipment	14/03	20/03
3.3	Profitability analysis	21/03	27/03
3.4	Scale-up and future scenarios	25/03	29/03
4	Report and Presentation	21/03	24/04
4.1	**First draft due April 10**	21/03	10//04
4.2	**Revision - final report due April 17**	11/04	17/04
4.3	**Presentation Design Day April 24**	18/04	24/04

Figure 2.1: Objective-Time Chart for this project timeline.

3 Market Analysis

3.1 Competitive Assessment

According to the 2016 market assessment report on the global algae industry from Transparency Market Research, the global algae market, valued at US$608.0 Million in 2015, is expected to continue growing at a compound annual growth rate of 7.39% into the next decade. The expected value in 2024 is over US$1.1 Billion at a volume of almost 30,000 of tons of biomass per year. This number could be even greater with a series of key technological advancements outlined below, with the aid of initial investment support, both public and private.

3.1.1 Carbon Conversion Technologies Landscape

In order for the global temperature rise to remain below the limits set by the Paris Climate Agreements – beyond which climate catastrophe is essentially inevitable – carbon dioxide levels in the atmosphere must be reigned in. This will occur not only by emissions reductions technologies, but by global adoption of an advanced profile of carbon conversion technologies. Carbon emissions from power plants are increasingly being recognized for their asset value, rather than simply as a harmful waste product. Carbon can be converted into many value-added products that have many industrial and day-to-day applications (Figure 3.1, obtained from the the XPRIZE Carbon Market Analysis). Unfortunately, the pace of carbon conversion technology is slow, due to technical and market challenges. While many carbon capture technologies (where captured CO_2 is merely stored) are near deployment readiness, carbon conversion technologies (where value-added products are created from the CO_2) are far behind. Current efforts to accelerate the research, development, and implementation of carbon conversion technologies are exceedingly important.

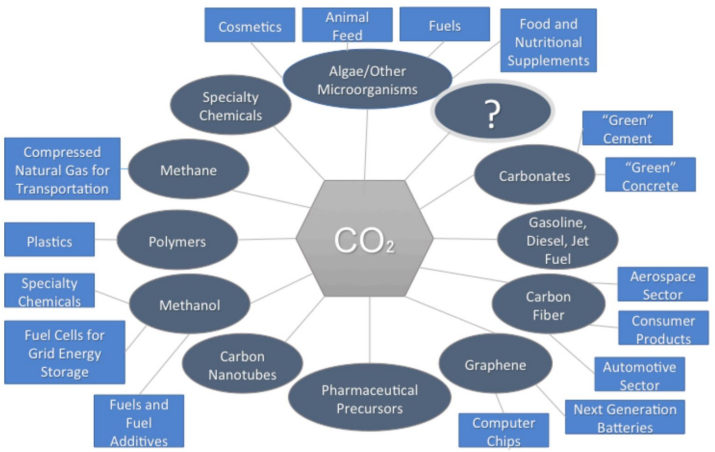

Figure 3.1: Various products that can be made from carbon dioxide through carbon conversion technologies. Obtained from the Carbon XPRIZE Market Analysis.

This project aimed to explore and overcome some of the technical and economic challenges associated with carbon conversion, and demonstrate the impressive potential of value-added microalgal production to contribute to the global carbon product market. The goals of this project were therefore in part motivated by the NRG Cosia Carbon XPRIZE, the ongoing $20 million international competition that aims to find and accelerate the development of the world's most innovative CO_2 conversion technologies. XPRIZEs are respected internationally for legitimizing highly important fields and providing visibility for creative and high-potential solutions to the world's most challenging problems. The foundational technological and market assessment for carbon conversion technologies that formed the Carbon XPRIZE criteria was therefore considered a legitimate assessment of the landscape and was used to provide perspective for this project.

Despite a move towards alternative sources of power generation, the International Energy Agency (IEA) anticipates that fossil fuels' share of the global power sector will only drop to 57% in 2035, from the 2011 level of 68%. This highlights the need for effective carbon conversion technologies. Carbon conversion technologies fall under three main categories: biological (organisms use processes like photosynthesis to absorb CO_2 and create a product), chemical (catalysts reconfigure carbon molecules from CO_2 with various substrates to form a product), and mineral (CO_2 is incorporated by way of solid carbonates into other products). Technologies under these classes are currently at a "Technology Readiness Level" (TRL) of approximately 1-4, meaning they are largely at the stage of initial conceptual research or laboratory-scale proof of concept. The timeline below (Figure 3.2), obtained from the the XPRIZE Carbon Market Analysis, depicts the path towards full commercial scale deployment. The presented timeline is an ideal schedule of research, development, and deployment. Carbon conversion technologies are only now breaking into pilot-scale operation.

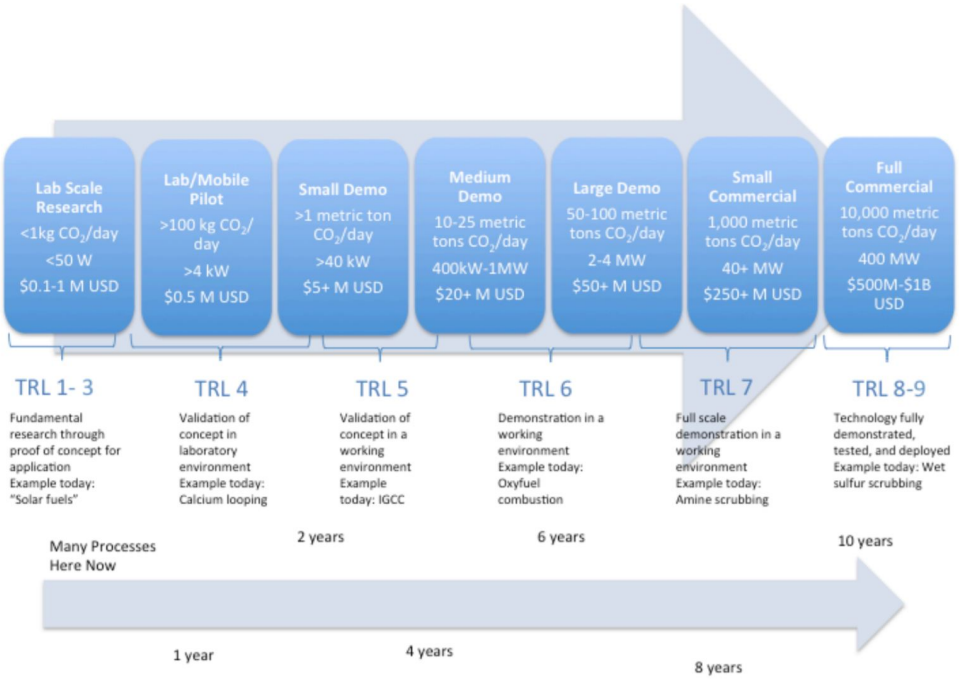

Figure 3.2: Timeline of the path to commercial viability of carbon conversion technologies, delineated by the "Technology Readiness Level". Carbon conversion technologies are currently generally at a TRL of 1-4. Obtained from the Carbon XPRIZE Market Analysis.

Another challenge in the path to viability is the need for conversion processes to be able to use a wide range of CO_2 sources. Currently, many concepts are being tested using pure CO_2 streams – the easiest source to utilize, as there are no other variables to account for. Eventually, conversion processes must be able to use industrial flue gas outputs that have a range of CO_2 concentrations, as well as other challenging properties such as physical characteristics like high temperatures, or changing compositions and presence of potentially harmful contaminants. On the other hand, another goal is to sequester large amount of CO_2 directly from air, where the challenge is instead achieving high and profitable volumes of product creation with the very small CO_2 concentration of air. Technologies are not currently at the point where highly variable gas streams can be utilized effectively.

3.1.2 Market Challenges of CO_2 Conversion Technologies

Some key challenges in bringing carbon conversion to market are considered to have played a prohibitive role in the realization of the full technological and economic potential of carbon conversion technologies such as algae production. The following section outlines some of these.

First, the range of products that can be created from CO_2 as a main building block is vast, and therefore hard to quantify, classify, and understand, which makes assessing the scale of potential impacts, the specific economic repercussions, and of course, the environmental benefits of all the possible processes complex. Furthermore, there is no standard method of life cycle analysis for carbon technologies. Since

the overarching goal is removing carbon from the atmosphere by closing the carbon cycle through carbon-neutral processes, it is important to standardize the way that carbon inputs and outputs of a process are measured and assessed. The large number of variables at play in a single process makes this very tricky. This makes measuring technological and economic progress difficult and obscure.

Second, industrial emissions reductions investment has been directed towards the simpler of carbon technologies: carbon capture and storage (CCS) technology. This leaves less funding for conversion R&D. Some CCS technologies have benefited from the investment; there are 12 commercial-scale projects around the world (XPRIZE Market Assessment). Unfortunately though, these processes actually force energy costs up, as CCS is a waste treatment process more-so than a value creation process. Third, conversion technologies must also compete with existing mature technologies that create the same products for much cheaper. For example, though algae can be used to produce valuable diesel, diesel production is performed on a large scale already, after decades of investment in the technology and its deployment.

Finally, navigating confounding and risk-averse rules and regulations embedded in the energy industry makes working with industrial emissions producers to test technologies at various scales difficult. Initial costs associated with deployment of new technology is a significant barrier to demonstrating potential for large scale viability. Of course, this is not aided by the fact that CO_2 emissions are heavily under-regulated in most of the world. Creating positive incentive for the widespread adoption of value-added carbon conversion technologies is crucial to their eventual success.

3.1.3 State of Algae Carbon Conversion Market

There is no shortage of reasons why algae is an attractive contender for large scale CO_2 capture and conversion into valuable products. With productivities orders of magnitude higher than other highly photosynthetically active plants such as soybean or sugarcane, and a biomass composition of 50% fixed carbon, microalgae is one of the fastest ways possible that CO_2 can be incorporated into a more carbon-dense material. However, large scale controlled and reliable microalgae production is difficult do to many technological and economic challenges. The technology for flue gas utilisation shows a lot of promise, but its long term economic viability as a profitable process depends on significant R&D investment in the present. Understanding how to harness the full biosynthetic potential of microalgae photosynthesis to be able to grow robustly under a wide range of conditions and high volumes of highly concentrated flue gas is crucial. From an economic perspective, unleashing the full potential of the algae biomass product market by boosting its expansion with positive incentives for industrial CO_2 emitters to use algae to offset emissions is going to be key. With increases in carbon regulation programs, there is growing interest in using algae to offset emissions in a number of industries. These include not only fossil-fuel power generation plants, but cement, iron, and steel plants, mining operations, petrochemical processes, and

many more. Programs like carbon crediting essentially adds a revenue stream for industrial producers utilizing algae as a carbon emissions mitigation method. Other government regulations could come in the form of subsidies based on amount of carbon emissions reduction, or tax reduction on algae products, or other initial cost offset such as land support. Many countries are actively interested in microalgae technology, including Brazil, where this project was designed for pilot deployment in.

Biological Understanding and Manipulation

Microalgae systems are complex. Though the knowledge landscape is large and rapidly expanding, much of the intricacies of algae growth and ecology remain largely unexplored or not understood. Application of advanced gene sequencing and engineering technologies to improve our understanding and control over microalgal carbon fixation will greatly improve yields. One of the major limitations of algae commerciability is the low productivity of algae under high lipid-producing conditions. Lipids can be extracted and converted to biofuels – one of the most commercially valuable products of algae – but for high lipid accumulation, algae must be grown under nitrogen starvation, which lowers growth rates overall. In the summer of 2017, Exxon Mobil and Synthetic Genomics released a breakthrough paper that reported the use of genetic engineering to double to lipid composition of Chlorella without sacrificing any biomass productivity (Dlouhy, 2017). Advancements of this significance are expected to rise in frequency in the coming years. This will be of particular importance in improving microalgae growth rates when fed a stream of gas with fractions of CO_2 as high as those in coal plant flue gas and higher. Improvements to the ability of microalgae to take advantage of other waste streams, such as using wastewater as a nutrient source instead of freshwater-based expensive nutrient medium, to create value and lower costs and overall footprint will also be important on large scales, and will make algae production facilities even more attractive for public and private investment.

Harvesting and Drying efficiency

Currently, harvesting, post-processing, and refining of algae cultivation volume is expensive and energy-intensive. In many cases, post-processing such as drying can represent the majority of production costs, and in some cases have been projected to be too high to even allow for implementation of a design (Slade, 2013). Improvements to heat integration and recycling within the water removal process will be particularly important. Microalgae refining is a relatively new field of research and engineering; there is a wide horizon for the invention of new and diverse methods for exploiting the most value possible from microalgae.

Carbon dioxide and oxygen concentration and mass transfer, temperature, pH, light availability, and nutrient availability all must be highly controlled when growing algae, especially if the desired productivity is high. Controlling these elements becomes significantly more complex when flue gas serves

as the main carbon source, and makes the above discussed improvements even more important. Mass transfer is a particularly pertinent issue when it comes to reactor design, as the surface area to volume ratio of a tank for good mass transfer may be much lower than what is required for good light transmission. Furthermore, balancing these factors often results in a large increase in cost. A further discussion on current methods of algae growth techniques can be found in Section 4.

The algae carbon conversion industry is still in its infancy, and so there are few examples of sustainable large-scale algae production operations. However, lab-scale demonstrations and some large-scale operations have shown promise. Importantly, life-cycle analyses even suggest that with the above discussed improvements, met with strong carbon legislature and investment support, the production cost of algae may even be on par with petroleum-based fuels in the the near future (Schenk et al. 2008, Lardon et al. 2009, Stephens et al. 2010).

3.2 Customer Requirements

The following subsections describe the ideal process and product specifications presented at the outlook for the presented design. They were informed by the above discussed Carbon XPRIZE technology and market assessments for moving towards an advanced pilot-scale carbon conversion facility, as well as reviews of algae carbon conversion technologies and industry challenges and prospects.

3.2.1 Process Specifications

This design is a pilot-scale direct flue gas-to-algae conversion process. A stream of 10% CO_2 v/v flue gas from a coal-fired power plant is sent to the algae reactor at a carbon dioxide input rate of 200 kg per 24 hours. Over the course of a 24-hour period, at least 30%, but ideally 50% of the incoming CO_2 must be converted to algae biomass through photosynthesis. This process should be designed to take advantage of renewable sources of power as much as possible in order to bring the process closer to carbon neutrality. Depending on the climatic profile of the chosen operating region, solar energy may be adequate to maintain higher growth rates during eight peak daylight hours, but there will also be a need for some level of growth maintenance overnight. Artificial lighting could be used to maintain growth during nighttime or less than ideal sunlight conditions, but a majority of the total daily CO_2 conversion goal should be met using solar energy in order to stay true to the goal of accelerating carbon neutral technologies for a cleaner future.

3.2.2 Product Specifications

The algae should be continuously harvested at a rate matching its specific growth rate (to maintain constant cell density and cultivation volume). It should then be sent to post-processing where the water

content is reduced to result in a product with less than 10% moisture content. This product can be sold to a variety of users for direct use in applications such as livestock and aquaculture feed, or sold to refineries to extract further product value by way of many processes such as lipid extraction, combustion for power generation, or nutraceutical compound extraction.

3.3 Presented Innovative Edge

The presented design provides an optimistic outlook for large-scale algae production. There are many ways in which the design is innovative and may have an edge in the algae industry. The design is highly flexible and tailorable to meet specific consumer needs. Currently, it operates at over 50% carbon conversion of a 200 kg CO_2 input rate from a 10% CO_2 v/v flue gas input.

Perhaps most importantly, this design functions on a scale-able modular base, where the entire system provides economies of scale and low cost of transitioning to larger scales. The design revolves around a series of "petals", horizontal tubing branches that extend from a central gas exchange column. These petals are optimized for high productivity and profitability. Scale up is simply a matter of adding more petals and increasing the size of the gas exchange column, up to a maximum capacity, after which total units are multiplied. The unit space requirements are also optimized to be very low while still providing a practical layout for operation and maintenance, and keeping added friction loss from bends and turns in the piping under reasonable limits.

Because the system is a closed system that also involves an internally-illuminated tank, the system could be operated in a range of conditions that may not be as ideal as the location selected for this project (Ceara, Brazil). The enclosed tank offers protection against particularly unfavourable weather or emergency conditions, opening up the potential for operation in a wider range of climatic profiles. Refer to Section 12 for a further discussion of the benefits of the tank.

The sales projections for the pilot process are small, but would rise with scale. Overall return on investment is also expected to rise. Furthermore, at a larger scale, there would be the ability to include further biorefinery treatment that would allow the products to be sold at higher cost, perhaps even orders of magnitude higher. Overall, this proposed design offers key improvements to typical algae production facilities, providing a high level of flexibility, capacity, conversion efficiency, and support for a wide range of growth conditions.

4 Preliminary Process Synthesis

4.1 Process Overview

This design project aimed to tackle some of the biological, technological, and economic challenges associated with using microalgae to sequester a high fraction of the CO_2 present in flue gas from a coal-fired power plant. A pilot-scale complete flue gas-to-algae conversion facility was designed that successfully met the ambitious target of converting over 50% of input CO_2 into biomass. Following requirements, the process utilizes a stream of flue gas (10% CO_2v/v) containing 200 kg of CO_2 per day. These specifications are on par with technical goals of the flue gas CO_2 conversion sector.

The open-endedness of the requirements left much room for challenging problem-solving and creative decision-making and resulted in a novel reactor design, dubbed the "Hybrid Petal Reactor". The following sections outline the design considerations and methods of decision-making for key aspects of the design including product type, species type, lighting source, location, nutrient formula and delivery, pH control, reactor configuration, and harvesting and post-processing. Also discussed are biological constraints of algae systems and information on how these limits were taken into account in the final design.

4.2 Design Considerations

4.2.1 Product Selection

Algae have many applications in a wide range of industries. The major applications include biofuels and power generation (from extracted lipids or from biomass), feed material (human or fish/livestock), health (nutraceuticals and well-known products such omega-3's) and green materials such as biomass-based plastics. Though unrefined algae biomass can be utilized as-is in a wide range of products, it is often further refined to take advantage of the potential for more specific or valuable products (for example lipid extraction and transesterification to diesel fuel) or to meet regulatory standards for food and drug applications. The product type is also specific to the species of algae. Some algae species produce highly specific (and valuable) products, such as the Astaxanthin-producing *Haematococcus Pluvialis*. Other species are more diverse in their eventual end use. Often though, the more tailored the species is to a certain product, the more specific and highly controlled the growth conditions must be, such as in the case of *H. pluvialis*. This is often more expensive and subject to failure. It was therefore determined that a product that could be further refined in a large range of ways was desirable. Biomass that contains about 20% lipids would be adequate for use as-is in many applications, but is also a high enough fraction to make lipid extraction (and use of leftover biomass) worth it. The dried biomass exiting this process will be sold to buyers that may include farmers/aquaculturers or other refineries such as bioethanol/biodiesel producers or pharmaceutical producers. Dried biomass can also be burned directly to generate power,

as it has a similar heating value to coal.

4.2.2 Species Selection

Though the designed system is capable of cultivating many typical algae species without modification, the design was based on the growth properties of a single chosen species. This provided a set of requirements of which to base design decisions off. It also allowed productivity to be accurately modelled and predicted under the chosen cultivation conditions. *Chlorella Vulgaris* was chosen to be the model species for the following reasons:

- The dried biomass can be used for a wide range of applications both as-is or following a variety of further refinery processes
- It is highly studied; there is a wealth of information available on its behaviour under various growth conditions
- It does not require highly demanding or controlled growth conditions, such as very high temperatures
- It is used commonly in larger scale algae cultivation operations
- It is robust under changing conditions
- It is not particularly subject to being out-competed by potential contaminants
- Biomass productivity is among the highest of well-known species
- Lipid content under normal nitrogen conditions (good for growth) is adequate at approximately 20%.
- The nutrient profile is excellent for many human health applications as well as livestock and fish feed supplements
- It can be grown on standard Bold's Basal Medium which has readily available components
- It can still grow well on 10% CO_2 v/v flue gas (many species require much lower concentrations of CO_2)

Use of a species that can grow on saltwater rather than freshwater was considered, in order to lower to freshwater requirements of the process. However, the advantages of using *C. Vulgaris*, a freshwater species, ultimately out-weighed the disadvantage of freshwater requirement.

Growth Model for Chlorella Vulgaris It was necessary to understand the growth properties of *C. Vulgaris* in order to help inform later decisions in the development of the design.

Algae growth is a complex and widely studied subject. Algae require nutrients, CO_2, H_2O, and light to photosynthesize and grow, but they also exhibit growth inhibition in certain conditions. In many cases this inhibition is not well understood. In this process design, a growth model was developed by compounding information from several studies on *C. Vulgaris*. The growth model is not a perfect description of algae growth, but it accounts for the primary resource requirements and causes of inhibition as accurately as is practical.

The rate of algae growth is proportional to algae concentration, so growth is described by an equation of the form:

$$\frac{\mathrm{d}X}{\mathrm{d}t} = \mu_g X \tag{4.1}$$

where the specific growth rate μ is a function that depends on the degree of resource limitations and growth inhibition. In the remainder of this section, a quantitative function for μ_g (as a function of resource availability) is developed that is used in the process simulation described in Section 8.

First, resource requirements are modelled for CO_2 and light using Monod models. Nutrients will be provided in excess so that they will not be a limiting factor to growth, and therefore did not need to be considered in the growth model. Similarly, the algae will be kept at dilute concentrations in water during the entire growth process, so H_2O will not be a limiting resource (in fact, inhibition due to overcrowding of algae in solution would occur well before photosynthesis becomes limited due to lack of water). Thus, the resource-constrained growth rate μ_{Res} is of the form:

$$\mu_{Res}(I, C_{CO_2}) = \mu_{max} \frac{I}{K_I + I} \frac{C_{CO_2}}{K_C + C_{CO_2}} \tag{4.2}$$

where I is the intensity of light incident on the algae, and C_{CO_2} is the dissolved CO_2 concentration. K_I, K_C, and μ_{max} are constants, the values of which were found from published studies on *C. Vulgaris* growth. These values are shown in Table 4.1.

Table 4.1: Growth Model Parameters

K_C	0.000167 mol/m^3	(Han et. al., 2015)
K_I	18.7 W/m^2	(Han et. al., 2015)
μ_{max}	0.27 hr^{-1}	(Blanken et. al., 2015)

Note that this equation for μ_{Res} applies to a volume element of algae solution in which light intensity I can be considered constant. In solution of any substantial depth, light intensity decays exponentially with depth due to light absorption by algae. This dependence of intensity on depth is accounted for separately using Beer's law, as discussed in Section 8.1.2.

A major cause of growth inhibition that must be accounted for is high O_2 concentrations. Published data (Shelp and Canvin, 1979) was found that reported the degree of O_2 inhibition at three concentrations, shown in Figure 4.1. In order to obtain a continuous function that models O_2 inhibition, a quadratic fit (indicated by the dotted line in the figure) was applied to this data.

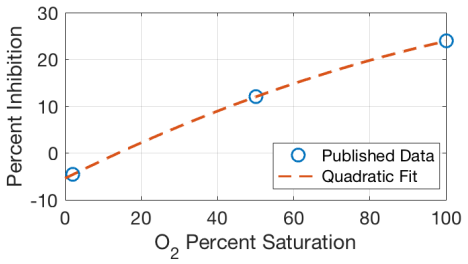

Figure 4.1: Percent growth inhibition as a function of O_2 percent saturation. Percent growth inhibition is the percent by which the growth rate decreases due to dissolved O_2, relative to the growth rate in atmospheric conditions. Note that the percent inhibition is negative for conditions with lower O_2 levels than in atmospheric conditions.

In Figure 4.1, percent inhibition is the percent by which the growth rate decreases due to dissolved O_2, relative to the growth rate in atmospheric conditions. Note that the percent inhibition is negative for conditions with lower O_2 levels than in atmospheric conditions. O_2 percent saturation is equal to $\frac{C_{O_2}}{H_{O_2}P}$.

The quadratic fit to this data is given by

$$f_{Inhib}(C_{O_2}) = -0.0011\Big(\frac{C_{O_2}}{H_{O_2}P}\Big)^2 + 0.403\frac{C_{O_2}}{H_{O_2}P} - 5.40 \tag{4.3}$$

The full function for μ_g is then given by

$$\mu_g = \mu_{Res}(I, C_{CO_2})\Big(1 - \frac{f_{Inhib}(C_{O_2})}{100}\Big) \tag{4.4}$$

An additional cause of inhibition is extended periods with no exposure to light. When algae are not exposed to sufficient light, they enter a stagnation phase in which they do not grow. Before beginning to grow again, algae must be exposed to light for a substantial period of time. Thus, it is essential that sufficient light is provided so that the algae do not enter this phase. The exact conditions that cause algae to enter this phase are not fully understood, but the following requirement was maintained: in any given several-minute interval, the algae must spend at least 1 second exposed to light for every 9 seconds in darkness. The ratio of time in light to time in darkness is referred to as the Light/Dark Ratio (LDR). Thus, this additional requirement is the following:

$$LDR > 1/9 \tag{4.5}$$

The amount of light needed to qualify as *'exposed to light'* is an amount sufficient to maintain growth, which was approximated as an amount sufficient to ensure $\mu_g > 0.01\mu_{max}$, as determined with Eq. 4.4.

4.2.3 Algae Cultivation Methods: Open vs Closed Reactors

One of the first steps in the design synthesis was to determine whether or not the system would be "open" or "closed" to the surroundings. This would then inform succeeding decisions such as location and illumination supply. There are a multitude of reactor setups available for cultivation of algae. They range from the most basic pond setups, where algae are grown in large shallow ponds, often in a raceway shape (Figure 4.2), to highly controlled tank photobioreactors with advanced illumination and CO_2 input systems (Figure 4.3).

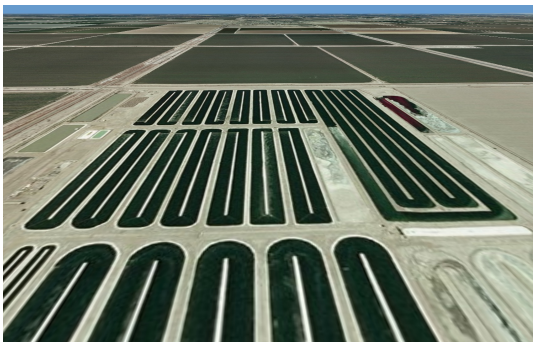

Figure 4.2: Algae raceway ponds in Southern California, courtesy of Pacific Northwest National Laboratory (Mark, 2011).

Figure 4.3: Pond Technologies' internally illuminated 1000L tank photobioreactors.

All methods of cultivation can be classified as either "open" or "closed" systems. Table 4.2 below (selected rows obtained from Table 1 of *Design of Closed Photobioreactors for Algal Cultivation (Koller, 2015))* describes some of the important criteria considered when deciding between an open or closed photobioreactor system.

Table 4.2: Criteria for Considering Open vs. Closed Algae Photobioreactors.

Criterion	Open Systems	Closed Systems
Space requirements	High	Low
Contamination risk	Very high	Very low
Water evaporation	Very high	None
CO2 supply	Exchange with air (limits rate of input)	Sparging (much higher rates of input possible)
Risk of CO2 loss	High	Low
O2 removal	Exchange with air	Degassing often required
Flexibility of process	Very low	Highly versatile and tailorable
Controllability of process	Very low	Possible
Dependency on weather conditions	Entirely dependent	None given artificial illumination, some given solar
Required cultivation volume	Very high	Low
Typical biomass concentrations	Low (below 1g/L)	Medium to high (few g/L)
Optimal lighting for productivity	Not possible	Variety of advanced illumination schemes
Initial investment cost	Lower	Often higher

Considering the rigorous carbon sequestration goals of this project, it was decided that a closed system would be more likely to provide the adequate conditions for both the higher rates of CO_2 input and the higher biomass productivities required to achieve the goals.

4.2.4 Light Sources: Natural vs Artificial

After having decided that a closed system was desirable, the next step in the design synthesis was selecting a source of illumination. Closed systems can be designed to support the utilisation of either solar energy (by way of flat panel or tubular reactors) or artificial illumination (often employed in bubble column or tank reactors). Two main factors were considered when deciding on the lighting method: electricity consumption, and tailorability of the process for optimal growth conditions.

It is desirable for the algae growth reactor to be designed for continuous operation for multiple reasons. First, a power plant emits flue gas continuously, so a sequestration facility should also operation continuously. Second, though sunlight can be utilized for some hours of the day, it is only adequate for algae growth for about eight hours. Without an adequate source of light energy, CO_2 is not being

consumed in photosynthesis, and high levels of CO_2 can even become harmful to the algae. A drop in cell density during the night, or during suboptimal weather conditions was not desirable.

Artificial lighting offers the ability to reach the biosynthetic potential of the algae, which can be much higher than is achieved using only natural sunlight. The wavelengths of provided light can be optimized to be in the right range of the photosynthetically active radiation spectrum, the light/dark duty cycle can be manipulated to achieve the highest productivity, and the algae can be provided with just enough light to be most photosynthetically productive while not running into the issue of either photoinhibition (too much light and not enough CO_2) or oxygen inhibition (too little light and too much oxygen), both of which can irreversibly harm a culture. However, artificial lighting configurations can reach prohibitively high operating costs quickly.

Perhaps most important when considering the purpose of carbon conversion systems in the first place, using artificial lighting can result in high carbon emissions throughout the lifecycle. If artificial light is relied on for cell growth, it is probable that the carbon emissions from lighting alone would greatly exceed the carbon sequestered by the algae. This is, of course, undesirable. Solar energy is freely available, and by using it to grow algae and sequester carbon, the process is brought closer to carbon neutrality. For this reason, it was decided that solar energy should be used to perform almost all of the required carbon conversion.

Of course, sunlight is only adequate for reasonable growth rates for at most 8 hours of a day, given ideal weather conditions. A drop in population during the 16 hours of night when biomass is not accumulating, or during less than optimal weather conditions, is undesirable for a continuously operating process. It was determined that a hybrid system should be designed, where solar energy is harnessed during hours of highest sunlight intensity, and artificial lighting is employed to prevent cell density drops at night or during sub-optimal conditions.

4.2.5 Conceptualizing the Novel "Hybrid Petal Reactor"

At this point in the synthesis it had been decided that the designed reactor would be closed, and would utilize a combination of both solar and artificial lighting. The exact configuration had to be chosen to optimize light use, land use, and method of gas transfer. Table 4.3 below (selected rows obtained from Table 2 of *Design of Closed Photobioreactors for Algal Cultivation (Koller, 2015))* describes some of the important criteria considered when deciding between types of closed reactor configurations.

Table 4.3: Criteria for Considering Bubble Column vs. Horizontal Tubular Algae Photobioreactors.

Criterion	**Bubble Column**	**Horizontal Tubular PBR**
Surface-to-volume ratio	Low	High
Mixing efficiency	High	Medium
kLa	High	Low
Risk of self-shading	Medium-high	Low if tube diameters are small
Risk of biofouling	Low	High
Investment costs	Low	Medium-high
Space occupation	Low	Medium
O2 release	Easy	Very hard
Shear forces	Low	High
Scalability	Difficult because higher volumes make illumination and mixing less efficient	Easy with addition of more tubing but restrictions on gas exchange

Light Use

Typically, flat panel or horizontal tubular reactors are the closed system of choice when designing a system for sunlight usage (Figure 4.4).

Figure 4.4: Transparent horizontal tubes are used for growing algae, often outdoors, to take advantage of sunlight (Climate Tech Wiki).

However, these layouts are not ideal for efficient artificial lighting, as the surface area-to-volume ratio is far too high to be cost effective or energy efficient. It was thus decided that a hybrid reactor that

combined an outdoor horizontal tubular reactor (to be used during adequate sunlight hours) and an internally-illuminated tank (to be used at night or during bad weather, maintenance, or unexpected population drops, etc.) should form the base of the design.

Gas Transfer

Adequate gas transfer is easily possible in a closed tank setup via sparging throughout the larger volume. Mass transfer coefficients are typically higher in these tank setups. However, the designed system must also be able to support gas transfer during the day time, when the algae will be cultivated in horizontal tubes. It was determined that in-line sparging and $O_2 2$ degassing throughout the tubes would be prohibitively expensive and unlikely to be able to support the high rates of mass transfer required to meet the CO_2 sequestration goals. Therefore, it was decided that there must be a central gas exchange column, where the cultivation volume would be cycled through continuously to receive fresh CO_2 and be degassed of built-up oxygen. This column would have to be as small as possible, to ensure that the algae are spending negligible time in the column, as the column volume would not be receiving adequate sunlight.

Pulling together all of the above criteria, the "Hybrid Petal Reactor" was conceptualized. During eight peak sunlight hours of the day, the algae will be grown in an outdoor tubular system that allows for adequate sunlight distribution to the cultivation volume. A small central gas exchange will be used for CO_2 transfer into the volume and O_2 transfer out. Almost all of the total daily carbon sequestration goal will be met during these eight hours. During the sixteen nighttime hours, the algae will be grown in a closed tank with an artificial LED/optical fibre lighting configuration that supports the baseline level of biomass increase necessary to sustain population densities at daytime operating levels. This results in the majority of the carbon sequestration being performed using solar energy. The light setup could, in theory, be easily configured to support a significantly higher growth rate, but this would come at a high dollar and emissions cost. To bring the process even closer to carbon neutrality, electricity for any artificial lighting could be obtained from renewable sources, or eventually, on-site solar collection and storage. See Section 7 for a detailed description of the reactor setup, and Sections 8 and 9 for a discussion of the simulation and optimization of the setup.

Other Important Biological Constraints

Algae are complex organisms, and the exact design of the growth system must take into account a number of biological requirements. The most pertinent are listed below:

- The presence of oxygen in the cultivation volume can inhibit growth, so the oxygen concentration throughout the tube length should be monitored and the effect on growth rate calculated and considered in the calculation of average growth rate.

- The algae volume should not be circulated at velocities higher than 30cm/sec in order to avoid cell damage due to shear stress.
- The residence time spent in the dark while receiving high levels of CO_2 should not exceed approximately 10-20 continuous minutes, as irreversible damage to the cells can occur after this point.
- The light:dark ratio should be high enough to support a reasonable average specific growth rate. The volume should also be well mixed as to ensure that statistically, a cell does not spend inhibitory amounts of time in darker zones. The flow through the tubular sections should be turbulent to promote uniform cell density.
- The cell density of the volume should be reasonable (approximately 2g/L) in order to mitigate the issue of light attenuation due to self-shading.
- The temperature should be maintained as close as possible to 30C and should not rise above 35C.

4.2.6 Location Selection

Given that the design would operate outdoors, relying in some part on sunlight availability and weather conditions, location choice was of particular importance. This process was designed to be located in the state of Ceará in Northeast Brazil, as highlighted in red in Figure 4.5. The algae growth system could be retrofitted to Porto de Pecém, a 1085 MW coal-fired power station. The following section describes how this location was chosen.

Figure 4.5: The state of Ceara, Brazil, where the Porto Do Pecem Power Station is located. This power station would be a suitable contender to retrofit the Hybrid Petal Reactor to (Wikipedia: Ceara, Brazil).

Choice of location is a function of many factors; not only were geographical and physical properties considered, but political and economic situations were assessed when determining where to locate this

pilot-plant. The first step was determining a set of criteria to base location selection off of. The ideal location would meet the following criteria:

- There must be a coal-fired power plant available for retrofitting the algae system
- There is adequate sunlight year-round, allowing for maximum daylight hours year-round
- There are not large temperature swings (during days or seasons)
- There are not periods of intense weather (monsoons, etc.) that would inhibit growth or present significant risk of damage to the equipment
- Non-arable land is available without significant habitat loss
- There is the potential for scale-up in the region
- There is reliable access to freshwater (if growing a freshwater species)
- There is reliable access to power
- Land should be cheap
- Utilities should be cheap
- There must be a market for the products
- There is political/social/economic investment in sustainability and renewable energy
- Bonus: there are existing flue gas regulations, carbon credit systems, or other sequestration and emissions reductions programs that will support the algae industry

For the geographic criteria, data on sunlight intensity, microalgae productivity, agricultural land usage, and temperature and climate profiles was compiled from major reviews including the "Global evaluation of biofuel potential from microalgae" (Moody et al, 2014), and mapping and imaging resources such as the NREL System Advisor Model and National Solar Radiation Database. Figure 4.6, sourced from Moody et al shows predicted biomass productivities around the globe.

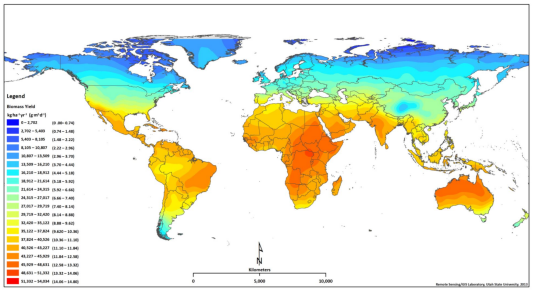

Figure 4.6: World map of average predicted biomass productivity of algae (Moody, 2014).

Based on the above criteria and data, a shortlist of five countries was compiled after which the final choice was made based on process of elimination. The shortlist consisted of the United States, India, Australia, Kenya, and Brazil. Figure 4.7 depicts the average lipid productivity predicted by Moody et. al. for India, China, Brazil, and Australia.

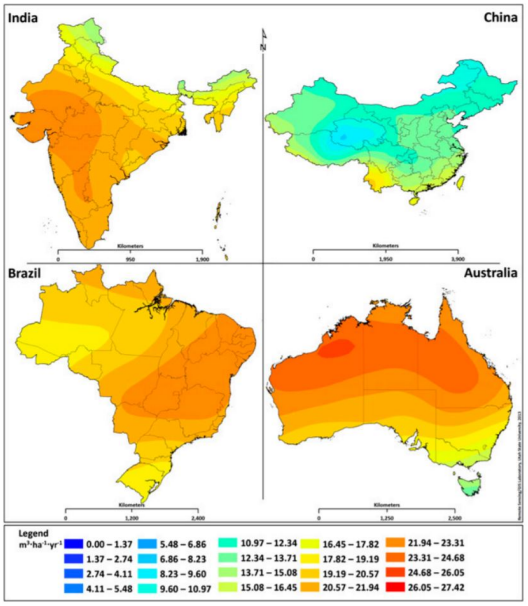

Figure 4.7: Average lipid productivity predicted by Moody et al for India, China, Brazil, and Australia.

US: The US receives a reasonable level of sunlight in the south but low non-arable land availability and the higher cost of land and utilities were disadvantages. Though there is interest in algae biofuels and biomass products, enthusiasm is lacking (especially in coal power generation regions) and share of energy consumption from renewable sources is low.

India: Though India has some very favourable characteristics such as warm temperatures year round, a high fraction of non-arable land suitable for algae production, low/no transportation costs due to proximous power plants, and adequate sources of nutrients and water, India was ultimately eliminated due to the risk posed by natural disasters during the rainy/monsoon season. Low light during this time as well as threats such as mud slides were too risky.

Australia: Areas in the North West and East of Queensland were determined to be suitable for algae production due to low land value, availability of non-arable land, and proper climatic condition. Furthermore, industrial activity in the Western regions provide supporting infrastructure and sources of CO_2, as well as a potential market for the products. Unfortunately, Australia has one of the highest utility costs among the countries on the shortlist, and freshwater was not as readily available as would have been optimal.

Kenya: Kenya exhibits optimal climatic zones with some of the most suitable sunlight and tempera-

ture profiles on the globe. Almost half the land in Kenya is non-arable land that would not compete with food crop land. Not only is Kenya attractive for microalgae cultivation, but Kenya is actively seeking methods to fulfil the "Kenya Vision 2030" goals for sustainable development. Furthermore, the health and economic benefits that a growing algae industry would bring would be extremely beneficial to local communities. Unfortunately, freshwater and power are not as available, and are high in cost. As well, the political and economic situation in Kenya would present too great of challenges to be worth establishing a pilot plant with limited guidance. Kenya would have been the second choice and could be a great location for expansion of operations.

Brazil: Brazil was chosen due in part to its optimal climatic profile. There is intense sunlight and high median temperatures with little fluctuation during the seasons. In the considered regions, seasonal natural disasters are not a significant threat. There is adequate water availability (and significant interest in future potential to develop algae wastewater treatment), and readily available power, both of which are not expensive. Apart from the physical advantages, Brazil stood out in the political and economic sphere. Brazil is pioneering renewable energy generation (over 85% of domestically produced electricity comes from renewables) and is rigorously pursuing further R&D into new clean energy generation processes– algae included. Investment into algae production is expected to grow in Brazil. Furthermore, Brazil already has much of the refinery infrastructure needed to transform harvested algae biomass into a diverse set of refined products. Using power plant mapping tools, the Porto do Pecém power station was located in the Northeast region. This location is near a source of freshwater and has land available for future scale-up.

4.2.7 Nutrient Delivery System

The algae are grown autotrophically (photosynthetically, with the sole carbon source being CO_2). After a literature review on appropriate nutrient formulas for autotrophic growth of Chlorella vulgaris, it was determined that Bold's Basal Medium (BBM) would result in the highest biomass productivity. Standard BBM and modified versions of it are the most commonly used nutrient formula for this algae. As recommended by the Canadian Phycological Culture Center, the BBM formula from the Handbook of Phycological Methods (Stein, 1973) was chosen, as it has been shown to support high levels of *C. Vulgaris* growth. The formula was then modified to support the biomass productivity goals of the design in the most economic manner possible. Refer to the Appendix for the formula. Nutrients will be stored on site and highly concentrated fresh stock solutions will be made up manually on a frequent basis. The stock solutions will be continuously injected into a freshwater stream that will then be delivered to the reactor. Refer to Section 7 for the process diagram and description.

4.2.8 pH Control

The transfer of NO, NO_2, SO_2, and CO_2 from the flue gas into the algae solution can cause pH to drop to toxic levels if not properly controlled. To maintain a neutral pH in the photobioreactor, NaOH is added to the nutrient stream before it enters the gas exchange column. The rate of NaOH addition will manipulated by a control system to maintain a neutral pH at all time. This method is very low cost relative to other pH control methods such as upstream removal of NO, NO_2, SO_2 from the flue gas. Dissolved NO, NO_2, SO_2, and the salts they form upon reaction with NaOH, are nontoxic to *C. Vulgaris* (Lee et. al., 2002). Therefore the presence of these species is not a concern so long as pH is properly controlled.

4.2.9 Harvesting and Post-Treatment

Collection and dewatering of the algal biomass is often described as one of the obstructions to efficient production of fuels and other value-added products from algae. For the biomass to be of value for biofuels production, it is agreed upon that the moisture content of the water should be less than ten percent by mass wet basis (w.b.). Dewatering of the produced biomass is energy intensive, inflicting high operational costs on the overall process. In an effort to reduce these costs, a three-step process is proposed, consisting of flocculation, flotation, and drying.

In general, after the algal biomass is grown, a flocculation step is desired to aggregate the individual clusters of algae cells dispersed throughout the medium. For the disruption of these suspensions to occur, the surface charges of the particles must be negated, so that van der Waals attractions will bring the cells together. *C. Vulgaris* cells have a negative surface charge for pH of solution at or above about 5 due to carboxyl and amine groups on their surface (Vandamme, 2013). To induce the aggregation, a compound with some form of positive charge is needed in the solution with the algae. After some consideration, it was decided that $MgSO_4$ would be used in a pH-induced flocculation process. Once exiting the harvesting port of the reactor, NaOH would be added to the harvested volume to increase the pH to approximately 11. Flocculation will then be induced via addition of Mg2+ (Vandamme, 2011). Other aluminum and polysaccharide-based flocculants such as alum and chitosan were considered, but the concentration of magnesium flocculant required is much lower while producing trace precipitate in the harvested biomass (Zhang, 2016).

Flocculation must always be accompanied by a second harvesting step to remove the biomass from the bulk of the aqueous growth medium. This can be accomplished by any number of processes, such as sedimentation, flotation, filtration, or centrifugation. Having a continuous process means sedimentation is not an option, as the time scale required for the flocs to settle is much too long. Selection of *C. Vulgaris* as the microalgae for cultivation ruled out most types of filtration, as the cells are too small

for traditional filtration and could lead to caking problems in a microfiltration process. Centrifugation is commonly used for biomass harvesting; however, it can be cost-prohibitive for a pilot-scale process due to significant required energy input. As a result, dissolved air flotation (DAF) was selected for the separation. In DAF, water saturated with air passes through a pressure release valve, causing air to come out of solution. When performed on flocculated algae, the less-dense cells adhere to the air bubbled through and rise to the top of the medium, where they can be effectively skimmed to remove the bulk of the moisture. However, as the size of the algal production process increases, the costs associated with dewatering should be reconsidered.

Although the bulk of the water has been removed, a drying process is still needed to remove the remaining moisture from the algal cake. The maximum amount of mass transfer allowed is dictated by the equilibrium moisture content (EMC) of the system, or the lowest moisture content possible in the cake. This EMC can be determined directly from the Guggenheim, Anderson, de Boer (GAB) equation using constants for algae predicted by Mohamed et.al (Mohamed, 2005). The equation is reproduced below:

$$EMC = \frac{ABC(RH_{eq})}{(1 - B(RH_{eq}))(1 - B(RH_{eq}) + BC(RHeq))} \tag{4.6}$$

in which RH_{eq} is the equilibrium relative humidity.

A belt drying process utilizing the input flue gas was initially considered, although the flue gas was already near saturated with water, and the low-grade heat provided by the flue was not adequate for evaporation of the water. Instead, it was decided that the algal cake would be sent to a rotary steam tube dryer in which the remaining water is evaporated, producing a dry algae product with approximately ten percent moisture content w.b. Indirect heat transfer is necessary for this process to maintain a low equilibrium moisture content. A detailed description of this process can be found in Section 7.5.

4.2.10 Hours of Operation and Biomass Productivity

As described above, the system will operate at two different modes of steady state over the course of a 24-hour period: "Daytime mode" and "Nighttime mode." Essentially all of the total carbon conversion will occur during daytime operation. A very small amount of CO_2 by way of air sparging will be input at night to maintain daytime operation cell density. The expected biomass productivity calculations were performed with the intent of meeting an ideal carbon sequestration fraction of over 50% of the input stream– the ideal and most ambitious scenario – resulting in a total amount of 100kg of CO_2 sequestered in a 24-hour cycle. The fraction of total daily CO_2 that is converted to biomass in the daytime set-up versus the nighttime setup could be optimized against costs of setup, operation, scale, and the effect of operating in range of geographic and economic scenarios outside the scope of this project. For this design, to bring the process as close to carbon neutrality as possible, the majority of sequestration is to

be performed using solar energy. Summary of biomass production during daylight:

Length of Daytime operation: 8hr

Total amount of CO_2 sequestered during Daytime = 100kg CO_2

Rate of CO_2 sequestration during Daytime = 100kg CO_2/8hr = 12.5kg CO_2 removed/hr

Rate of carbon assimilation = (12g C/mol / 44g CO_2/mol) * 12.5kg CO_2/hr = 3.4kg carbon fixed/hr

Fraction of algae biomass that is fixed carbon = 0.5

Rate of biomass output during Daytime = (3.4kg carbon/hr)/(0.5kg carbon fixed/kg biomass)

= **6.8kg biomass/hr**

5 Database

The following tables list all physical and biological constants used in the following sections. The source for each value is provided in the third column of the tables. The section in which the values are used is provided the table caption.

Table 5.1: Gas Transfer constants: used in Section 8.1.1

H_{CO_2}	34 mol/m^3 atm	(Sander, 1999)
H_{O_2}	1.3 mol/m^3 atm	(Sander, 1999)
H_{NO}	1.9 mol/m^3 atm	(Sander, 1999)
H_{NO_2}	24 mol/m^3 atm	(Sander, 1999)
H_{SO_2}	1200 mol/m^3 atm	(Sander, 1999)
$k_{L,CO_2}a$	0.26 s^{-1}	(Talbot et. al, 1990)
$k_{L,O_2}a$	0.77 s^{-1}	(Talbot et. al, 1990)

Table 5.2: Growth Kinetics: used in Section 8.1.2

K_C	0.000167 mol/m^3	(Han et. al., 2015)
K_I	18.7 W/m^2	(Han et. al., 2015)
μ_{max}	0.27 hr^{-1}	(Blanken et. al., 2015)
$Y_{CO_2/X}$	41.63 mol/kg	(Hu et. al., 2011)
$Y_{O_2/X}$	41.63 mol/kg	(Hu et. al., 2011)
$\hat{H}_{alg}$	15,000 kJ/kg	(Orosz and Forney, 2008)
B	187 m^2/kg	(Blanken et. al., 2015)

Table 5.3: Flue Gas Properties: used in Section 8.1.1

vol% CO_2	10%	Problem Statement
vol% O_2	10%	(Xu et. al., 2003)
vol% NO+NO_2	420 ppm	(Xu et. al., 2003)
vol% SO_2	420 ppm	(Xu et. al., 2003)
Flue Gas Temp from Power Plant	200^{o}C	Estimation by Consultants

Table 5.4: Physical Properties used in Section 8

Heat capacity of water at 30^{o}C	4178 kJ/kg K	(Incropera, 2003)
Density of water at 30^{o}C	999 kg/m^3	(Incropera, 2003)
Dynamic viscosity of water at 30^{o}C	769 $\times 10^{-6}$ N s/m^2	(Incropera, 2003)
Kinematic viscosity of water at 30^{o}C	0.8007 $\times 10^{-6}$ m^2/s	(Incropera, 2003)
Kinematic viscosity of air at 30^{o}C	0.00001349 m^2/s	(Incropera, 2003)

Table 5.5: Environmental Properties at plant location: used throughout report

Daytime Sunlight Intensity	917 W/m^2	(Alves and Schmid, 2014)
Underground Temperature	26^{o}C	(Alves and Schmid, 2014)
Average Daytime Temperature	27^{o}C	(Alves and Schmid, 2014)
Maximum Daytime Temperature	33^{o}C	(Alves and Schmid, 2014)

6 Process Model

6.1 Block Flow Diagram

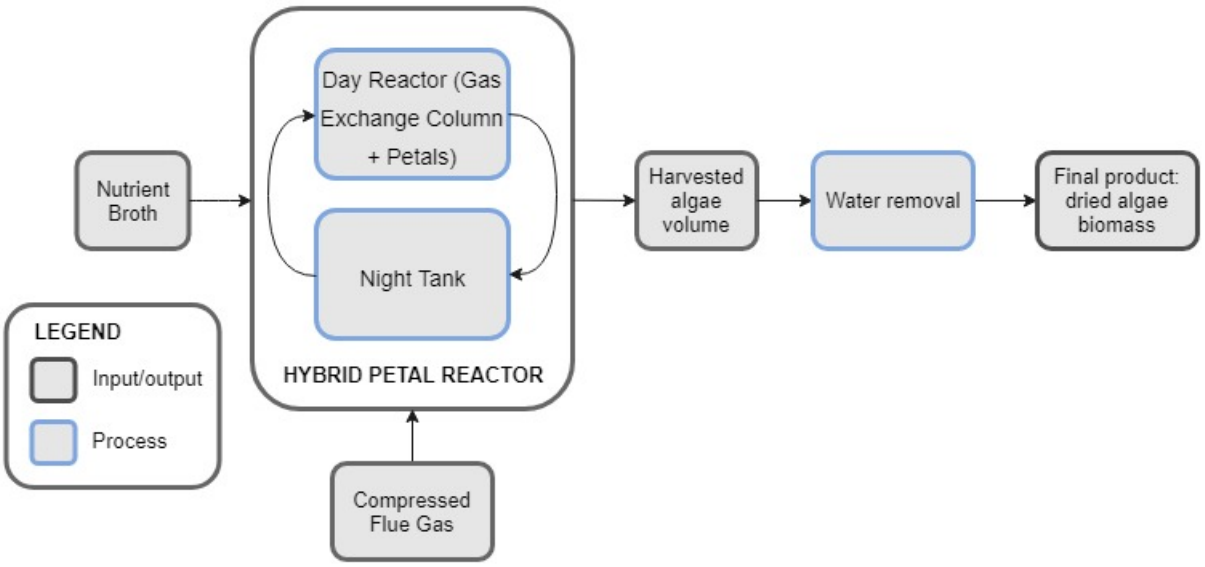

Figure 6.1: The Block Flow Diagram for this process. The algae growth reactors are supplied with nutrients and freshwater, as well as flue gas. They are grown during eight peak sunlight hours in the daytime outdoor horizontal tubular "Petal Reactor" setup and transferred to the night tank for cell density maintenance during the sixteen hours of night. During the day, the algae are continuously harvested and sent for post-processing to remove water.

6.2 Overall Process Flow Diagrams

Process flow diagrams for both the daytime and nighttime processes are shown on the following pages.

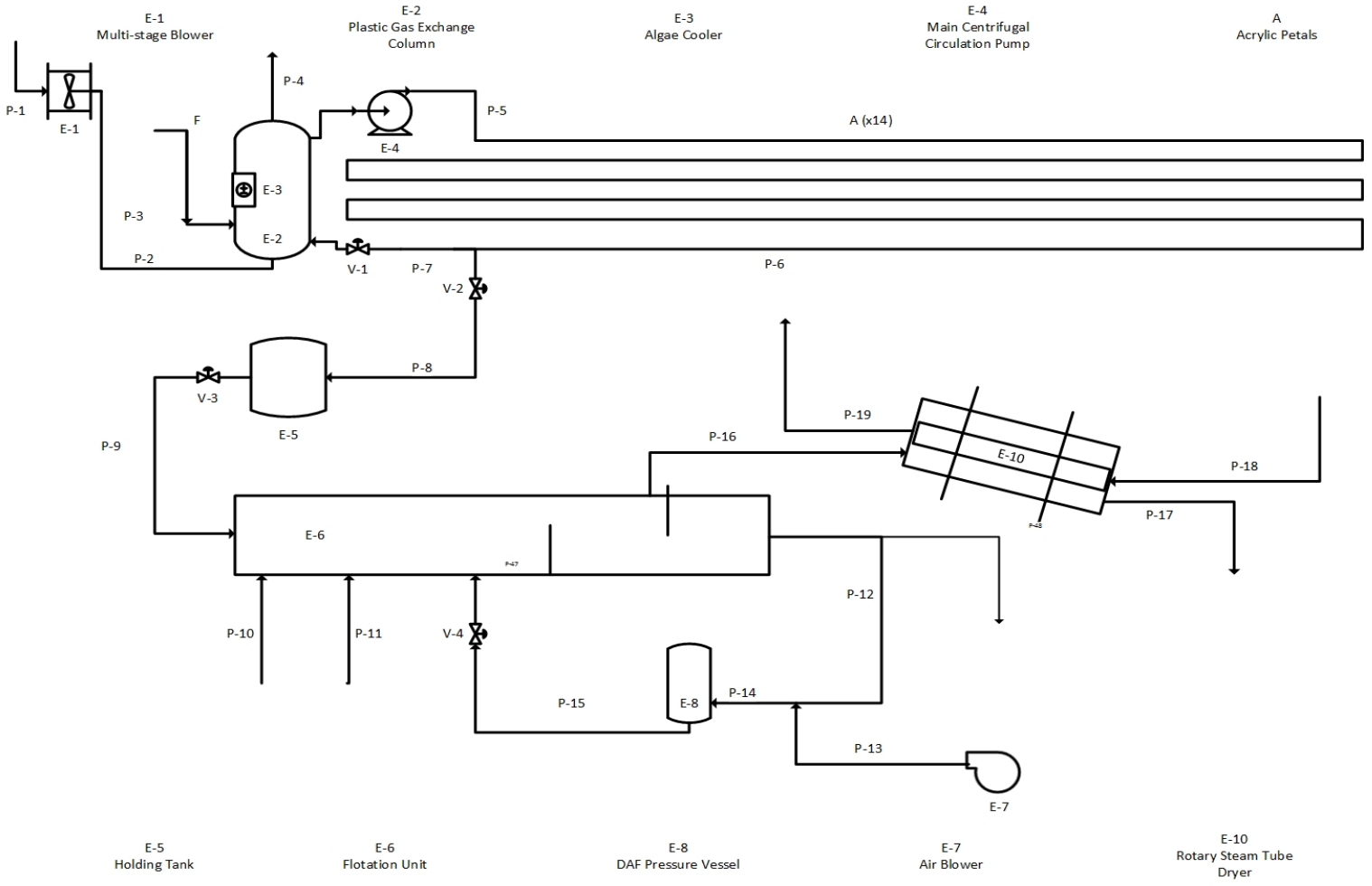

Figure 6.2: Overall process flow diagram for the daytime algae production process

Stream	P-1	P-2	P-3	P-4	P-5	P-6	P-7
Temperature (°C)	200	27	27	30	30	31.4	31.4
Pressure (bar)	1.013	1.405	1.013	1.013	1.326	1.013	1.013
Mass Flow (kg/h)	-	-	-	-	-	-	-
Volumetric Flow (m^3/h)	141.125	141.125	2.71296	134.0688	24.8616	24.8616	24.52248
Stream Components (kg/m^3)							
Chlorella	0	0	0.0	0	1.663	1.663	1.686
CO_2	0.113334	0.15716	0		0.065105	0.065105	0.022963

Stream	P-8	P-9	P-10	P-11	P-12	P-13	P-14	P-15
Temperature (°C)	30	27	27	27	27	27	27	27
Pressure (bar)	1.013	1.013	1.013	1.013	1.013	1.013	1.013	1.013
Mass Flow (kg/h)	-	-	0.0592	0.2671	-	-	-	-
Volumetric Flow (m^3/h)	2.71296	1.48	-	-	0.7432	1.7	0.79	0.79

Stream	P-16	P-17	P-18	P-19
Temperature (°C)	27.0	100.0	160.0	111.4
Pressure (bar)	1.013	1.013	1.5	1.5
Mass Flow (kg/h)	39.005	39.005	44.897	44.897
Volumetric Flow (m^3/h)	0.4744	-	-	-
Vapor Fraction	0	0.9290	1	0.0997
Moisture Content (wet basis)	0.936034	0.09907	-	-
Dried Algae (kg/hr)		2.495		

Figure 6.3: Overall material balances for the process

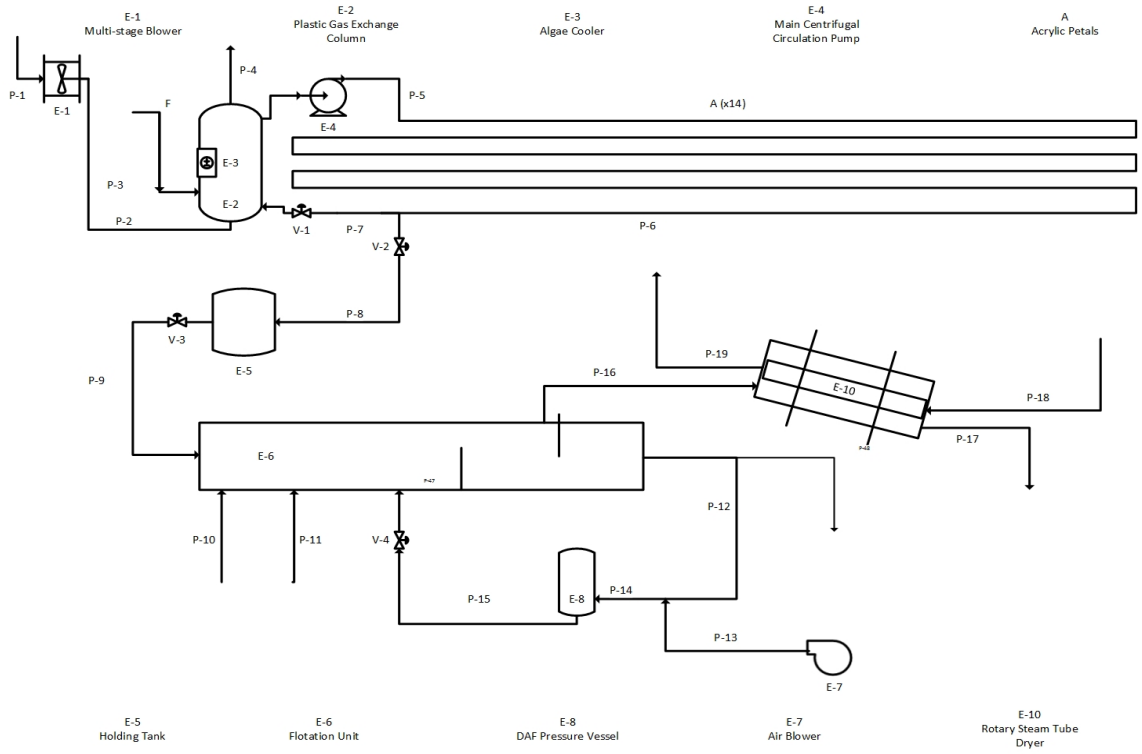

Figure 6.4: The process shown above depicts the entirety of the daytime algae growth process. Flue gas from the connected power plant flows through a multi-stage blower (E-1) to increase pressure for both transport from the plant and bubbling through the gas exchange column (E-2). The buildup of temperature in the system due to incident sunlight is mitigated by a cooling coil run through the tank (E-3). The CO_2-saturated growth media flows out the top of the tank, through the main circulation pump (E-4), to one of thirteen petals in direct sunlight (a fourteenth petal will be out of operation for cleaning at any given time). These petals run back to the base of the gas exchange column. Just prior to reentry of the column, the contents of the petals are combined, and a small portion is harvested for algae removal (stream P-8). The harvested slurry is sent to a holding tank (E-8), which accumulates volume during the day to be depleted overnight. This is required because the harvesting operation is continuous over the course of 24 hours, but the grown algae is only harvested during daytime hours. Flow from this tank is metered into the flotation unit (E-6), where the additions of NaOH and $MgSO_4$ occur. Recycled growth media is saturated with pressurized air (E-8) and sent through a pressure release valve (V-4) to facilitate the bubbling required for flotation. Algae cake is skimmed from the top of the flotation unit and sent to the rotary steam tube dryer (E-10) flowing opposite low pressure steam (P-18) to bring the biomass to the required moisture content

6.2.1 Nighttime Tank Process Flow Diagram

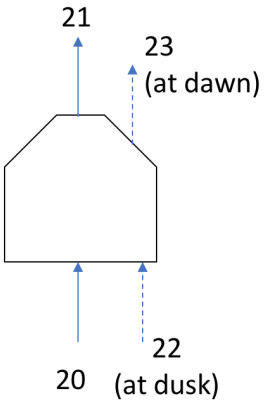

Figure 6.5: Process flow diagram for the nighttime tank.

Stream	Description	Flow Rate
20	Air In	9.1 m^3/min
21	Air Out	9.1 m^3/min
22	Algae Feed (at dusk)	1.5 m^3/min
23	Algae Exit (at dawn)	1.5 m^3/min

Table 6.1: Stream properties for the nighttime tank process.

7 Process Descriptions

The following sections detail the individual elements of the process, including the hybrid reactor set-up, the nutrient storage and delivery system, the harvesting and post-treatment system, and the nighttime lighting configuration. Detailed process diagrams and narrative descriptions are presented. Refer to Section 8 for simulation calculations, Section 9 for optimization algorithms, and Section 10 for equipment specification information.

7.1 Hybrid Petal Reactor

Figure 7.1 presents a schematic of the Hybrid Petal Reactor in which the algae are continuously cultivated. During the daytime operation (eight peak sunlight hours in a 24-hour period), the cultivation volume is circulated between the central Gas Exchange Column (GEC) and external "Petals". A Petal is a length of horizontally inclined acrylic tubing that branches out from the GEC, carrying the algae cultivation volume through the tubing, before returning into the GEC. The Petals are designed to receive incident sunlight as a source of lighting. To achieve the specified carbon sequestration goals of this project, 13 Petals of length 304m and inner area 0.02303m2, extending from the GEC, are required.

In the GEC, both CO_2 transfer into the volume and O_2 transfer out of the volume occurs by way of compressed flue gas sparging at the base of the column. The sparging action also serves to mix the cultivation volume in the column. Exhaust gas leaves from a mesh-protected exit port at the top of the column. A central pump is employed that draws liquid from the top of the column through a central distribution line for distribution into and through the Petals. Before re-entry into the GEC, a fraction of the total flow is taken off for harvesting. Lost fluid to harvesting is replaced continuously with fresh nutrient broth. The harvesting rate (dilution rate) is set to match the average specific growth rate of the algae, in order to maintain constant cell density and constant volume in the system. The harvested volume is collected from the section of the Petal tubing right before re-entry into the GEC to ensure that the algae have had the most time possible to consume CO_2 and accumulate biomass before being harvested. Throughout the Petal tubing are small bubble release vents; though oxygen transfer occurs in the GEC, oxygen bubbles build up in the tube once the liquid reaches saturation, therefore necessitating these release vents. CO_2 loss from the cultivation volume into the air through these oxygen bubbles was determined to be negligible, as described in Section 8.1.2.

After the eight hours of daylight operation, the total cultivation volume is collected and drained into the underground nighttime tank, where sparged air with a small amount CO_2 required for cell density maintenance provides mixing in the tank. LEDs and fibre optic light pipes are used to internally light the tank (see next section). After nighttime operation, the central pumping line is used to draw the cultivation volume above ground and back into circulation between the GEC and the Petals. The

nighttime tank is cooled to near 27C due to heat conduction to the ground, and no additional cooling of the nighttime tank is required. Refer to Sections 8 and 9 for detailed design parameters, and Section 10 for equipment specifications.

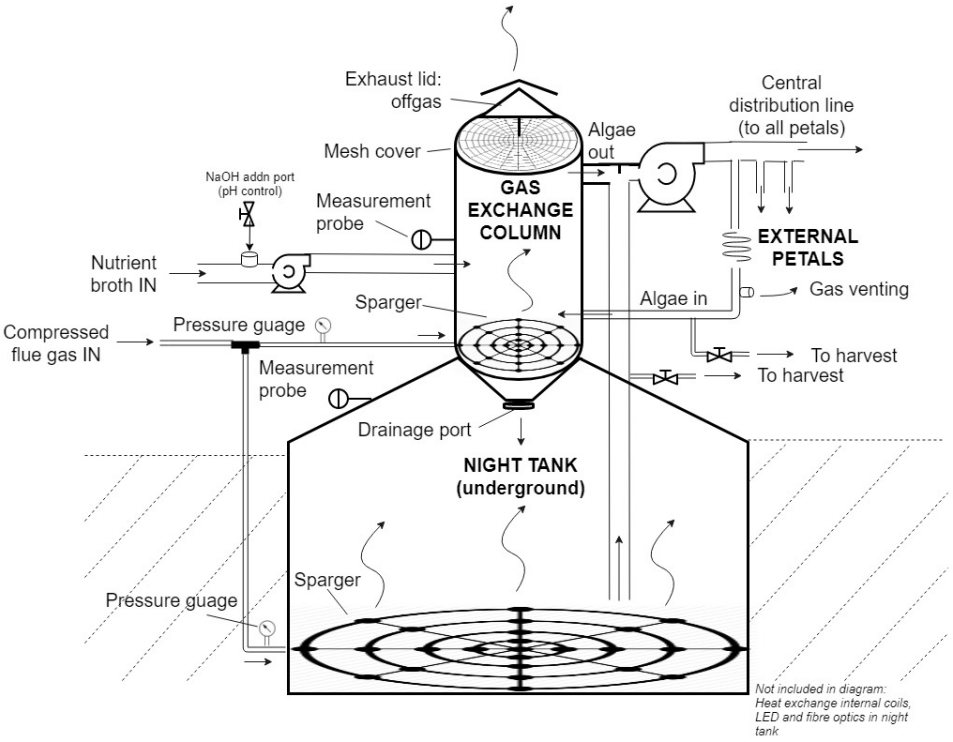

Figure 7.1: Diagram of the Hybrid Petal Reactor setup (not to scale). Only one petal input/output branching port is depicted here, for clarity. All petals will branch outward from the central distribution pumping line, labelled here, and return into the bottom of the bubbler.

7.2 Plant layout

The system is designed to be retrofit to a power station, potentially the Porto do Pecém power station, allowing for easy access to the flue gas from the power plant. There is adequate land available for the pilot plant, as well as opportunity for further expansion. There are also adequate transportation routes in and out of the area. Figure 7.2 shows satellite images of the Porto do Pecém power station and surrounding region.

Figure 7.2: Satellite images of the Porto Do Pecem Power Station in Ceara, Brazil. Obtained using Google Maps.

This scale of the Hybrid Petal Reactor consists of one central gas exchange column with the ability to attach up to 16 petal branches of length 304m each. Though only 13 are required to meet the goals of this design, the option to rotate out petals for maintenance, add more petals, or configure the specific petal configuration to suit customer space needs is desirable. The total area of the 16-petal lay out is 1615m2. The layout of the petals was designed to minimize space requirements give the following set of practical and cost restraints:

- All tubes must leave the bubbler and return after 304m of length.
- Pipe fittings and number of pipe fittings should be chosen to keep added equivalent length of fittings below 20% of the total tube length.
- There should be negligible overlapping of tubes in order to mitigate shading.
- Adjacent pipe lengths should be a minimum of 10cm apart.
- There should be space for periodic walkways for access by operators.
- Tube sections should not be unreasonably small or large.

Figure 7.3 depicts the chosen spacing and elbow configurations.

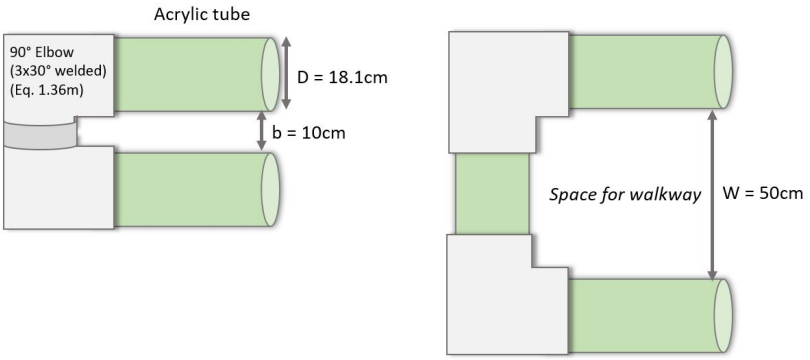

Figure 7.3: Spacing for 90 degree pipe fittings for reversing the tube direction. Most loops adopt a 10cm gap, except for some loops that have a 50cm gap to allow for space to walk through the tubes.

The 16-petal layout (Figure 7.4) involves 4 quadrants containing 4 petals of slightly different dimensions each, depicted below respectively as quadrants "I" through "IV" and petals "A" through "D". The gas exchange column is located at the origin between the quadrants. Table 7.1 lists the specific dimensions referred to in Figure 7.5. In the individual petal figures, the GEC is pictured at the bottom left.

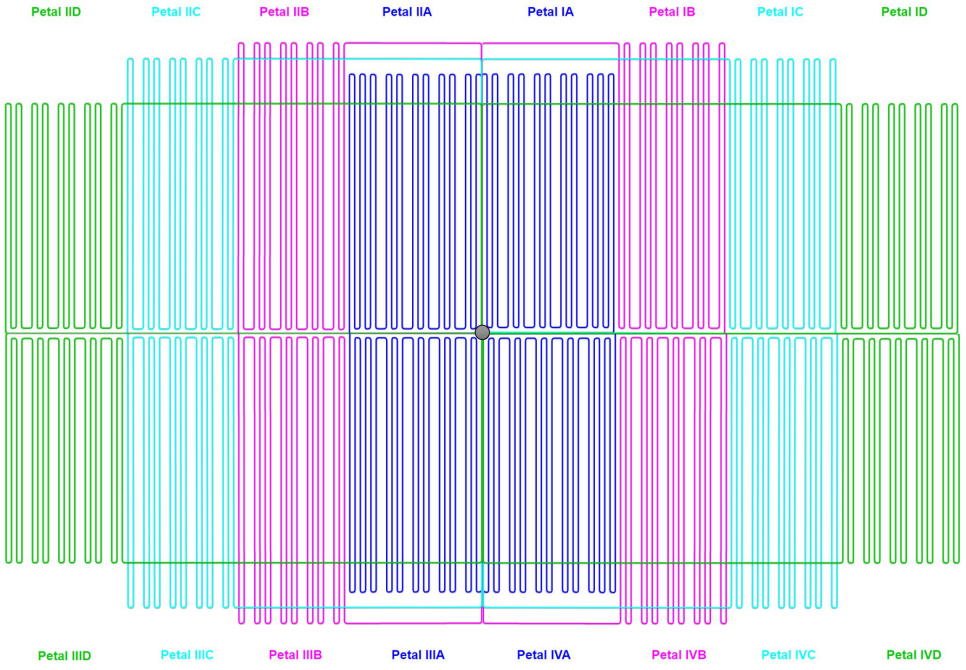

Figure 7.4: The petals will be laid out in 4 quadrants each containing 4 petals of slightly different dimensions, depicted as quadrants "I" through "IV" and petals "A" through "D".

Table 7.1: Dimensions of the Petals corresponding to quadrant location shown in Figure "16-Petal".

Petal type	No. sections	L (m)	p (m)	Total length (m)	Single Petal Area (m2)
A	22	13.0	7.66	303.8	107.2
B	18	14.5	6.54	305.0	101.4
C	18	13.7	6.54	303.7	96.14
D	20	11.6	7.10	304.4	89.46

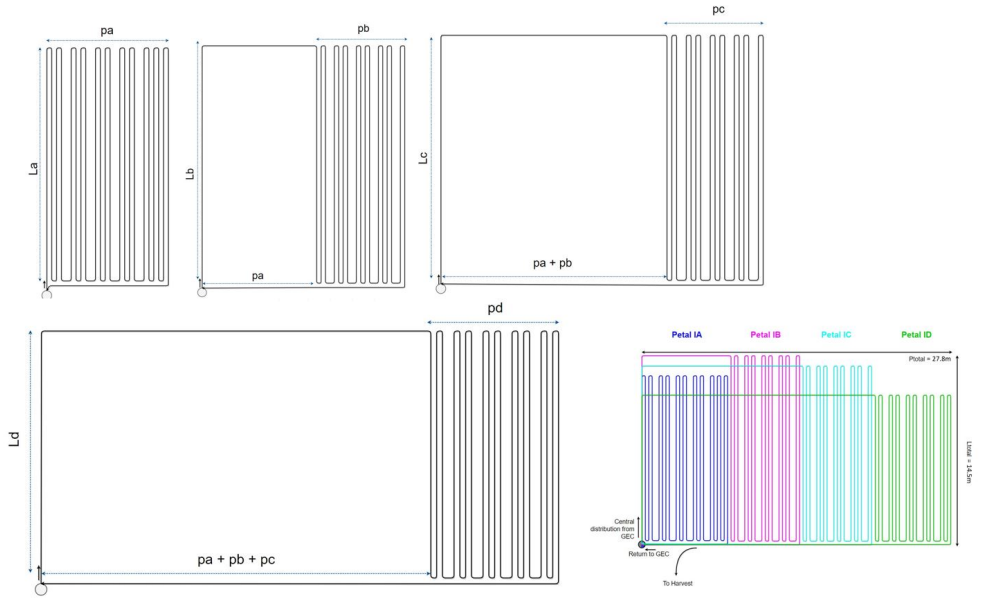

Figure 7.5: Specific dimensions of each petal type.

Figure 7.6 below shows an example of how 14 petals (one additional petal is added so that it can be used to rotate out petals that require maintenance) could be configured. Other process equipment such as gas and water input tubing, controls systems, harvesting holding tanks, or entry port into the underground night tank would be placed in the empty space.

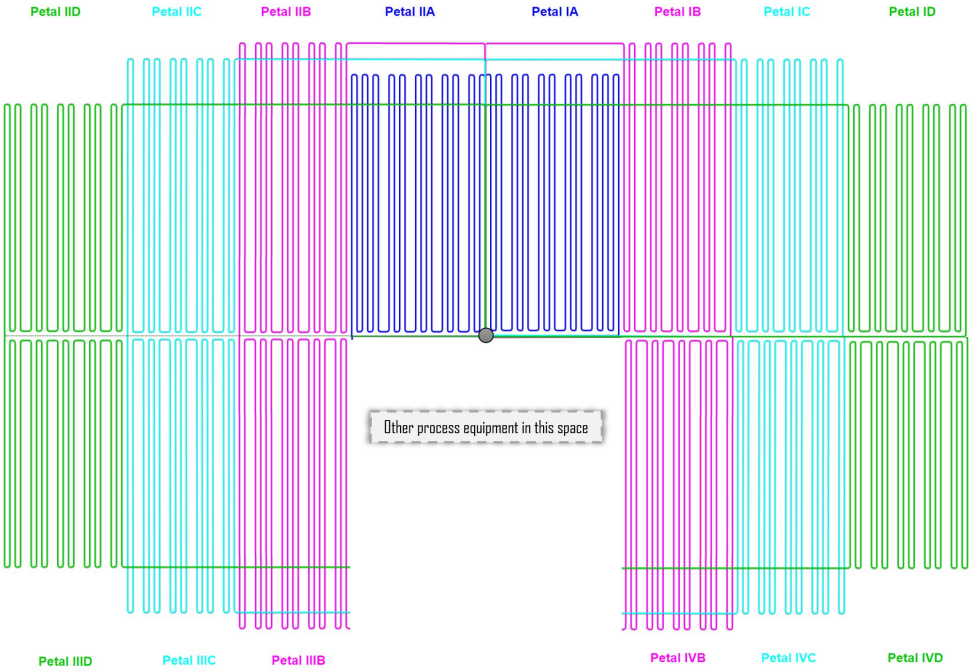

Figure 7.6: A sample layout of 14 petals (13 required for this scale of carbon intake, plus one extra for rotation during maintenance). Other process equipment or service facilities could be placed in the space not being taken up by petals.

7.3 Nighttime Lighting Configuration

The Nighttime tank will be illuminated using LEDs mounted to thin cylindrical optical light guides arranged in an array through the tank. High intensity red and blue LEDs within the photosynthetically active radiation region will be mounted to the base of light pipes, which are designed to distribute light evenly along the pipe length. These light pipes will be arranged in a hexagonal array emerging from the base of the tank, in order to provide even lighting throughout the tank volume. This configuration is shown in Fig. 7.7. The intensity of the LEDs, size and spacing of the light guides was chosen in order to provide the most economical setup to meet the specific growth rate required for the night time biomass productivity goals.

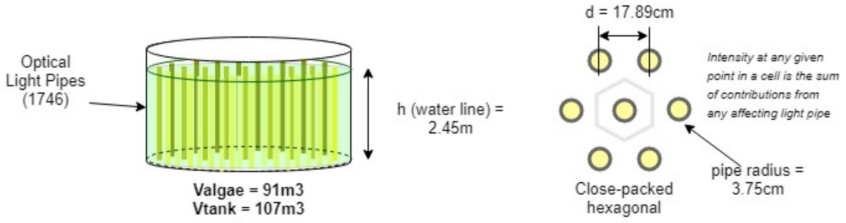

Figure 7.7: Nighttime tank setup with optical light guides spaced throughout tank to provide even light distribution.

Optical light guides allow for a more efficient use of light than conventional lighting methods, and are

less harmful to algae. Using conventional lighting, the required light intensity to provide enough photons necessary for growth would create a large "kill zone" surrounding the source where the intensity is too bright and the temperature too high for the algae cells to withstand. Furthermore, the use of specially designed light guides where light diffuses uniformly through the tube tank allows for more of the tank volume to receive light of intensity within the optimal range. This allows for a reasonable desired growth rate to be met given good mixing of the volume.

In this design, it was desired to provide the algae with sufficient light to maintain healthy cultures and daytime level cell densities throughout the night, while using as little electricity as possible. The daytime photobioreactor is designed to meet the entire daily growth requirements during the eight daytime hours, and so only as much light as is necessary to avoid a drop in cell density overnight is provided in the night tank. This biological requirement dictates that the algae must spend at least 10% of their time exposed to light (light/dark ratio $> 1/9$). The minimum light intensity for a portion of algae solution to be considered 'exposed to light' is an amount high enough for algae to carry out growth. This value is approximated as the light intensity needed to achieve a growth rate of at least 1% of μ_{max}. An optimization procedure (described in Section 9) was used to choose the diameter and spacing of light guides, and the number of LEDs mounted to each guide, in order to minimize the annual cost of the the nighttime tank and lighting system under the given biological constraints. The results of this optimization are shown in Table 7.2, and the detailed method used for the optimization is described in Section 9. This design ensures that greater than 10% of the tank volume is exposed to light, given adequate mixing. Air is sparged through the tank at a low rate to ensure adequate mixing.

Table 7.2: Nighttime Tank size and Lighting Setup. Empty volume refers to the tank volume minus the volume occupied by the light guides.

Tank Volume	107 m^3
Tank Height	2.45 m
Tank Diameter	7.46 m
Empty Volume	91 m^3
Light Guide Spacing	17.9 cm
Number of Guides	1476
LEDs per Guide	2

Note that the Empty Volume listed in Table 7.2 is the volume of the tank that is not occupied by the light guides. Additionally, although 2 LED mounts will be installed on each guide, only 55% power will be supplied to the mounts during typical operation. This lower power setting is sufficient to provide enough light to meet the light/dark ratio requirement, but the supplied power can be increased if higher growth rates are desired.

Figure 7.8 below depicts the LED mount setup on the base of the light pipe. The LEDs will be blue and red in color, optimized for the Photosynthetically Active Radiation range that is considered to be

the most efficient use of energy for microalgal growth. If higher growth rates are desired, many more LED mounts could be added to the light pipes.

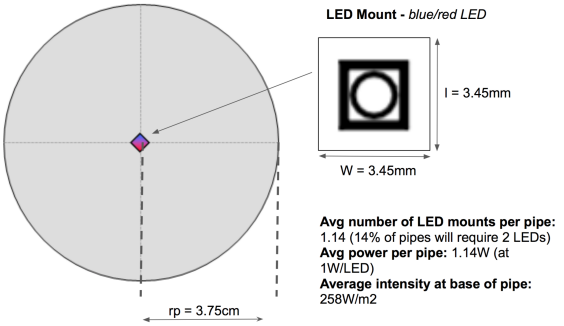

Figure 7.8: LED mounting setup on end of light guide.

7.3.1 Design and Manufacture of Light Guides

The light guides are manufactured from a Poly methyl methacrylate (PMMA) core surrounded by a Polytetrafluoroethylene (PTFE) cladding. PTFE and PMMA have indices of refraction of 1.36 and 1.489, respectively. The inner surface of the PTFE will be roughened to extract light from the core to be dispersed outside of the pipe. The surface will be roughened in a particular non-uniform way that causes light to evenly distribute along the length of the guides; the specifics of this process are described in a 1998 patent [3M, 1998]

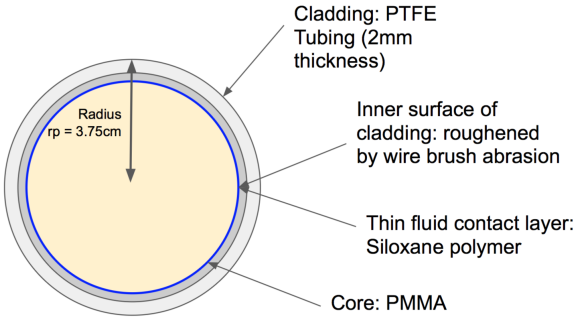

Figure 7.9: Cross-section of light guide showing layered structure.

Roughening will be performed by securing the hollow PTFE pipe to a mount and inserting a rotating wire brush through the tube, slowing the velocity of travel through tube by a set amount as length increases, in order to create more roughening.

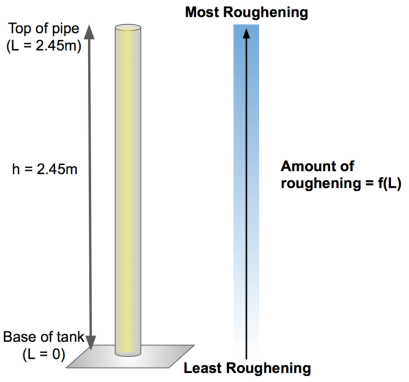

Figure 7.10: Illustration of the degree of roughening to achieve uniform light distribution

7.4 Nutrient Storage and Delivery

Bulk chemicals will be restocked monthly. The chemical storage unit was designed to be large enough to store monthly chemical requirements for the BBM formula. It will be enclosed and sectioned off from sources of contamination. Fresh concentrated stock solutions will be made up for each component once every two days, so as to mitigate the risk of contamination in the stock solutions. Standard sterilization procedures will be employed for all equipment involving nutrient storage, preparation, and delivery. Peristaltic pumps will be used to inject stock solution into the freshwater supply stream, as shown in Figure 7.11. Mixing of the stock solution into the freshwater will occur by turbulent flow before reaching the reactor input. This broth-water supply enters the reactor continuously at a flow rate equal to the harvest rate of the algae (which is in turn equal to the growth rate), in order to maintain constant cell density and volume. Refer to Section 10 for detailed equipment specifications.

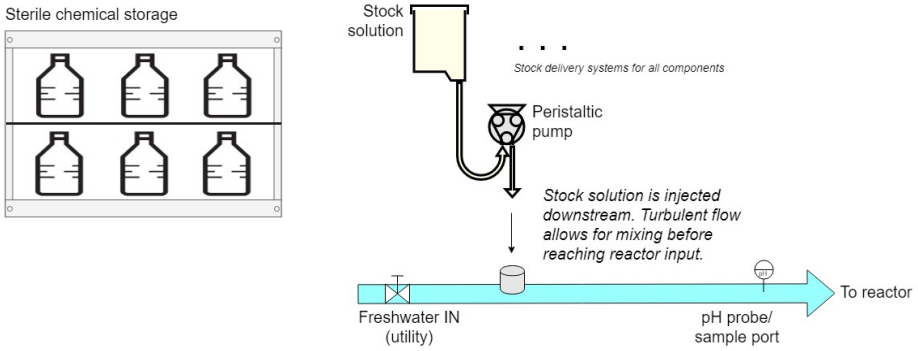

Figure 7.11: The nutrient stock solutions are injected into a turbulent input stream of freshwater before being sent to the reactor.

7.5 pH Control

Dissolved NO, NO_2, SO_2, and CO_2 in the algae solution react with water to form acids that can lower pH to harmful levels if not properly controlled. In order to maintain a neutral pH in the photobioreactor, NaOH is added to the fresh water input (stream 3) at a rate determined by a control system, with a set-point pH of 6.5.

The quantity of NaOH needed to neutralize the CO_2 can be calculated as follows:

$$\frac{[H^+][HCO_3^-]}{[CO_2]} = K_a \tag{7.1}$$

where $K_a = 4.45 \times 10^{-7}$ and square brackets "[ ]" denote concentration. The CO_2 concentration in the bubbler with no pH control would be 3.36×10^{-2} mol/l, therefore the CO_2 concentration with pH control is given by

$$[CO_2] = 3.36 \times 10^{-2}\text{mol/l} - [H^+] - [NaOH] \tag{7.2}$$

because 1 mole of NaOH neutralizes 1 mol of carbonic acid, which forms from 1 mol of CO_2. Similarly,

$$[HCO_3^-] = [H^+] + [NaOH] \tag{7.3}$$

Inserting Eqs. 7.2 and 7.3, Eq. 7.1 and solving for $[NaOH]$, and neglecting the negligible term $[H^+]^2$ yields

$$[NaOH] = \frac{1.49 \times 10^{-7}\text{mol/l}}{[H^+] + 4.45 \times 10^{-7}\text{mol/l}} \tag{7.4}$$

With a target $[H^+]$ of $10^{-6.5}$, the required [NaOH] input to neutralize the CO_2 is 11.1mol/hr.

Due to the complex chemistry of NO, NO_2, and SO_2 in water, a precise calculation of required NaOH input was not feasible. Instead, an upper-bound on the NaOH requirement to neutralize these components was estimated. If it is assumed that all NO, NO_2, and SO_2 react with water to form acid, and that the acidic H+ dissociates completely for each species, the required rate of NaOH input is equal to sum of the rates of mass transfer into solution for NO, NO_2, and SO_2. This quantity is given by the process simulation (described in Section 8) to be 0.73mol/hr. Thus, the total NaOH requirement is 11.8mol/hr.

7.6 Harvesting and Post-Processing

Figure 7.12 depicts the three process steps required to dewater and dry the wet algae to produce a viable biomass product. The first of these, flocculation, focuses on the clumping of the microalgal cells dispersed through the medium. Algae cells in medium have a negative surface potential, causing them to repel each other naturally when in solvent. Chemical flocculation seeks to mitigate the repulsive effects of these charges in such a way that the cells prefer to aggregate in the liquid. For the proposed process, pH-induced chemical flocculation with magnesium will be used. Once the biomass has left the reactor

via the harvesting port, epsom salts (MgSO4) will be added to reach a dissolved Mg2+ concentration of 1.5mM. Immediately after, enough sodium hydroxide is added to raise the medium to a pH of 11. At this higher pH, magnesium precipitates, occasionally as cationic particles (Vandamme, 2011). These positively charged particles form a double layer about the surface of the algal cells, reducing the repulsive forces until they are on the order of the van der Waals attractions between the cells. DLVO (Derjaguin, Landau, Verwey, and Overbeek) Theory states that these forces are superimposed, causing the cells to aggregate at a distance apart at which the repulsive and van der Waals forces are balanced and potential energy between the cells is at a minimum (Derjaguin, Landau, 1941); (Verwey, Overbeek, 1948).

Once the cells have aggregated, the second process step, dissolved air flotation (DAF), brings the flocs to the surface for skimming. During DAF, water saturated with air is sent into the algal medium, with a pressure release valve causing air to be released as it enters. The flocs adhere to the bubbles and are pushed to the to surface, where they remain due to their relatively low density. The flocs can then be easily skimmed, while a portion of the wastewater is recirculated to a pressure vessel to be resaturated with compressed air. Flocculation alone is typically attributed to approximately 85 percent biomass recovery (Zhang, 2016); however, with a second dewatering step yields are improved significantly, in some cases as high as 95 to 98 percent (Sim, 1988).

To remove the remaining water from the biomass, more rigorous separations must be used. The proposed rotary steam tube dryer makes use of the high latent heat of steam as it condenses to efficiently transfer heat to the algal paste to evaporate the remaining water. Low pressure steam at 1.5 bar and 160 degrees Celsius will be run through a bundle of inner tubes 15 feet long and six inches in diameter. The algal paste will enter the shell and run countercurrent to the steam. Both the shell and tube will be rotated to encourage evaporation as well as move the algae along the dryer, as its pitch will allow the algae to exit via gravitational forces. A schematic is shown below in Figure 7.12. The drying process was modeled as a heat exchanger using Aspen Plus; a description of the setup and results are presented in Section 8.2, and detailed information about the simulation is included in Section A.3 of the Appendix.

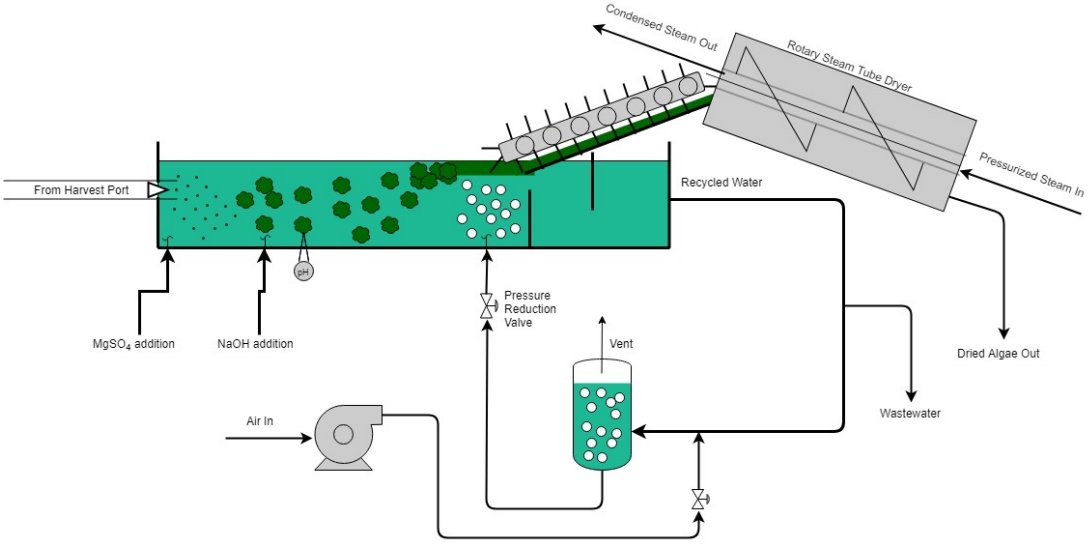

Figure 7.12: Downstream algae biomass dewatering and drying process.

8 Design Calculations and Process Simulation

8.1 Simulation of Photobioreactor

The daytime photobioreactor has two primary process elements: the bubbler, in which CO_2 is transferred from rising flue gas bubbles to the algae solution, and the petals, which are transparent tubes in which algae are exposed to sunlight. This setup is shown in Figure 8.1. In the liquid leaving the bubbler (stream 5), the CO_2 concentration is high and the algae concentration is at a set-point level maintained by control of streams 3 and 8. As the liquid from stream 5 moves through the tubes, the algae use energy from sunlight to photosynthesize, converting CO_2 into O_2, H_2O, and biomass. By the end of the petal tube (streams 7 and 8), the algae concentration has risen and CO_2 has fallen. A portion of this flow is redirected to the flocculation process for post treatment (stream 8). The flow rate of stream 8 is set such that the algae flow rate (kg/s) out of the bubbler through stream 5 is equal to flow rate into the bubbler through stream 7. The flow rate of stream 3 is set equal to the flow rate of stream 8 to replenish the removed liquid and to bring fresh nutrients into the system.

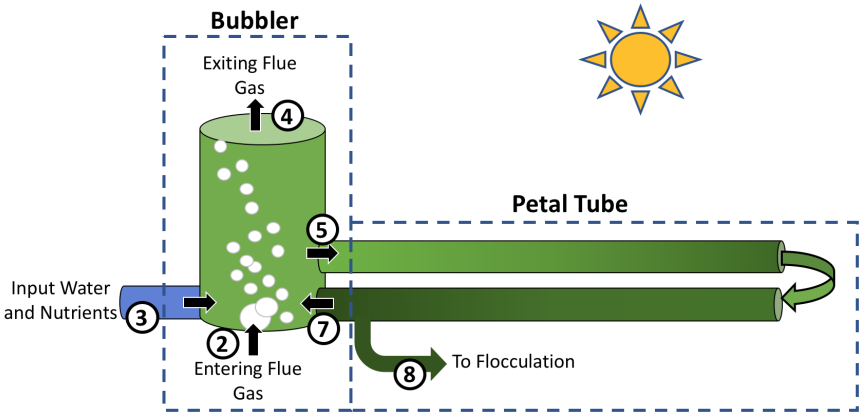

Figure 8.1: Schematic of the daytime photobioreactor. The two process elements, bubbler and petal tube, are outlined with dotted lines. The pilot plant has 13 identical petal tubes and one central bubbler.

In the first two sections that follow, the design of each process element is described independently. For each process element, the input streams are treated as given. Of course, the two process elements are coupled in that the output of one is an input to the other; thus, self-consistent mass balances are required in which the calculated output of one is equal to the expected input to the other. In the section 8.1.3, an iterative procedure to find such a self-consistent solution is described. The result is a procedure, which has been automated in Matlab, to calculate all stream properties given 4 input parameters: the cross sectional area of the petal tubes (A), the length of each petal tube (L), the algae concentration in the bubbler (X), and the flue gas flow rate through the bubbler per petal tube (F_2). It is desirable to have high flue gas flow rates to maximize the concentration of dissolved CO_2 for algae to consume. However, our prescribed CO_2 sequestration rate of 50% puts an effective upper bound on F_2 because excessively

high flue gas flow rates lead to high CO_2 concentrations in the liquid which lead to an insufficient driving force for CO_2 transfer into the liquid. Thus, F_2 is set to ensure a CO_2 sequestration rate of $52\% \pm 1\%$, given values for L, A, and X. The method for selecting F_2 to meet this constraint is then described. The result is a procedure, again automated in Matlab, for the complete process simulation that meets all production and sequestration requirements, given the input parameters L, A, and X. In section 9, an optimization method is developed to select the values for L, A, and X that maximize profits per tube. The Matlab code that conducts the procedures described in this section is given in Appendix A.1.

In the following sections, the notation F_n and C_i, n is used to refer to the volumetric flow rate of stream n and concentration of component i in stream n for streams 2 through 8 depicted in Fig. 8.1 and components CO_2 and O_2.

8.1.1 Bubbler Design

In this section, a model for the mass transfer of CO_2, O_2, NO, NO_2, and SO_2 from the flue gas into the algae solution is described. This model is then used for a mass and energy balance on the system. A more detailed diagram of the bubbler is shown in Figure 8.2.

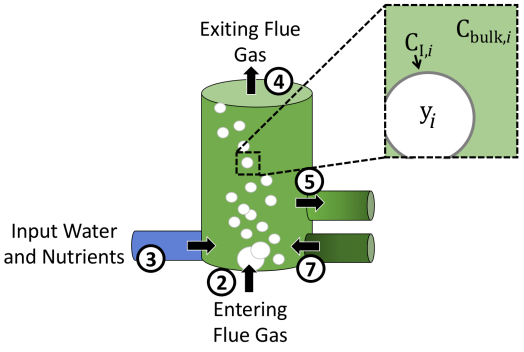

Figure 8.2: Schematic of the bubbler. In the inset depicting mass transfer, $i \in \{CO_2, O_2, NO, NO_2, SO_2\}$. The direction of mass transfer is from gas phase to liquid phase for CO_2, NO, NO_2, and SO_2, and is from liquid phase to gas phase for O_2.

Note that CO_2, NO, NO_2, and SO_2 are transferred from the flue gas into the liquid. O_2, however, is transferred from them liquid to the flue gas due to the high O_2 concentration in the liquid that results from photosynthesis.

Bubbler Mass Balance Several assumptions are made in the mass transfer model. First, C_{Bulk}, the CO_2 concentration in the liquid, is assumed to be constant everywhere in the bubbler. This is likely a good assumption because the liquid will be well-mixed. Second, mass transfer of CO_2 from the gas bulk to the bubble interface is assumed to be fast relative to CO_2 transfer from the interface to the bulk liquid. Thus, mass transfer from the liquid side of the bubble interface into the liquid bulk is treated as

the rate limiting step of mass transfer.

Under these assumptions, the rate of mass transfer is given by

$$\begin{aligned} k_{L,i}a(C_{I,i} - C_{Bulk,i}) &= k_{L,i}a(H_i P y_i - C_{Bulk,i}) \\ &= -\frac{P}{RT}\frac{\mathrm{d}y_i}{\mathrm{d}t} \ . \end{aligned} \tag{8.1}$$

where C_I, the dissolved-gas concentration on the liquid side of the bubble interface, is given by Henry's law (with Henry's Law constant H_i), and $C_{Bulk,i}$ is the concentration of component i in the bulk liquid. The bubbler pressure P is 1 atm and bubbler temperature T is maintained at 30^{o}C with a heat exchanger. The gas transfer coefficients $k_{L,i}a$ are estimated on the following page. This differential equation has the solution

$$y_i(t) = \frac{C_{Bulk,i}}{H_i P} + (y_i|_{t=0} - \frac{C_{Bulk,i}}{H_i P}) \exp(-RTk_{L,i}aH_i t) \ . \tag{8.2}$$

where t is the contact time between the bubble and liquid, and $y_i|_{t=0}$ is the mole fraction of component i in the flue gas. The contact time when the bubbles exit the bubbler, t_{exit}, is estimated from Stokes Law:

$$v = \frac{2(\rho_{H_2O} - \rho_{fluegas})gR^2}{9\mu} \tag{8.3}$$

where R is bubble radius and μ is fluid dynamic viscosity.

These equations are used to perform a mass balance on the bubbler for CO_2 and O_2. The small amount of NO, NO_2, and SO_2 that transfers into solution is partially converted to aqueous $NaSO_3$, $NaNO_2$, and $NaNO_3$ by adding NaOH to stream 3 (NaOH is added for pH control, as described in section 7.5). The NaOH reacts with the acids that form due to reaction of NO, NO_2, and SO_2 with water. These dissolved gases, and the sodium salts, are harmless to algae (Lee et. al., 2002), therefore it is not necessary to perform complete mass balances on these components.

The mass balances for CO_2 and O_2 are given by

$$(y_{CO_2}|_{t=0} - y_{CO_2}|_{t_{exit}})\frac{PF_2}{RT} + C_{CO_2,7}F_7 = C_{CO_2,5}F_5 \ , \tag{8.4}$$

and

$$C_{O_2,7}F_7 = C_{O_2,5}F_5 + (y_{O_2}|_{t_{exit}} - y_{O_2}|_{t=0})\frac{PF_2}{RT} \ . \tag{8.5}$$

Note that in equations 8.4 and 8.5, F_2 is used as bubble volumetric flow rate for the entire bubbler, which implicitly assumes that bubble volume is constant in spite of the mass transfer. However, the volume of transferred gas is a small fraction (less than 5%) of the total flue gas volume, so this is a quite good approximation.

In equations 8.4 and 8.5, $y_{CO_2}|_{t_{exit}}$ and $y_{O_2}|_{t_{exit}}$ are substituted with Eq. 8.2 evaluated at t_{exit}. The resulting equations can then be solved for the bubbler outlet concentrations $C_{CO_2,5}$ and $C_{O_2,5}$, which yields

$$C_{CO_2,5} = \frac{(y_{CO_2}|_{t=0})(\exp(-K_{CO_2}t_{exit}) - 1) - C_{CO_2,7}F_7\frac{RT_{bub}}{PF_2}}{\frac{\exp(-K_{CO_2}t_{exit})-1}{H_{CO_2}P} - \frac{RT_{bub}}{PF_2}F_5} \tag{8.6}$$

where $K_{CO_2} = PH_{CO_2}k_{L,CO_2}aRT_{bub}$, and

$$C_{O_2,5} = \frac{(y_{O_2}|_{t=0})(1 - \exp(-K_{O_2}t_{exit})) + C_{O_2,7}F_7\frac{RT_{bub}}{PF_2}}{\frac{1-\exp(-K_{CO_2}t_{exit})}{H_{O_2}P} + \frac{RT_{bub}}{PF_2}F_5} \tag{8.7}$$

where $K_{O_2} = PH_{O_2}k_{L,O_2}aRT_{bub}$.

In equations 8.6 and 8.7, F_5 is given by

$$F_5 = Av \tag{8.8}$$

where v is the fluid velocity in the petal tubes and A is the tube cross-sectional area. All other variables are input parameters into the bubbler model.

Equations 8.6, 8.7, and 8.8 give the stream flow rate and composition of stream 5, the bubbler output, as a function of the input stream properties and the model parameter A.

With this model, the fraction of input CO_2 that is sequestered can also be calculated. A requirement of the pilot plant is that at least 50% of input CO_2 be sequestered, so it is essential that the process simulation calculate this value. The CO_2 sequestration fraction is calculated with the following equation.

$$\%\ \text{Sequest.} = \frac{(C_{CO_2,5} - C_{CO_2,7})F_5}{F_2 y_{in}/RT_{bub}} \tag{8.9}$$

where $y_{in} = 0.10$ is the volume fraction of CO_2 in the input flue gas and R is the gas constant.

Sparger Design and Estimation of Mass Transfer Coefficients It is essential that high CO_2 transfer rates are attained in the bubbler to provide the algae with sufficient CO_2 and to meet the 50% CO_2 sequestration goal.

Published data for mass transfer coefficients for CO_2 bubbles rising from a perforated-plate sparger in water at 30^{o}C was obtained (Talbot, 1990). According to this data, bubbles of diameter $d_B > 9.5mm$ have a mass transfer coefficient of $k_{L,CO_2} = 5.32 \times 10^{-4}$ m/s. To obtain the $k_{L,CO_2}a$ value, a is estimated by assuming spherical bubbles, for which $a = 6/d_B$. For bubbles of diameter $d_B = 12.2mm$ (which is the expected diameter, as described in the sparger design section below), this gives a $k_{L,CO_2}a$ value of 0.26 s^{-1}.

The sparger is designed from tubing with 1mm diameter pores from which the flue gas escapes into the bubbler. The sparger contains a total of 1,200 pores, distributed evenly over the sparger surface. In our pilot-scale design described in Section 7, flue gas enters the bubbler at a rate of 63.2 L/s, thus the gas flow rate per pore, $4F_{pore}$, is 53mL/s. Eq. 8.10 can be used to estimate the d_B based on these parameters (Cao et. al., 2009).

$$d_B = 0.19 d_P^{0.48} \Big(\frac{4F_{pore}\rho_{gas}}{\pi d_P \mu_{gas}}\Big)^{0.32} \tag{8.10}$$

where d_P is pore diameter (m), F_{pore} is the gas flow rate through each pore (m^3/s), ρ_{gas} is the flue gas density (kg/m^3), and μ_{gas} is the pore dynamic viscosity (kg/m s). With this correlation, d_B was estimated as 12.2mm, as expected in the previous paragraph.

Bubbler Energy Balance The bubbler temperature is controlled with a heat exchanger connected to a refrigeration unit in order to maintain a temperature of 30^oC, the ideal temperature for algae growth. The temperature of the input streams (streams 2, 3, and 7) are all very near this temperature, but fluctuate due to variations in ambient air temperature. As a result, the required rate of heat removal is low, but the percent change in rate of heat removal with weather fluctuations can be high. Here, an energy balance is performed using unusually high ambient air temperature in order to put an upper-bound to the required rate of heat removal. 306K is used as the ambient air temperature, which is equal to the record monthly highs for most summer months (though due to the plants proximity to the equator, temperatures are fairly constant throughout the year.)

The total rate of heat removal is equal to the amount of heat that must be removed (or added) from streams 2, 3, and 7 to bring them to 30^oC.

$$Q_{Bub} = F_2\rho_2 C_{p,2}\Delta T_2 + F_3\rho_3 C_{p,3}\Delta T_3 + F_7\rho_7 C_{p,7}\Delta T_7 \tag{8.11}$$

The fresh water flow rate (stream 3) is assumed to be an average of 30^oC, but a conservative estimate of 306K (the ambient air temperature) is made here. The entering algae solution from stream 7, calculated using the petal tube model described below, is 32^oC. The entering flue gas temperature (stream 2) is equal to the ambient air temperature of 306K. The flue gas exits the power plant at 200^oC and flows 100m to the bubbler through a 10cm diameter pipe. If plug flow is assumed, the heat transferred from a differential plug in a time dt can be related to the differential change in flue gas temperature dT as follows:

$$dQ \ = hA(T - T_{air})dt = F_2\rho C_p dT \tag{8.12}$$

where ρ and C_p are the flue gas density and specific heat capacity. The thermal resistance of the thin metal duct carrying the flue gas is neglected, and uniform flue gas temperature is assumed due to the turbulent flow ($Re = 6 \times 10^5$). Thus, T represents both the pipe surface temperature and the flue gas temperature. The heat transfer coefficient h is given by

$$h = \frac{Nu\,k}{dL} \tag{8.13}$$

and Nu can be estimated with the following correlation for flow over a cylinder (Incropera et. al., 2003):

$$Nu = 0.3 + \frac{0.62Re_D^{1/2}Pr^{1/3}}{[1 + (0.4/Pr)^{2/3}]^{1/4}}\Big[1 + \Big(\frac{Re_D}{282,000}\Big)^{5/8}\Big]^{4/5} \tag{8.14}$$

where

$$Re_D = \frac{v_{wind}D}{\nu} \tag{8.15}$$

Thus, wind speed v_{wind} has a significant effect on heat transfer rate. Eq. 8.12 can be integrate from $t = 0$ to the pipe residence time $t = Vol/F_2$ to determine the temperature of the flue gas exiting the pipe. For a wind speed of 1m/s (well below the average wind speed of 3.3m/s for the region), then flue gas is cooled to a temperature equivalent, up to at least 4 significant figures, to that of the ambient air. Even with negligible wind, the flue gas is cooled to a temperature only 0.76^{o}C above the ambient air temperature.

With the estimated temperatures of 33^{o}C, 33^{o}C, and 32^{o}C, for streams 2, 3, and 7, respectively, the ΔT values in Eq. 8.11 become 3^{o}C, 3^{o}C, and 2^{o}C, respectively. Inserting these values into Eq. 8.11 yields an upper-bound an cooling requirements of 1.3kW. The heat exchanger used in the bubbler was chosen in order to have sufficient capacity to meet this requirement.

For very low ambient air temperatures, the bubbler temperature is allowed to drop to as low as 288K without harming the algae. However, this temperature is lower than the lowest temperature every recorded in Fortaleza, Brazil. Thus, heating of the bubbler liquid is not expected to ever be required.

On an average day (average daytime mean temperature is 27^{o}C), virtually no cooling is required. Eq. 8.11 predicts that only 0.49kW must be removed from the bubbler. The coefficient of performance for the heat exchange process is estimated to be 3.4, a typical value for small refrigeration units (Commercial Refrigeration). Thus, the energy requirements of running the refrigeration unit on an average day is 0.49kW/3.4=0.15kW. This value is used in our Utilities costing.

8.1.2 Petal Tube Design

To model the petal tubes, plug flow is assumed, and the tubes are divided into differential cross-sections (plugs) on which a mass and energy balance is performed. The model for each differential plug is described below, and this model is used to integrate the mass and energy balances over the length of the tubes to obtain balances on the full system.

Figure 8.3 depicts a generic differential plug in a petal tube.

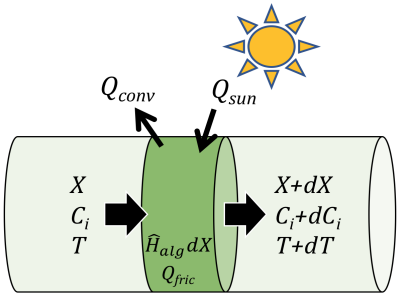

Figure 8.3: Differential plug in a petal tube. X is algae concentration, C_i dissolved gas concentration ($i \in \{CO_2, O_2\}$, T is liquid temperature. Heat enters the plug liquid due to sunlight (Q_{sun}) and frictional heating (Q_{fric}), and exits the plug liquid due to algae growth ($\hat{H}_{alg}dX$). The direction of convective heat transfer (Q_{conv}) is from the petal tube to the ambient air, except in unusually hot weather, when the direction is reversed.

Differential Mass Balances Performing mass balances on the differential plug for C_{CO_2} and C_{O_2} yields the following equations.

$$dX = \mu_{plug} X \tag{8.16}$$

$$dC_{CO_2} = (-Y_{CO_2/X})dX \tag{8.17}$$

$$dC_{O_2} = (Y_{O_2/X})dX \tag{8.18}$$

In equation 8.16, μ_{plug} is an average of the specific growth rate μ_g through the plug volume. μ_g is a function of light intensity, which varies substantially throughout the plug due to light attenuation in the algae solution. μ_g is also a function of C_{CO_2} and C_{O_2} which vary substantially along the length of the tube due to CO_2 consumption and O_2 generation, but the concentrations are treated as constant within each differential plug. The calculation of μ_{plug} is described in the following paragraph. In equations 8.17 and 8.18, $Y_{CO_2/X}$ and $Y_{O_2/X}$ are the amount of dissolved gas (moles) sequestered (for CO_2) or released (for O_2) by the algae per kg algae growth.

Calculation of μ_{plug} and Light/Dark Ratio As discussed in section 4.2.2, the specific growth rate at a given point in the differential plug is given by

$$\mu_g(I, C_{CO_2}, C_{O_2}) = \mu_{max} \frac{I}{K_I + I} \frac{C_{CO_2}}{K_C + C_{CO_2}} \left(1 - \frac{f_{Inhib}(C_{O_2})}{100}\right) \tag{8.19}$$

where

$$f_{Inhib}(C_{O_2}) = -0.0011 \left(\frac{C_{O_2}}{H_{O_2} P}\right)^2 + 0.403 \frac{C_{O_2}}{H_{O_2} P} - 5.40 \tag{8.20}$$

The intensity I at a depth D and concentration X in the tube is estimated with the Beer-Lambert relation as follows:

$$I(D) = I_0 e^{-BXD} \tag{8.21}$$

where the attenuation constant B is $187 m^2/kg$ for Chlorella algae in water (Blanken et. al., 2016). Figure 8.4 shows the light intensity at each point in a cross-section of the petal tube. As expected from

Eq. 8.21, the intensity is highest along the surfaces of the tube facing the sun, and intensity decreases exponentially along paths moving away from the sunlit surface.

To determine the amount of algae growth dX in the plug, an average growth rate over the entire tube cross-section, μ_{plug}, must be calculated. This calculation is done using Eq. 8.22.

$$\begin{aligned}\mu_{plug} &= \frac{1}{A}\int_A \mu_g(I, C_{CO_2}, C_{O_2})dA \\ &= \frac{2}{A}\int_0^R \int_0^{2\sqrt{2Rr-r^2}} \mu_g(I(D), C_{CO_2}, C_{O_2})dD\,dr\end{aligned} \tag{8.22}$$

where R is the tube radius.

In addition, the biological constraint that the light dark ratio (LDR) be at least 1/9 must be considered. The petal tube model calculates the LDR in the following way, in order to check that the process does not break this constraint. First, because the flow in the petal tubes is turbulent, the fraction of time that an algae spends in a given region of the tube is approximately equal to fraction of the tube's volume that the region occupies. With this observation, the LDR requirement reduces to the requirement that at least 10% (i.e. $100\% \times \frac{1}{1+9}$) of the area of the tube cross-section has sufficient light intensity that $\mu_g > 0.01\mu_{max}$. This calculation is performed by the process simulation code, and the value of LDR is reported.

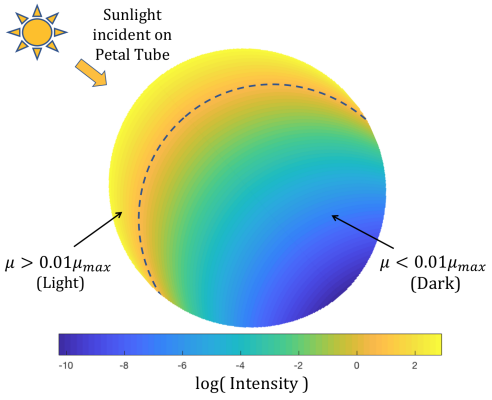

Figure 8.4: Cross-section of petal tube depicting penetration of light into algae liquid. Color indicates log-base 10 of light intensity (W/m^2) at each point in the tube (see colorbar). The dashed line indicates the boundary between light ($\mu > 0.01\mu_{max}$) and dark ($\mu < 0.01\mu_{max}$).

Differential Energy Balances Performing an energy balance on the differential plug yields

$$dT = \frac{1}{C_p \rho dV}(dQ_{sun} + dQ_{fric} + dQ_{conv} - \hat{H}_{alg}dX) \tag{8.23}$$

where T is the liquid temperature in the differential plug, dV is the volume of the differential plug, and C_p is the specific heat capacity (J/m^3K) of the algae solution. C_p is assumed to be equal to the specific heat capacity of water, which is a good approximation because the algae solution is over 98wt% water. dQ_{sun}, dQ_{fric}, and dQ_{conv} are the amount of heat transferred into the plug due to sunlight, frictional

heating, and convective heat transfer with the ambient air, in the differential residence time $dt = dV/F_6$. dQ_{sun} and dQ_{fric} are both greater than 0, and the sign of dQ_{conv} depends on ambient air temperature. $\hat{H}_{alg}$ is the specific enthalpy of algae biomass (J/kg), relative to the photosynthetic reactants CO_2 and O_2 (i.e. it is effectively the heat of combustion of algae biomass). $\hat{H}_{alg}$ is estimated to be 15,000kJ/kg (Orosz and Forney, 2008). This figure captures both the enthalpy of reaction of photosynthesis and of all other metabolic processes in the algae. This approach to the energy balance avoids the need to estimate what portion of sunlight energy is used for photosynthesis and what portion goes to heating the algae solution, which greatly simplifies the task.

Heat input from sunlight is estimated as

$$dQ_{sun} = I D \, dL \, dt \tag{8.24}$$

where I is the intensity of light incident on the petal tube, D is the tube diameter, dL is the length of the differential plug, and dt is the differential residence time.

$$Q_{fric} = dP \, dV \tag{8.25}$$

where dP is the pressure drop across the differential plug due to friction. dP is estimated using the Darcy-Weisbach equation,

$$dP = dL f_D \frac{\rho v^2}{2D} \tag{8.26}$$

where ρ is the liquid density, v is liquid velocity, D is tube diameter, and f_D is the Darcy friction factor. f_D is estimated using the following correlation for smooth pipes in turbulent flow:

$$\frac{1}{\sqrt{f_D}} = -1.93 \log \frac{1.90}{Re\sqrt{f_D}} \tag{8.27}$$

The Reynolds number is given by $Re = \frac{vD}{\nu}$ where ν is the kinematic viscosity of the liquid. For tube diameter used in the final design, $Re = 6.4 \times 10^4$, so the flow is in the turbulent regime. Turbulent flow is important to the design of the petal tubes because it ensure turnover of algae in the lit region of the tube, so that no cells spend extended periods in darkness. ν was approximated as the kinematic viscosity of water, which is a good approximation because the liquid is over 98wt% water. The f_D that solves equation 8.27 was estimated using the *fzero* function in Matlab.

Convective heat transfer to the ambient air is estimated with

$$dQ_{conv} = h(T_{air} - T)\pi D \, dL \, dt \tag{8.28}$$

where T is the temperature of the algae liquid, T_{air} is the temperature of ambient air, and h is the convective heat transfer coefficient. Not that Eq. 8.28 makes the assumption that the temperature of the tube surface is equal to the temperature of the the algae solution. This approximation can be justified by the fact that turbulent flow in the tube keeps the liquid temperature nearly uniform, and the tube walls are quite thin (0.5 cm). The convective heat transfer coefficient h is given by

$$h = \frac{Nu \, k}{dL} \tag{8.29}$$

where k is the thermal conductivity of air and the Nusselt number is estimated using Eqs. 8.14 and 8.15. Typical wind speeds v_{wind} at the plant location are 2 to 4 m/s, and a correlation for the kinematic viscosity of the ambient air as a function of time $\nu_{air} = \nu_{air}(T_{air})$ was developed by fitting a quadratic function to tabulated data. A correlation for the Prandtl number $Pr = Pr(T_{air})$ was also developed by fitting a quadratic function to tabulated data.

Integration of Differential Balances Equations 8.16 through 8.23 can now be integrated over the length of the petal tube to yield complete mass and energy balances for the petal tubes. Algorithm 1 displays the procedure for numerical integration of the mass and energy balances. As shown in the algorithm, the petal tube was partitioned into 500 differential plugs. The numerical integral was tested with convergence with respect to this partitioning, and the outputs of the algorithm were found to be well converged.

Algorithm 1: Numerical Integration of Petal Tube Differential Mass and Energy Balance. The integration was found to be very well converged using by partitioning the tubes into 500 differential plugs. $dVol$ is the volume of a differential plug.

input : X, C_{CO_2}, C_{O_2}, and T at the tube entrance
output: X, C_{CO_2}, C_{O_2}, and T at the tube exit
$O_{2,vented} \leftarrow 0$
for *step* $\leftarrow$ *(1,2,...,500)* **do**
  $X \leftarrow X + dX$
  $C_{CO_2} \leftarrow C_{CO_2} + dC_{CO_2}$
  if $C_{O_2} < H_{O_2}P$ **then**
    $C_{O_2} \leftarrow C_{O_2} + dC_{O_2}$
  else
    $O_{2,vented} \leftarrow O_{2,vented} + (dC_{O_2})(dVol)$
  end
  $T \leftarrow T + dT$
end

In Algorithm 1, the differential changes in concentrations and temperature are given by Eqs. 8.16, 8.17, 8.18, and 8.23. Note that the O_2 balance in Algorithm 1 accounts for the possibility that the algae solution becomes saturated with O_2. In this case, the O_2 produced by the algae bubbles out of solution and is released through vents placed every 3 meters along the tubes (no vents are placed in the first 95m of each tube because the liquid is not yet saturated in O_2, as discussed in the following paragraph. Algorithm 1 tracks the total amount of vented O_2 through the $O_{2,vented}$ variable. As the bubbles form, some CO_2 enters the gas phase as well and exits through the vents. This process is described in the following subsection.

The result of Algorithm 1 is a procedure which calculates the properties of the tube output (stream 7) from the properties of the tube input (stream 5), and the model parameters L and A.

O_2 and CO_2 Venting As O_2 bubbles form in the petal tubes, some dissolved CO_2 will enter the gas phase bubbles as well. This CO_2 is then vented from the system along with the O_2. It is essential that only a small portion of the CO_2 that enters the petal tubes is vented, in order to keep growth rates and sequestration fraction high. The rate at which O_2 is vented from each vent, calculated by tracking the $O_{2,vented}$ variable in Algorithm 1, is shown in Figure 8.5.

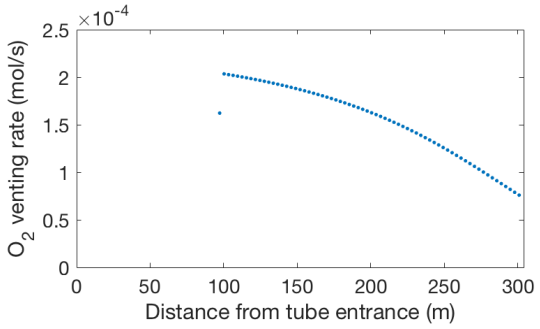

Figure 8.5: Rate of O_2 venting at each vent along length of petal tubes. Vents are not placed for the first 95m, where no O_2 bubbles form because O_2 concentration is lower than the saturation concentration.

The total rate of O_2 venting for an entire petal tube is 10.5mmol/s. The rate at which CO_2 is vented is lower than the rate at which O_2 is vented by a factor of $H_{O_2}/H_{CO_2} = 0.038$, thus CO_2 is vented at a rate of 0.40mmol/s. This rate is 1.7% of the rate at which dissolved CO_2 enters the petal tube, thus CO_2 loss through the O_2 vents is not a significant concern.

8.1.3 Iterative Approach to Self-Consistent Mass and Energy Balances

Section 8.1.1 describes the procedure to calculate stream 5 properties using stream 7 properties and other model parameters. Section 8.1.2 describes the procedure to calculate stream 7 properties using stream 7 properties and other model parameters. There exists a set of properties for the two streams for which each procedure outputs the stream properties that the other procedure takes as an input; this set of properties is the self-consistent solution to the mass and energy balances on the photobioreactor.

Algorithm 2 describes an iterative procedure that converges to the self-consistent solution.

Algorithm 2: Iterative procedure to find the self-consistent mass and energy balances for the photobioreactor.
input : L, A, X, and F_2
output: Stream Properties for streams 5, 7, and 8
$C_{CO_2,5} \leftarrow H_{CO_2}P$
$C_{O_2,5} \leftarrow H_{O_2}P$
while *Change in concentrations from previous iteration are sufficiently large* **do**
  $C_{CO_2,7}$, $C_{O_2,7}$, $F_7 \leftarrow$ TubeModel($C_{O_2,5}$,$C_{CO_2,5}$)
  $C_{CO_2,5}$, $C_{O_2,5} \leftarrow$ BubblerModel($C_{O_2,7}$,$C_{CO_2,7}$,F_7)
end

In Algorithm 2, the functions TubeModel($C_{O_2,5}$,$C_{CO_2,5}$) and BubblerModel($C_{O_2,7}$,$C_{CO_2,7}$,F_7) do the

procedures described in sections 8.1.1 and 8.1.2, respectively. All parameters in Algorithm 2, including those within the TubeModel and BubblerModel functions, have set values, except for the parameters L, A, X, and F_2. Thus, a complete process simulation has been developed for the photobioreactor that takes these four parameters as inputs.

Now that a full model for each petal tube has been developed, it remains to be determined how many petals to use in the pilot-scale design. A requirement of the pilot-scale design is that it sequester 100kg of CO_2 each day, thus the number of tubes is chosen to meet this requirement. For the pilot-scale design presented in this report, 13 tubes were required to achieve this sequestration goal.

Sequestration constraint Although the process can be simulated effectively for any given values of L, A, X, and F_2, the process only achieves the carbon sequestration goal of 50% for F_2 values below some threshold. It is desirable to set F_2 as high as possible without passing this threshold in order to provide the algae with high CO_2 concentrations. Thus, F_2 should be set right at the threshold necessary to achieve the sequestration requirement. For a given set of values of L, A, and X, the threshold F_2 value can be found by minimizing the objective function

$$f(F_2) = \Big(\text{SeqFrac}(F_2, L, A, X) - 0.52\Big)^2 \tag{8.30}$$

where SeqFrac(F_2, L, A, X) is a function that returns the fraction of input CO_2 sequestered, as calculated with the BubblerModel code using the self-consistent balances. The function is minimized at a sequestration fraction of 0.52, which provides a margin of error so that the pilot plant achieves the sequestration target even if the process simulation is not perfectly accurate. Minimizing f(F_2) is a simple one-variable minimization problem, and it is achieved efficiently using the *fminbnd* function in Matlab.

A procedure that runs this minimization and reports the self-consistent mass and energy balance results at the minimizing F_2 was automated in Matlab. This procedure takes values for L, A, and X as inputs and returns all stream properties from the process simulation. The values of L, A, and X used in the pilot plant are chosen to optimize estimated profits per tube, as described in section 9.

8.2 Design of Rotary Steam Tube Heat Exchanger Using Aspen Plus

To model the evaporation of the remaining water after skimming the flocculated algae, Aspen Plus was used. In the process, Chlorella was modeled as a nonconventional solid by specifying its elemental composition (Mandalam, Palsson, 1998). Detailed information about the specifications can be found in Section A.3 of the Appendix. The dryer was modeled using the HEATX block; the algal paste was assumed to enter the dryer at ambient temperature, while the low pressure steam entered at 150C and 1.5 bar gauge. The conditions for the low pressure steam were determined based on a constraint requiring

that 90 percent of the steam condensed as it passed through the exchanger in order to make good use of the latent heat.

The HEATX block was specified to model the dryer as a single-pass shell-in-tube heat exchanger with no baffles. This is a close approximation, as the heat exchange between the two fluids occurs primarily at the outer surface of the tube carrying the steam, and the rotary drum will only rotate at the speed necessary to move the biomass (approximately 7.5rpm).

Stream information from the simulation is reproduced from Section 6.2 below.

Table 8.1: Stream Results from Aspen Plus Simulation

Stream	P-16	P-17	P-18	P-19
Temperature (°C)	27.0	100.0	160.0	111.4
Pressure (bar)	1.013	1.013	1.5	1.5
Mass Flow (kg/h)	39.005	39.005	44.897	44.897
Volumetric Flow (m^3/h)	0.4744	-	-	-
Vapor Fraction	0	0.9290	1	0.0997
Moisture Content (wet basis)	0.936034	0.09907	-	-
Dried Algae (kg/hr)		2.495		

From the table, one can see that algal paste entering the dryer, stream 16, has a wet basis moisture content of over 93 percent. The content of this stream is obtained based on the 98 percent removal of water attributed to the magnesium-based flocculation and flotation process with nearly total biomass recovery [García-Perez et. al 2013]. In order to produce a valuable biomass product, the moisture content of the exiting algal paste must be at or below ten percent. In order to accomplish this goal, it was determined that 44.9 kg/h of low pressure steam would be required.

9 Process Optimization

9.1 Photobioreactor Optimization

The process simulation created in Matlab performs mass and energy balances on the process, given the PBR tube dimensions (length and cross-sectional area) and algae concentration in the bubbler. An optimization procedure was used to find the values of the parameters that maximize estimated profits per tube. The method of profit estimation, which is described in detail below, is intended to reflect the profits per tube in a hypothetical full-scale plant, not the profits in the pilot-scale plant proposed in this report. The rationale for this approach is that the pilot-scale plant is intended to demonstrate the features of a full-scale plant and provide data to aid the design of the full-scale plant. Thus, the PBR tubes used in the pilot scale plant should be identical to those that would be used in a full scale design.

The formal problem statement of the optimization and a description of the optimization methods are provided in the following sections.

9.1.1 Optimization Problem Statement

Define $\vec{x} = (L, A, X)$ where L is tube length (m), A (m^2) is tube cross-sectional area, and X is biomass concentration (kg/m^3). It was desired to find the $\vec{x}$ that maximizes profits (or minimizes losses), under the constraints that L, A, and X are positive and that reactor temperature and depth of light penetration remain at ideal levels for algae health. Specifically, the temperature change ΔT between the tube entrance and exit must be below 20^oC, and the light/dark ratio LDR must be greater than 0.10. The problem is stated formally below.

$$\begin{aligned} \min_{\vec{x}} \quad & f_o(\vec{x}) \\ \text{s.t.} \quad & x_i > 0 \text{ for } i = 1, 2, 3 \\ & \Delta T(\vec{x}) < 20^oC \\ & LDR(\vec{x}) > 0.10 \end{aligned} \tag{9.1}$$

The function $f_o(\vec{x})$ to be minimized is given by $f_o(\vec{x}) = Costs - Revenue$, and a formal definition is given below.

$$f_o(\vec{x}) = C_{cooling} + C_{pumping} + C_{nutrient} + C_{acrylic} + C_{land} - (\text{Productivity}) * (Price) \tag{9.2}$$

In Eq. 9.2, C_i is the cost per unit time of input i, per tube. Productivity is the biomass output per unit time, per tube. $Price$, the selling price of the output biomass, is taken as constant, but all other terms in Eq. 9.2 are functions of $\vec{x}$. Productivity is given directly by the Matlab process simulation code, and Eqs. 9.3 through 9.7 define how costs are estimated for each input.

$$C_{cooling} = Q(\frac{1}{COP})p_{elec} \tag{9.3}$$

where Q is required rate of heat removal, COP is estimated coefficient of performance of the refrigeration unit, and p_{elec} is the price of electricity.

$$C_{pumping} = (\Delta P)F\frac{1}{\varepsilon_{pump}}p_{elec} \tag{9.4}$$

where ΔP is pressure drop from the tube entrance to exit, F is volumetric flow rate through tube, ε_{pump} is pump efficiency, and p_{elec} is the price of electricity.

$$C_{nutrient} = (\text{Nutrient Consumption Rate})(p_{nutr}) \tag{9.5}$$

where p_{nutr} is nutrient price.

$$C_{acrylic} = (\text{Mass of Acrylic})\Big(\frac{1}{\text{Tube Lifetime}}\Big)(p_{acryl}) \tag{9.6}$$

where p_{nutr} is price of acrylic.

$$C_{land} = (\text{land cost})(\text{interest rate}) \tag{9.7}$$

where the cost of land ownership C_{land} is estimated as the foregone interest that would be earned if the land were sold. In Eqs. 9.3 through 9.7, p_{elec}, p_{nutr}, p_{elec}, ε_{pump}, and COP are constants, and all other variables depend on $\vec{x}$ and are obtained from the process simulation code.

It was decided that a gradient descent method would be used to minimize f_o under the inequality constraints described above. To account for these constraint, the problem is reformulated into an unconstrained minimization problem, as described in the following section.

9.1.2 Reformulated Problem

To reformulate the constrained optimization problem into an unconstrained optimization problem, a penalty is added to the objective function when one of the constraint parameters $p_i \in (L, A, X, \Delta T, LDR)$ is near to its constraint C_i. The penalty approaches infinity as p_i approaches C_i. This penalty causes gradient-based minimization methods to avoid breaking the constraint.

Formally, the reformulated problem is:

$$\min_{\vec{x}} f_1(\vec{x}) \tag{9.8}$$

where

$$f_1(\vec{x}) = f_0(\vec{x}) + \sum_i b_i(p_i(\vec{x})) \tag{9.9}$$

Here, $b_i(p_i(\vec{x}))$ is the penalty for the ith constraint (described below), and the sum is over the 5 inequality constraints. The values $p_i(\vec{x})$ are calculated with the process simulation code described in Section 8.

It is desired that the penalty b_i is 0 for p_i far from the constraint, that the penalty smoothly takes effect at a point near the constraint, and that the penalty approaches infinity as $p_i \to C_i$. The value of p_i at which the penalty takes effect is denoted as $C_{i,soft}$ (the soft constraint) and the value at which

the penalty reaches infinity is denoted as $C_{i,hard}$ (the hard constraint). These requirements are satisfied with the following function:

$$b_i(E_i) = \begin{cases} \infty & E_i < 0 \\ E_i - \ln E_i - 1 & 0 \leq E_i < 1 \\ 0 & E_i \geq 1 \end{cases} \tag{9.10}$$

where

$$E_i = \frac{p_i(\vec{x}) - C_{i,hard}}{C_{i,soft} - C_{i,hard}} \tag{9.11}$$

Note that $\frac{\mathrm{d}b_i}{\mathrm{d}p_i} = 0$ at $p_i = C_{i,soft}$, so that the objective function remains differentiable at all $\vec{x}$ that obey the constraints. Table 9.1.2 shows the hard and soft constraints used for the PBR optimization.

Table 9.1: Hard and Soft Constraints used in $f_1(\vec{x})$

i	p_i	$C_{i,soft}$	$C_{i,hard}$
1	L	1.0	0 m
2	A	10^{-5}	0 m^2
3	X	0.01	0 $\mathrm{kg/m}^3$
4	ΔT	18	20 ^{o}C
5	LDR	0.12	0.10

It is now possible to minimize $f_1(\vec{x})$ using a standard gradient descents algorithm like that shown in Algorithm 1.

Algorithm 1: Gradient Descents.

input : An initial guess $\vec{x}_0$
output: The vector $\vec{x}$ that locally minimizes $f_1(\vec{x}_0)$
while $\nabla f_1 > \varepsilon$ **do**
  $\nabla f_1 \leftarrow$ Gradient($\vec{x}$)
  $\alpha \leftarrow$ LineSearch($\vec{x}$,∇f_1)
  $\vec{x} \leftarrow \vec{x} - \alpha \nabla f_1$
end

In Algorithm 1, the Gradient($\vec{x}$) function calculates the gradient of f_1 at point $\vec{x}$, and the LineSearch($\vec{x}$,∇f_1) function finds the minimum value of f_1 along a line through $\vec{x}$ in the ∇f_1 direction. The algorithms for both functions are provided below.

This simple implementation is ill-suited for cases in which the components of ∇f_1 significantly differ in magnitude. In the case of $f_1(\vec{x})$, the tube length x_1 is on the order of 10^2 whereas cross-sectional area is on the order of 10^{-2}, and the magnitudes of f_1's derivatives with respect to each variable differ on a similar scale. Panel A in Figure 9.1 illustrates the consequence of this feature, which is that a highly indirect zig-zag path is taken towards the minimum, leading to very slow convergence.

To mitigate this problem, the components of $\vec{x}$ can be re-scaled (effectively a unit-conversion) so that their numerical values are on a similar scale. Alternatively, the direction of the line search can be

modified to imitate this scaling effect while retaining physically-meaningful coordinates in convenient units. The specific modification that is needed is developed as follows.

First, the notation $\vec{a}.*\vec{b}$ (or $\vec{a}./\vec{b}$) will be used to denote element-wise multiplication (or division) of vectors $\vec{a}$ and $\vec{b}$ (as is used in Matlab). Define a function $g(\vec{x})$ such that $g(\vec{x}.*\vec{w}) = f_1(\vec{x})$ where $\vec{w}$ is a vector of weights that achieve the desired scaling of components (the choice of $\vec{w}$ is discussed below). Now, consider the parallel problems of conducting a line search of f_1 beginning at point $\vec{x}_o$ and conducting a line search of g beginning at point $\vec{x}_o.*\vec{w}$. For the line search of g, the direction ∇g is a good choice of minimization direction, as the components of $\vec{x}$ are properly scaled such that the traditional Gradient Descent algorithm converges efficiently. As described previously and as shown in Panel A of Figure 9.1, ∇f_1 is not a good choice for the direction of the line search of f_1, and the direction $\nabla g./\vec{w}$, which is the desired direction for g re-scaled for the function f_1, is chosen instead. Note that $\nabla g = \nabla f_1./\vec{w}$, so the desired direction for the line search of f_1 is $\nabla f_1./(\vec{w}.*\vec{w})$. The scaling factor $\vec{w}$ should be chosen so that the components of $\vec{x}_0.*\vec{w}$ are on a similar scale, in order to avoid a zig-zag path. It was chosen to set $\vec{w} = 1./\vec{x}$ so that $\vec{x}_0.*\vec{w} = (1,1,1)$. Thus, the direction of the line search of f_1 becomes $\nabla f_1.*(\vec{x}_0.*\vec{x}_0)$. This modified algorithm is outlined formally in Algorithm 2 below. (Note that a similar approach is used in the common Conjugate Gradient (CG) algorithm. The main difference is that CG makes a more nuanced choice of $\vec{w}$).

Figure 9.1 illustrates the increase in performance of this modified Gradient Descent algorithm (Alg. 2) relative to the basic Gradient Descent algorithm (Alg. 1).

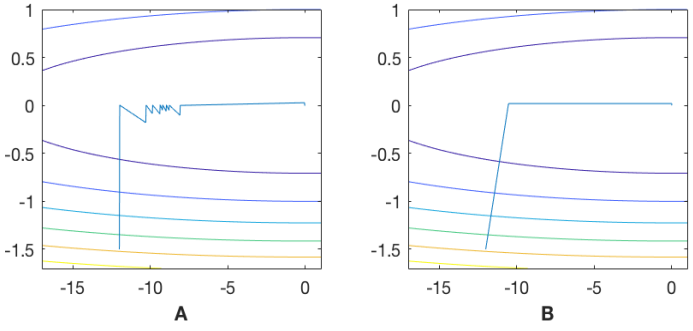

Figure 9.1: Comparison of Algorithm 1 (Panel A) to Algorithm 2 (Panel B). The objective function in this figure is $f(x,y) = (x/23)^2 + y^2$, and smooth colored lines indicate level sets of this function. As can be seen, Algorithm 2 converges in much fewer iterations than Algorithm 1.

The Gradient($\vec{x}$) and LineSearch($\vec{x}, \vec{dir}$) functions used in Algorithms 1 and 2 are outlined in Algorithms 3 and 4 below.

Algorithm 2: Modified Gradient Descents

input : An initial guess $\vec{x}_0$
output: $\vec{x}$ that minimizes $f_1(\vec{x}_0)$
while $\nabla f_1 > \varepsilon$ **do**
  $d\vec{i}r \leftarrow$ Gradient$(\vec{x})$.*$\vec{x}$.*$\vec{x}$
  `// Note: .* denotes element-wise multiplication`
  $\alpha \leftarrow$ LineSearch($\vec{x}$,$d\vec{i}r$)
  $\vec{x} \leftarrow \vec{x} - \alpha d\vec{i}r$
end

Algorithm 3: Gradient

input : A vector $\vec{x}$ at which the gradient will be evaluated.
  A vector $d\vec{x}$ defining the desired differential steps for derivative calculations.
output: a vector ∇f_1 whose ith component is $\frac{\partial f_1}{\partial x_i}$.
for $i \leftarrow$ *(1,2,3)* **do**
  $d\vec{x}_i \leftarrow d\vec{x}.*(\delta_{1i}, \delta_{2i}, \delta_{3i})$
  `// Note: ` δ_{ji} `denotes the Kronecker delta`
  $\nabla f_{1i} \leftarrow \frac{f_1(\vec{x}+d\vec{x}_i)-f_1(\vec{x})}{|d\vec{x}_i|}$
end

Algorithm 4: LineSearch

input : A vector $\vec{x}$ at which the line search is to begin.
  A vector $d\vec{i}r$ specifying the direction of the line search.
output: A number α specifying the distance in the $d\vec{i}r$ from $\vec{x}$ at which a local minimum occurs, measured in multiples of $d\vec{i}r$.
$\alpha_{Low} \leftarrow 0$
$\alpha \leftarrow \alpha_0$
$L_0 \leftarrow f_1(\vec{x})$
$L_1 \leftarrow f_1(\vec{x} - \alpha d\vec{i}r)$
while $L_1 < L_0$ **do**
  $\alpha_{Low} \leftarrow \alpha$
  $\alpha \leftarrow 2\alpha$
  $L_0 \leftarrow L_1$
  $L_1 \leftarrow f_1(\vec{x} - \alpha d\vec{i}r)$
end
$\alpha_{High} \leftarrow \alpha$
$\alpha_{Low} \leftarrow \alpha_{Low}/2$
$\alpha \leftarrow$ BisectionSearch(α_{Low},α_{High})

The BisectionSearch(α_{Low},α_{High}) function used in Algorithm 4 performs a bisection search minimization of $h(\alpha) = f_1(\vec{x} - \alpha d\vec{i}r)$ on the interval (α_{Low},α_{High}) within which it is known that a local minimum exists and on which it is assumed that $\frac{\mathrm{d}h}{\mathrm{d}\alpha}$ is monotonically increasing (i.e. it is assumed that there is only one minimum in the interval).

9.1.3 Results of PBR Tube Optimization

The optimization procedure was run with an initial guess of $L = 100\text{m}$, $A = 0.005\text{m}^2$, and $X = 2.0\text{kg/m}^3$. At this initial guess, $f_1 = -3.76 \times 10^{-5}$. The optimization converged after 4 iterations to the values

$L = 304.03\text{m}$, $A = 0.002303\text{m}^2$, and $X = 1.663\text{kg/m}^3$, and the objective function was reduced to $f_1 = -19.7 \times 10^{-5}$. These values are the parameters used in the pilot-scale design presented in this paper. Note that the objective function is negative, which indicates negative losses (i.e. positive profits) per tube.

9.2 Nighttime Tank Lighting Optimization

The lighting configuration in the nighttime tank was optimized in order to find the lowest-cost method of providing adequate lighting to the algae. Adequate lighting was defined as a light/dark ratio of 10%. It was determined that the light guides would be arranged in a hexagonal array, as described in Section 7.3, however the light guide radius, spacing (distance between guides), and LED intensity were parameters that could be adjusted to minimize costs. Formally, the problem is

$$\begin{aligned} \min_{\vec{x}} \quad & f_o(\vec{x}) \\ \text{s.t.} \quad & LDR > 0.10 \end{aligned} \tag{9.12}$$

Here, $\vec{x} = (r, d, P)$ where r is light guide radius, d is guide spacing, and P_{LED} is LED power per guide. LDR is the light/dark ratio. The objective function $f_o(\vec{x})$ is an estimate of the annual cost of the tank. It is defined as follows.

$$f_o(\vec{x}) = \Big(\frac{C_{guide}}{\text{Guide Lifetime}} + (P_{LED})(p_{elec})\Big)N_{guides} + \frac{C_{tank}}{\text{Tank Lifetime}} \tag{9.13}$$

Where the cost of one guide C_{guide} is estimated to be \$4.71 based an material and manufacturing costs. Guide Lifetime is estimated to be 20 years. p_{elec} is the price of electricity, which is $\$0.16/kWh$. C_tank was estimated to be $(\$30/m^2)(V_{Tank})$, where V_{Tank} is tank volume, and Tank Lifetime was estimated to be 10 years. N_{guides}, the number of light guides in the tank, and V_{Tank}, are implicitly functions of r and d. N_{guides} is determined by finding the number of rods (light guides) of radius r and arranged in a hexagonal grid with spacing d that are needed to fill a space with empty volume of 91m^3. V_{Tank} is then the volume of these rods plus the empty volume of 91m^3. Equations for V_{Tank} and N_{guides} in terms of r and d are given below.

$$N_{guides} = \frac{121.8}{\pi d^2(2.45 - 8.33r^2/d^2)} \tag{9.14}$$

$$V_{Tank} = N_{guides}(7.98r^2) + 91 \tag{9.15}$$

where units for r and d are meters and units for V_{Tank} are m^3.

In order to ensure that the constraint on LDR is met with the minimal electricity costs, P_{LED} was fixed at the value that guarantees $LDR = 0.10$, for a given r and d. This removes one degree of freedom from the problem and removes the constraint. The result is a new minimization problem

$$\min_{\{r,d\}} \quad f_1(r, d) \tag{9.16}$$

where the new objective function f_1

$$f_1(r,d) = f_0(r,d,E_{LED,min}(r,d)) \tag{9.17}$$

where $E_{LED,min}(r,d)$ is a function that returns the value of E_{LED} that achieves an LDR of 0.10, for given r and d. $f_1(r,d)$ was minimized using the same technique described for the PBR optimization to determine the optimal values of light guide radius and spacing.

9.2.1 Results of Nighttime Tank Lighting Optimization

The optimization procedure was run with an initial guess of $r = 0.5$cm and $d = 10$cm. At this initial guess, $f_1 = 8.42 \times 10^3$. The optimization converged after 5 iterations to the values $r = 0.0375$cm and $d = 17.89$cm, and the objective function was reduced to $f_1 = 3.64 \times 10^3$. These values are the parameters used in the pilot-scale design presented in this paper.

10 Descriptions of Equipment

This section provides specification and cost information for all process equipment used in the pilot-scale plant. Due to the pilot-scale and custom nature of the design, most of the equipment costs were estimated by searching B2B-provided listings. An example provider is cited for each of the equipment items that reflects what was found to be a typical cost for a given item. Prices for each item are reported in USD, but were estimated with the aim of reflecting a cost closer to what may be found in Brazil, rather than American suppliers.

Identification:	**Item**	Plastic Gas Exchange Column Tank
	PFD Ref. No.	E2
	No./Amt. Req.	1

Function: Central tank for gas exchange (CO2 transfer in and O2 transfer out)

Operation: 8 hours/day

Example supplier: Zhangjiagang Sanofi Machinery Co., Ltd.

Supplier unit name: 3000L PE Food Grade Plastic Water Storage Tank

Cost per unit ($): 100

Specifications:

Property	**Value**
Volume	3000L
Material	PE
Height	3m
Grade	Food grade

Other notes: Transition area of interior wall on tank adopts arc to ensure no dead corner

Insect resistant sanitary breathing cover

Input and output pipes at bottom and top as nessecary

Identification:	**Item**	Acrylic Tubing
	PFD Ref. No.	A
	No./Amt. Req.	14259kg

Function: Acrylic tubes for horizontal tubular bioraector petals. See Section 7 for tubing layout.

Operation: 8 hours/day

Example supplier: Wuxi Ludery International Trading Co., Ltd.

Supplier unit name: Custom LDR Acrylic Tubing

Cost per unit ($): 1$/kg

Specifications:	**Property**	**Value**
	Material	Acrylic
	Thickness	5mm
	Inner Diameter	17.12cm
	Length	Custom
	Color	Transparent

Other notes: Dimensions are custom to order

Identification:	**Item**	Multi-stage Blower
	PFD Ref. No.	E-1
	No./Amt. Req.	1

Function: Gas transport to reactor (through spargers at base of column/tank)

Operation: 24hr/day

Example supplier: HIS

Supplier unit name: Model 31

Cost per unit ($): 2700

Specifications:

Property	**Value**
Stages	1-11
Operating speed	3550 RPM (dierct drive), 5075 RPM (belt drive)
Shaft Power	9hp
Power Rating	7kW
Flow rate	0-500m3/hr
Pressure Ratio	3.5PSIG

Identification:	**Item**	Water Chiller
	PFD Ref. No.	E-3
	No./Amt. Req.	1

Function: Internal coil HX for cooling algae volume in the central gas exchange column

Operation: 8hr/day

Example supplier: Shanghai Wenheng Electric Equipment Co., Ltd.

Supplier unit name: CW-5200

Cost per unit ($): 380

Specifications:	**Property**	**Value**
	Certification	CE, CE, ISO
	Cooling agent	R134a
	Dimenison	72 X 44 X 62 cm
	Max heat duty:	1400W
	Avg. op. heat duty:	150W

Other notes: Alarm function: can use state real-time monitoring

Easy installation (small, light weight)

Identification:	**Item**	Main Centrifugal Circulation Pump
	PFD Ref. No.	E-4
	No./Amt. Req.	1

Function: Circulating algae cultivation volume

Operation: 24hr/day

Example supplier: Hebei Yuandong Pumps Manufacturing Co., Ltd.

Supplier unit name: BYD, 100CYZ-40

Cost per unit ($): 2933

Specifications:	**Property**	**Value**
	Type	Centrifugal, self-priming
	Power	Electric
	Pressure	12-75m
	Flow capacity	610m3/hr
	Speed	2900r/min
	Certificate	ISO9001:2000
	Temperature	-20 to 80C
	Head	75m

Other notes: Simple structure, convenient operation and maintenance

Identification:	**Item**	Night Tank
	PFD Ref. No.	E-11
	No./Amt. Req.	1

Function:	Underground water tank for night/other
Operation:	16 hours/day

Example supplier:	Shijiazhuang Zhengzhong Technology Co., Ltd.
Supplier unit name:	Center Enamel Water Storage Tank, ZZKJ-0010
Cost per unit ($):	5000

Specifications:	**Property**	**Value**
	Volume	>100m3
	Material	Titanium dioxide enhanced double enamel steel
	Fill Height	2.45m
	Roof	custom for purpose
	Service life	>30 years
	Permeability	Gas/liquid impermeable
	Cleanability	Easy: smooth, glossy, inert, and non-adhesive
	Corrosion resistance	High

Other notes: Dimensions are custom to order

Identification:	**Item**	High Intensity Blue and Red LEDs
	PFD Ref. No.	B
	No./Amt. Req.	2952

Function: Fixture to fibre optical light guides for artificial illumination

Operation: 16 hours/day

Example supplier: Shenzhen Dpower Optoelectronic Co., Ltd.

Supplier unit name: DPT-XT3535B

Cost per unit ($): 0.16

Specifications:	**Property**	**Value**
	Wattage	1W
	Working current	350mA
	Blue wavelength	450-500nm
	Red wavelength	610-730nm
	Lifespan	50,000hrs
	Mount width	3.45mm
	Mount length	3.45mm

Identification:	**Item**	PMMA Granules
	PFD Ref. No.	C
	No./Amt. Req.	13608kg

Function: Melted down to form inner core of optical light pipes

Operation: 16 hours/day

Example supplier: Inner Mongolia Zhishe Industry Trade Corporation

Supplier unit name: ZSSY, PMA-AAA

Cost per unit ($): 0.35/kg

Specifications:	**Property**	**Value**
	Form	Granules
	Grade	High quality virgin pure PMMA
	Color	Transparent
	Certification	SGS,BV,ISO9001:2000
	Refractive index	1.489

Other notes: High tensile strength, corrosion resistance

Easy to process and mold into custom shape

Used for optical applications

Identification:

Item	PTFE Granules
PFD Ref. No.	D
No./Amt. Req.	3650kg

Function: Melted down to form outter cladding of optical light pipes

Operation: 16 hours/day

Example supplier: Dalian Huanruntongshi Imp & Exp Co., Ltd.

Supplier unit name: HRTS, PTFE Resin

Cost per unit ($): 0.6/kg

Specifications:

Property	**Value**
Form	Granules, powder
Grade	High quality virgin pure PTFE
Color	Transparent
Refractive index	1.36

Other notes:

High tensile strength, corrosion resistance

Easy to process and mold into custom shape, esp. tubing

Used for optical applications

Identification:	**Item**	Chemical Storage Units
	PFD Ref. No.	-
	No./Amt. Req.	44 (variable sizes)

Function: Storage of nutrient chemicals, stock solutions.

Operation: 24hr/day

Example supplier: Plastic Container Suppliers

Supplier unit name: Sealable Airtight Chemical Storage Drum

Cost per unit ($): Large (200L): 26, Medium (10L): 4.50, Small (1L): 0.52

Specifications:

Property	**Value**
Material	Chemical Storage Plastic
Seal	Airtight
Dimensions	Variable: 200L, 10L, 1L

Other notes: Purchased by size requirements

Identification:	**Item**	Peristaltic Pump
	PFD Ref. No.	-
	No./Amt. Req.	1

Function: Nutrient Delivery

Operation: 8hr/day

Example supplier: Jining Luheng Machinery Equipment Co., Ltd.

Supplier unit name: LH GM1.6-2.1/50

Cost per unit ($): 150

Specifications:	**Property**	**Value**
	Power	Electric
	Capacity	2.1LPH
	Max Pressure	500bar
	kW	0.55

Other notes: Will be operated at half capacity

Identification:	**Item**	Rotary Drum Dryer
	PFD Ref. No.	E-10
	No./Amt. Req.	1

Function: Rotary drying drum for post-processing drying of algae

Operation: 24hr/day

Cost per unit ($): 2809

Specifications:

Property	**Value**
Material	Carbon Steel
Length	15ft
Shell Inner Diameter	2ft
Diamter	6in
Rotation velocity	7.5rpm
Max Op. Temp.	150C
Motor Power	3hp
Installed Capacity	178kg evaporated water/hr

Identification:	**Item**	Gas Blower
	PFD Ref. No.	E-7
	No./Amt. Req.	1

Function: Gas transport for post-processing

Operation: 24hr/day

Example supplier: Home Depot

Supplier unit name: PowerPro Technology, 2 Gal. Portable Electric Air Compressor

Cost per unit ($): 60

Specifications:

Property	**Value**
Max Pressure	100psi
Op. Pressure	40psi
Op. Flow Rate	1.5CFM
Motor power	1/3hp
Compressor Type	Light Duty

Identification:	**Item**	Pressure Vessel
	PFD Ref. No.	E-8
	No./Amt. Req.	1

Function: Pressurized saturation of water with air

Operation: 24hr/day

Example supplier: OEM

Supplier unit name: Commercial Tank

Cost per unit ($): 100

Specifications:

Property	**Value**
Diameter	24in
Material	PE Liner, FRP Filament winding
Pressure rating	150psi

Identification:	**Item**	Flotation Tank
	PFD Ref. No.	E-6
	No./Amt. Req.	1

Function: Post-processing flocculation and flotation

Operation: 24hr/day

Example supplier: Dezhou Huili Environmental Technology Co., Ltd.

Cost per unit ($): 208

Specifications:

Property	**Value**
Modular pieces	1x1m, 0.5x1m, 0.5x0.5m
Dimensions	6mx0.5mx0.5m
Material	Galvanized steel

Identification:	**Item**	Holding Tank
	PFD Ref. No.	E-5
	No./Amt. Req.	1

Function: Holding harvested algae for post-treatment

Operation: 24hr/day

Example supplier: Chongqing Dianfeng Plastic Containers Co., Ltd.

Supplier unit name: Dianfeng M-4000L

Cost per unit ($): 136

Specifications:	**Property**	**Value**
	Material	LLDPE
	Volume	4000L
	Diameter	2m
	Grade	Food grade

11 Economic Analysis

The following sections provide a break down of the economic analysis of the presented process, including a profitability assessment of the overall system. Bare module costs were estimated, from which total capital investment was derived. Production costs and annual sales were calculated. Then, profitability was assessed in terms of Return on Investment (ROI), Payback Period (PB), Venture Profit (VP), and Annualized Cost (AC).

The analyses were performed on two different bases to reflect the unique nature of this venture. The first method involved assuming that all equipment was purchased at the full cost up-front, and without taking into account the lifespan of certain equipment. This method is denoted as the "Up-front" column in the following tables. However, a longer lifespan means that for much of the high-cost equipment, the up-front cost does not accurately reflect the long-term capital needs of the pilot plant once in operation. For example, the rotary dryer only needs to be purchased once every 30 years, so costs could hypothetically be distributed over a longer time period. To take this into account, a second method of economic analysis was therefore employed, where lifespan of the equipment was used to determine an overall "10 Year cost", from which all analyses were also performed based on. This method is presented in the "10 Year" columns in the following tables. This second method was built assuming that with the aid of government support and loans (common for projects of this nature in Brazil), that some of the initial investment costs could be paid back over a longer period of time. This effect was estimated by obtaining lifespans for equipment and fabricated units and calculating a 10-year projected cost, allowing for equipment to be paid back over the period of its expected lifespan. For example, if a compressor costing $2700 up-front has a lifespan of 20 years and a bare module factor of 2.15, the first method would assume $5805 to be the Bare Module Cost, while the second method would assume it to be half of that (10years/20year lifespan), at $2903. This calculation also worked in the reverse, where if a unit had a lifespan under 10 years, the 10 year cost was raised to reflect the need to purchase new equipment in this time period. The Total Capital Investment profile, as well as ROI, PBP, VP, and AC, were all calculated using both of these methods. The 10 Year method is not meant to produce an exact financing scenario, but rather, provide an alternative perspective that is believed to be a closer reflection of a realistic financing scheme for this pilot plant under a start-up business scenario.

11.1 Fixed Capital Investment Summary

Table 11.1 presents an item-by-item list of the equipment costs associated with the process, split up by reactor costs, nutrient delivery costs, and harvesting and post-treatment costs. Due to the pilot-scale and custom nature of the process, most of the equipment costs were estimated by searching B2B-provided listings. Specifications can be found in Section 10. Bare Module Factors specific to each

piece of equipment were obtained from *Product and Process Design Principles: Synthesis, Analysis, and Evaluation* (Seider et al, 2016), or where appropriate, estimated by calculating expected values of indirect costs associated with purchase, manufacturing, and installation. A summary of how each Bare Module Factor was estimated is given in Section A.2 of the Appendix. Given the small scale of the operation, and the start-up nature of the management, costs associated with contracting were lumped into the bare module costs. It should be noted that the installed cost of the rotary steam tube dryer is based on a rule of thumb given for algae drying based on the total mass of water evaporated (Amos, 1998).

Table 11.1: Equipment Cost Summary

PFD Ref. No.	Unit Name	Direct Module Expense	Lifespan	10 Year Cost	Bare Module Factor	Bare Module Cost	10 Year Bare Module Cost
Day Reactor							
E-2	Plastic Gas Exchange Column Tank	100	15	66.7	2.1	210	140
A	Acrylic tubing	14259	10	14259	1.1	15684.9	15684.9
E-1	Multi-stage Compressor	2700	20	1350	2.15	5805	2902.5
E-3	Water Chiller	380	10	380	1.1	418	418
E-4	Centrifugal pump	2933	15	1955	1.1	3226.3	2151
Totals						**25344**	**21296**
Night Reactor							
E-11	Night tank	5000	30	1667	3	15000	5000
B	LEDs	472.32	8.6	549	1.05	496	577
C	PPMA Granules	4762.8	25	1905.12	2	9525.6	3810.24
D	PTFE Granules	2190	25	876	2	4380	1752
Totals						**29402**	**11139**
Nutrient Delivery							
	Chemical Storage	360.696	30	120	1.05	378.73	126
	Peristaltic Pumps	150	5	300	1.05	157.5	315
Totals						**536.2**	**441**
Harvesting and Post-treatment							
E-10	Rotary steam tube dryer	5024.8	30	1674.9	1.3	6532.24	2177.4
E-7	Gas blower	60	10	60	2.15	129	129
E-8	Pressure vessel	100	5	200	4.16	416	832
E-6	Flotation tank	208	20	104	1.2	249.6	124.8
E-5	Holding tank	136	15	90.6666667	1.05	142.8	95.2
Totals						**7470**	**3358.41**
					TBM	**62752**	**36235**

The fixed capital investment summary given in Table 11.2 quantifies the Total Capital Investment (TCI) required for the project, including estimates of the Total Bare Module Investment (CTBM), the Total Direct Permanent Investment (CDPI), the Total Depreciable Capital (CTDC), and the Total

Permanent Investment (CTPI).

The CTBM is a sum of the bare module costs of fabricated equipment and process machinery (tabulated above), and cost of spare equipment. Cost for spare equipment was considered zero, as the cost of halting operation for some number of days in order to repair a piece of process machinery is orders of magnitude lower than the cost of purchasing a second piece of equipment. Furthermore, the hybrid reactor setup of this process offers the ability to use either the day or night time setup as a "spare" for continued operation during maintenance of the other. If harvesting repairs need to be made, the night tank also offers the ability to be used as a temporary holding tank. This is further discussed in Section 12. At larger scales, spare equipment would be required. The CDPI required for the facility is a summation of the CTBM and costs associated with site preparation, service facilities, and utility production. Here, allocated costs for utilities are assumed to be zero as they are already available onsite at the Porto do Pecem power station to which our process is being retrofit. Site preparation was estimated by methods cited for standard agricultural land levelling (Salassi, 2001, and Land Levelling, 2013) The cost for service facilities was estimated by calculating space required to set up a tent warehouse for indoor nutrient storage and preparation space, harvesting and post-treatment equipment space, as well as space for an office cubicle. A 15% factor for contingencies was applied to the CTDC the give the CTPI (overall profitability analyses are also reported in Table 11.7 for contingency factors of 25% and 50% though). To give the CTPI, the amount of required depreciable capital was added to the non-depreciable investments.This included cost of land and production startup costs. Start-up costs included inoculation culture purchase, and the equipment and operation costs for small inoculation and start-up cultures (further discussed in Section 12).

To obtain a final value for the CTCI, it was necessary to estimate the on-hand working capital needed. This was assumed to be 30 days of cash reserves for operating costs, stores of necessary operating materials (like feedstock) to account for any delays in shipping, the value of 7 days of product inventory to account for weekly product shipments, minus 30 days of accounts payable.

Table 11.2: Fixed Capital Investment Summary

		Up-front	10 Year
CDPI			
CTBM		62752	36235
Csite	Cost of Site Preparation	200	200
Cserv	Cost of Service Facilities (incl. storage space)	450	450
CDPI		63402	36885
CTDC			
CDPI		63402	36885
Ccont	Cost of Contingencies	9510	5533
CTDC		72912	42417
CTPI			
CTDC		72912	42417
Cland	Cost of Land	468	468
Cstartup	Cost of Plant Startup	512	512
CTPI		73892	43397
CTCI			
CTPI		73892	43397
CWC	Working Capital	1725	1725
CTCI		**75617**	**45122**

11.2 Operating Costs

This section tabulates the costs associated with the day-to-day operation of the plant. The operating costs are broken into variable and fixed costs; the former are affected by the production level of the plant, while the latter do not change, regardless of the operational status of the plant. These costs are reported in Table 11.3 below. Table 11.4 lists the annual costs of each type of utility.

Table 11.3: Variable Costs of Biomass Production

Variable Cost Summary	
Raw Materials	2575
Utilities	13597
Total Annual Variable Costs	16172
Fixed Cost Summary	
Operations	
Direct Wages	2344
Operating Supplies and Services	50
	2394
Maintenance	
Wages	60
Materials and Services	100
	160
General Plant Overhead	186
Property Taxes and Insurance	9.75
Total Annual Fixed Costs	2750
TOTAL OPERATING	18922

Table 11.4: Annual Utilities Costs

Type	Amount	Price	Annual Cost
Electricity (kWh)	11.9	US$0.16 /kWh	8842.12
Steam (kg/h)	44.5	US$0.12 /kg	4677.84
Water (m3/hr)	4.44	US$0.0056 /m3	77
Total Annual Utilities (USD)			**13596.96**

Table 11.5 presents a breakdown of how each expense contributes overall to the production. As expected, harvesting and post-processing is the most significant cost. It will be important to lower this cost at a larger scale. The fixed costs fraction is higher than normal perhaps, due to the pilot scale. The nighttime operation currently may be high considering the growth rate is minimal under the current CO_2 day:night split, however the added benefit of the night tank is qualitatively large. Further discussion of this can be found in Section 12.

Table 11.5: Breakdown of the contribution of type of expense to biomass production listed by total annual cost, and fraction of total annual cost.

Expense	Total Annual Cost	Fraction of Total Annual Cost
Annual TCI	4512	19%
Day time operation	3988	17%
Night time operation	1585	7%
Harvesting and Post-treatment	10514.97548	45%
Fixed Costs	2833.75	12%
SUM	23434	100%

11.3 Return on Investment Analysis

Dried biomass will be sold at a rate of $1.23USD/kg. At a production rate of 21,668kg/yr, this is a total annual sales revenue is $26,651. Income tax in Brazil for this income bracket is 15% on gross income (annual sales minus production costs). Table 11.6 tabulates the Annual Sales (S), Annual Production Costs (C), Income Tax, Total Depreciable Capital (CTDC), Depreciation (D), and a Reasonable desired ROI, chosen as 5%. This would be reasonable for a plant of such new technology. Reported are an ROI, PBP, VP, and AC, for both the Up-front method of analysis and the 10 Year method. By both methods, this process will be profitable with up to a 15% Return on Investment.

Table 11.6: Assessment of profitability for both the Up-front method and the 10 Year method described above in the introduction to Section 11.

Assessment of Profitability	Up-front	10 Year
Factors		
S (Annual Sales)	26651	26651
C (Annual Production Costs)	18922	18922
CTCI (Total Capital Investment)	75617	45122
Income Tax	0.15	0.15
CTDC (Total Depreciable Capital)	72912	42417
D (Depreciation)	7291	4242
imin (Reasonable ROI)	0.05	0.05
Profitability Measures		
ROI	9%	15%
PBP	5.3	3.9
VP	2789	4314
AC	22703	21178

This profitability analysis shows that this process would be on par with the highly ambitious goals depicted in the "Paths to Commercial Viability" discussed in Section 3. Of course, because this technology is in its early stages, challenges will inevitably arise. The above reported values were calculated with a 15% contingency factor, given that this plant is small. However, higher contingency factors may be more reasonable. Table 11.7 presents a comparison of Profitability Measures calculated when 15%, 25%, and 50% contingency factors were applied. The process remains profitable.

Table 11.7: A comparison of Profitability Measures calculated when 15%, 25%, and 50% contingency factors were applied.

	Up-front			10 Year		
Contingency Factor	**15%**	**25%**	**50%**	**15%**	**25%**	**50%**
ROI	9%	8%	7%	15%	13%	7%
PBP	5.26	5.47	5.91	3.9	4.12	5.91
VP	2789	2472	1679	4314	4129	1679
AC	22703	23020	23812	21178	21363	23812

11.4 Scalability

The pilot scale plant designed in this report is intended to demonstrate the potential of algae growth as an economical method for carbon conversion. The pilot-scale design is predicted to be profitable, with

an ROI of up to 15%, but a larger scale plant is expected to be much more profitable due to economies of scale. The process element where the greatest economies of scale are expected are the post-processing process, and the flue gas exchange column. In addition, process equipment such as pumps and control systems have high relative costs for pilot scale plants, but will have relative costs that will decrease for larger systems. Opportunities for heat integration and recycling of nutrient-rich process water also grow for larger plants, leading to economies of scale. The photobioreactor tubes are designed at the optimal size for a full-scale plant, therefore there are not economies of scale for this process element. However, this makes the cost of transitioning to larger scales low, as it is a matter of adding more petals to a gas exchange column, up to a certain maximum unit size. Similarly, the lighting design in the nighttime tank was optimized and is not expected to change in a full-scale plant, but could be optimized for a range of desired growth goals, if need be.

Certain biological factors can affect the ability to scale algae growth processes, and the biological principles governing these factors are still in the relatively early stages of research. The large scale emergent properties are not well understood. For example, algae growth can be very sensitive to tank size and environmental factors. This presents an inherent risk to scale-up. A major advantage of the pilot scale design, and one that sets it apart from the field, is that the petal tubes in which the algae grow are identical to the tubes that would be used in a full scale plant, as they are optimized for profitable growth under the given conditions. This means that measurements of growth rates on the pilot scale plant can be used to make accurate predictions of growth rates for a full-scale plant, minimizing the risk of inhibition due to unexpected biological phenomena.

There is ongoing research in genetic engineering of microalgae in order to address these biological factors and to increase growth rates. Engineered algae strains may, in the future, have much higher growth rates than the growth rates estimated in this design, which would greatly increase the profitability of a full scale plant.

A further consideration to scale up is the set of regulations that influence fossil fuel and renewable energy use in the location of a full-scale plant. There is growing support for regulatory limits on CO_2 emissions, and many regions already have laws that limit or tax CO_2 output. These regulations increase the cost and/or decrease the supply of fossil fuel products, thereby increasing the competitiveness of fossil fuel alternatives such as microalgae. In addition, some regions have created subsidies for fossil fuel alternatives which directly improve profitability. In Brazil, the government uses an auction system to award funding to renewable energy projects, and a full-scale algae growth plant would likely be competitive for such funding. The decision of when and where to build a full-scale plant based on this pilot-scale design should take careful consideration of the regulatory outlook of the plant location.

11.5 Evaluation of Existing Carbon Credits and Subsidies

One of the deciding criteria in the selection of Brazil as the location of the pilot-scale production facility was the climate surrounding incentives for renewables, particularly in the biofuels sector. The initiatives put in place and overall level of monetary investment over the last ten years have provided a more stable environment than those of other countries for experimental ventures such as algal biomass production (Josling et. al, 2010). Perhaps most notably, the Brazilian Climate Change Plan, introduced in late 2008, has allocated funds for the development of processes that aim to reduce greenhouse gas emissions approximately 36 to 39 percent within the country by 2020 (GlobalData, 2017). Two of the plan's main focuses are categories which this proposed process falls under: Renewable Power, and Biofuels. In addition, in 2010, the Brazilian government enacted the 2010-2019 Decennial Plan for Energy Expansion, the aim of which was to end new fossil fuel power plant construction and replace the energy production capacity with renewables. Although the majority of this initiative was dedicated to hydroelectric power, biomass was the second largest focus, with the goal to increase installed capacities by 3.1 GW over the ten year period. The government placed a high priority on these goals, backing the plan with $236 billion, due to an estimated 52 percent increase in domestic electricity consumption over the course of the decade. Within each of these two programs, additional funds are allocated for R&D processes, which this proposed process would qualify for due to its pilot-scale nature. Finally, Brazil has taken keen interest in algae processes, particularly in integration with existing biorefinery processes. It is expected that there would be significant support for specifically algae-based R&D that the proposed process would be able to take advantage of.

12 Additional Considerations

12.1 Startup operation

The process will be continuous once in full operation mode. There will be two steady-state operation modes: daytime and nighttime, with constant volume and cell density maintained. The operating volume for over 50% CO_2 sequestration of 200kg of CO_2/day (13 petals) is 91m3. Reaching the steady state of operation where the full volume is in use will require a series of start-up cultures where cell density and cultivation volume is steadily increased. A series of primary start-up cultures will be maintained in basic bench-scale reactors at all times (Figure 12.1), as well as a well stocked and healthy culture collection. After this step, the cultivation volume can be maintained in either the nighttime tank at below-capacity volume or a number of petals while cell density increases. The culture can then be continuously diluted at a rate lower than the growth rate until the operating volume and operating cell density is reached. At this point, the harvesting operation begins and the volume is diluted at the rate of growth. This is at-capacity steady state operation.

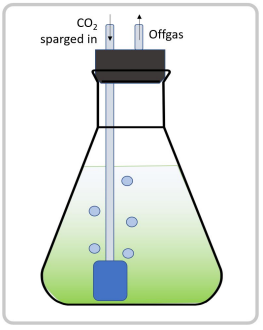

Figure 12.1: Small scale flask reactors for bench-scale startup cultures and culture line maintenance.

12.2 Environment, Safety, and Health

12.2.1 Wastewater

The volume of wastewater produced in this process is nearly identical to the volume of medium removed through the harvest port. After the flocculation and removal of biomass, the remaining water is at a basic pH and contains residual biomass as well as magnesium precipitate. To make the water suitable for disposal, the volume will first be chlorine bleached to kill the remaining algae, as per standard protocol. A small portion of the volume containing the magnesium precipitate will be removed and stored separately to be sent to the wastewater treatment facility used by the power plant. The remaining volume will be sent to sewage disposal.

For a larger algae production process, the likelihood is high that it would be cost-effective to remove biomass and growth metabolites from the wastewater and send it back to the photobioreactor rather

than use fresh water. In some cases, the presence of such metabolites increases the biomass productivity, mostly due to the extracellular polysaccharides providing an additional carbon source for the algae. This effect can persist for as many as 63 days before the metabolites significantly impact growth (Hadj-Romdhane et. al), although it should be noted that recycling water without treatment greatly increases the chances of bacterial contamination in the culture (Slade, 2013).

12.2.2 Disposal of algae

In the event that algae volume needs to be disposed of without harvesting (such as in the case of high contamination), the volume will be drained to a holding tank where it will be treated and killed using bleach before being sent to waste. This is standard protocol for disposal of algae.

12.2.3 Safety during operation

Consideration should be given to safe operation of the photobioreactor and downstream drying processes. Especially during the initial culture scale-up and when handling chemicals to mix the BBM medium, safe laboratory procedures must be followed according to MSDS information. Additionally, all Brazilian Regulatory Standards (NR) outlined in the Consolidation of Labor Laws (CLT) must be followed both on and off site. Special care should be taken around large process equipment such as the rotary dryer, or any process vessels and piping with high temperatures or pressures.

12.3 Process control

12.3.1 Transfer Between Day and Night Operation

Switching between day and night operation is a matter of draining the daytime system into the night tank. This is done by opening the drainage port at the bottom of the gas exchange column and utilizing the central pump line to feed the volume in the petals through the gas column into the night tank. To switch back to daytime operation, the drainage port is closed and the central line pump draws liquid back into circulation in the daytime system. The exact hour at which the switch occurs is determined by the hourly sunlight intensity profile in Northeast Brazil at any given point in the year so that the eight day operation hours are at peak intensity hours.

12.3.2 Manual vs. Dynamic control for steady-state operation

This pilot scale operation is controlled manually to operate at a steady state in both the day time and night time. This assumes constant cell density and growth rates throughout the periods of operation as well as a constant flow rate of flue gas with constant composition and properties, and constant growth conditions (outdoor temperature, sunlight during day hours, etc.). These are valid assumptions for a

process of this scale. If need be, operating conditions such as dilution rates and pH can be adjusted manually. For a larger scale operation though, dynamic control would need to be implemented. This would increase economy of scale. An ideal control system would constantly monitor cell density (and perhaps even other cell properties such as size of cells) and adjust parameters such as dilution rate or flue gas input rate in order to maintain constant and healthy cell growth. A thorough control system would also be able to alert operators if conditions fluctuate outside acceptable range (for example, if it is particularly hot one day and temperatures in the tubes rise significantly), or if a contaminant is present in the cultivation volume that presents significant threat to the health of the culture. Involving dynamic control in larger scale operations would allow for a more robust and tailorable process that could support a wider range of conditions and products. As well, it would reduce the need for on-site operators.

12.3.3 Maintenance and Emergency Control Procedures

The acrylic tubing will periodically require cleaning in order to remove build-up of dirt on the outside and/or biofouling on the insides. If the tubes are not operating at close to their optimal transmissivity, light access to the algae cells will be reduced and growth rates will slow. Therefore, periodic emptying of the tubular system will be required. While this occurs (likely during night hours), the volume will be maintained in the night tank to prevent halting operation.

Aside from maintenance, there may be events that fall significantly outside the expected range of operating conditions that result in the need for emergency action. These events include particularly drastic weather changes such as very high or very low temperatures, or extended storms, as well as sudden population drops or unacceptable levels of contamination. Depending on the circumstance, the algae volume may be able to be maintained in the night tank, which can provide a higher level of control and could be used to quickly boost population density. In the event of contamination, the cultivation volume will need to be drained to a holding tank where it will be treated and killed using bleach (standard protocol) before being sent to waste.

13 Conclusions and Recommendations

The novel Hybrid Petal Reactor for microalgae cultivation successfully converts over 50% of the carbon dioxide present in a stream of flue gas from a coal fired power plant. The process operates at a carbon dioxide input rate of 200 kilograms per day from a 10 vol% carbon dioxide flue gas stream. The project met a set of highly ambitious carbon conversion goals, and contributes to a positive outlook for the future of algae production for sustainable carbon emissions reduction and value-added product creation.

The innovative design incorporates a central gas exchange column with a horizontal tubular photobioreactor system that harnesses sunlight during the day, and an internally-illuminated nighttime tank that involves innovative use of optics. The outdoor system was designed to scale with a series of tubes that branch out like "petals" from the central gas exchange column. The tube design is optimized for high productivity and low costs. An emphasis was placed on designing a process highly considerate of biological constraints. The final design offers great flexibility and opportunity for scale-up.

A 9-15% Return on Investment is reported. This is an exciting result, as pilot plants rarely project profitability. Furthermore, this result stands out against a relatively unforgiving market landscape for carbon conversion technologies. This result is encouraging for the path to viability for high-capacity carbon conversion processes that utilise flue gases from fossil fuel power generation plants.

It is therefore recommended that a pilot-scale facility is built to test the design and collect empirical data in order to further optimize the process. This design is easily transitioned to larger scales, and economies of scale are expected. A move to larger scales would be encouraged. It is recommended that at larger scales, an emphasis be placed on decreasing power and water consumption through water recycling, heat integration, and the application of scale-able energy-saving post-processing methods. A carbon neutral process at all scales should be the goal. Not only could this process contribute to building and accelerating the development of the global carbon conversion market, but significant reductions in emissions could be achieved.

The global algae biomass market is currently projected to be valued at over $1.1 Billion at a volume of almost 30,000 tons per year by 2024. At the current scale, one pilot-plant of this design would produce enough biomass to support nearly 0.1% of projected volume. If ten operations with ten times the carbon conversion capacity were installed, this technology could support nearly 10% of the projected global algae biomass market volume for 2024. This is a promising prospect. It is expected that investment into technologies such as the Hybrid Petal Reactor presented in this report will catalyze a thriving algae carbon conversion industry, where carbon-neutral, value-added algae processes play a key role in the global effort towards a sustainable future.

14 Acknowledgements

We would like to thank Dr. Warren Seider and Geetanjali Yadav for sharing their expertise in microalgae growth and processing with us throughout the course of this project, as well as Dr. John Crocker for optical physics guidance. In addition, we greatly appreciate the guidance and helpful input during design meetings from the following industrial consultants: Mr Bruce Vrana, Dr. Michael Grady, Mr. Gary Sawyer, Mr. Adam A Brostow, Dr. Shaibal Roy, Dr. Richard Bockrath, and Dr. Arthur W. Etchells, III. The project author thanks the following for initial consulting during the project proposal phase: Dr Wen K. Shieh, Dr. Marylin Huff, and Dr Daeyeon Lee.

15 Bibliography

Alves, A. B., & Schmid, A. L. (2015). Cooling and heating potential of underground soil according to depth and soil surface treatment in the Brazilian climatic regions. *Energy and Buildings,90*, 41-50. doi:10.1016/j.enbuild.2014.12.025

Amos, W. A. (n.d.). *Report on Biomass Drying Technology* (Rep.). National Renewable Energy Laboratory. (NTIS No. NREL/TP-570-25885)

Blanken, W., Postma, P. R., De Winter, L., Wijffels, R. H., & Janssen, M. (2016). Predicting microalgae growth. *Algal Research,14*, 28-38.

Cao, C., Zhao, L., Xu, D., Geng, Q., & Guo, Q. (2009). Investigation into Bubble Size Distribution and Transient Evolution in the Sparger Region of Gas−Liquid External Loop Airlift Reactors. *Industrial & Engineering Chemistry Research,48*(12), 5824-5832. doi:10.1021/ie801700s

CarbonX Prize Competition Guidelines. (2016, March 1). NRG Cosia. V 1.4. Obtained from https://carbon.xprize.org/about/guidelines

"Commercial Refrigeration." Commercial Refrigeration Equipment Overview, www.fridgesolutions.com/terms-considerations.html.

Derjaguin, B.; Landau, L. (1941), "Theory of the stability of strongly charged lyophobic sols and of the adhesion of strongly charged particles in solutions of electrolytes", *Acta Physico Chemical URSS*, **14**: 633.

Dlouhy, J. A. (2017, June 19). Exxon Makes a Biofuel Breakthrough. Retrieved April 15, 2018, from https://www.bloomberg.com/news/articles/2017-06-19/genome-decoder-s-fatty-algae-is-biofuel-breakthrough-for-exxon

Ferguson, A., & Frangione, C. (2014). Carbon Conversion Landscape Analysis. *Carbon XPRIZE*. Retrieved from http://www.xprize.org/sites/default/files/carbon_conversion_landscape_analysis_2014.pdf

Gale, J., Bradshaw, J., Chen, Z., Garg, A., Gomez, D., Rogner, H., . . . Williams, R. (2005). Special Report on Carbon Dioxide Capture and Storage. IPCC.

García-Pérez, J. S., Beuckels, A., Vandamme, D., Depraetere, O., Foubert, I., Parra, R., & Muylaert, K. (2014). Influence of magnesium concentration, biomass concentration and pH on flocculation of Chlorella vulgaris. *Algal Research, 3*, 24-29. doi:10.1016/j.algal.2013.11.016

Ghadiryanfar, M., Rosentrater, K., Keyhani, A., & Omid, M. (2017). A review of macroalgae production, with potential applications in biofuels and bioenergy. Renewable & sustainable energy reviews, 54. doi: 10.1016/j.rser.2015.10.022

GlobalData. (2017). *Brazil Renewable Energy Policy Handbook 2017* (Rep. No. GDAE1102P).

Han, S., & Wu, W. (n.d.). Biofuel production from microalgae as feedstock: Current status and potential. *Critical Reviews in Biotechnology,35*(2), 255-268. doi:DOI: 10.3109/07388551.2013.835301

Huang, G., Chen, F., Kuang, Y., He, H., & Qin, A. (2015). Current Techniques of Growing Algae Using Flue Gas from Exhaust Gas Industry: a Review. Applied Biochemistry and Biotechnology,178(6), 1220-1238. doi:10.1007/s12010-015-1940-4

Hu, D., Li, M., Zhou, R., & Sun, Y. (2012). Design and optimization of photo bioreactor for O2 regulation and control by system dynamics and computer simulation. *Bioresource Technology,104*, 608-615. doi:10.1016/j.biortech.2011.11.049

Incropera, F. P., Dewitt, D. P., Bergman, T. L., & Lavine, A. S. (2003). *Fundamentals of heat and mass transfer*(7th ed.). Hoboken, NJ: John Wiley.

International Energy Agency. (November 12, 2013). World Energy Outlook 2013 factsheet. Retrieved from www.worldenergyoutlook.org/media/weowebsite/factsheets/WEO2013_Factsheets.pdf

Josling, T., Blandford, D., & Earley, J. (2010). *Biofuel and Biomass Subsidies in the U.S., EU and Brazil: Towards a Transparent System of Notification* (Issue brief). International Food & Agricultural Trade Policy Center.

Koller, M. *Design of Closed Photobioreactors for Algal Cultivation, 2015.* Retrieved from Part I of Algal Biorefineries, A. Prokop et al. (2015), DOI 10.1007/978-3-319-20200-6_4

Land Levelling. (2013). Chp 4.5 In *Best Management Practices for Agricultural Water Users*. Texas Water Development Board.

Lardon L Helias A Sialve B Steyer JP Bernard O . 2009. Life cycle assessment of biodiesel production from microalgae. Environmental Science and Technology 43: 6475–6481.

Lee, J., Seo, K. A., & Oh, Y. (2014). Effects of nitrogen and organic carbon sources on growth and lipid production of Chlorella sp. KR-1 in flask cultures. *Journal of Marine Bioscience and Biotechnology,6*(2), 110-117. doi:10.15433/ksmb.2014.6.2.110

Mandalam, R. K., & Palsson, B. (1998). Elemental balancing of biomass and medium composition enhances growth capacity in high-density Chlorella vulgaris cultures. *Biotechnology and Bioengineering, 59*(5), 605-611.

Matos, J., Cardoso, C., Bandarra, N. M., & Afonso, C. (2017). Microalgae as healthy ingredients for functional food: a review. Food Funct., 8(8), 2672-2685. doi: 10.1039/c7fo00409e

Micro-algae for mitigating carbon dioxide. (n.d.). Retrieved from http://www.climatetechwiki.org/technology/co2-mitigation-micro-algae

Minnesota Mining And Manufacturing Company, 1998: https://encrypted.google.com/patents/WO1999056158A1?cl=tr

Mohamed, L., Kouhila, M., Lahsasni, S., Jamali, A., Idlimam, A., Rhazi, M., . . . Mahrouz, M. (2004). Equilibrium moisture content and heat of sorption of Gelidium sesquipedale. *Journal of Stored Products Research*. doi:10.1016/s0022-474x(04)00023-2

Moody, J., McGinty, C. M., Quinn, J. C. 2014. Global productivity potential of microalgae, Proceedings of the National Academy of Sciences Jun 2014, 111 (23) 8691-8696; DOI: 10.1073/pnas.1321652111

NREL National Solar Radiation Database: https://nsrdb.nrel.gov/

NREL System Advisor Model: https://sam.nrel.gov/

Pond Technologies Gallery 1. (n.d.). Retrieved from http://pondtechnologiesinc.com/media/attachment/pond-technologies-gallery-01/

Sadeghizadeh, A., Farhad dad, F., Moghaddasi, L., Rahimi, R. (2017). CO capture from air by microalgae in an airlift photobioreactor. Bioresource Technology, 243, 441-447. doi: 10.1016/j.biortech.2017.06.147

Salassi, M. S. (2001). Estimated Costs of Precision Land Grading With On-Farm Labor. *Journal of the ASFMRA*. Retrieved from http://citeseerx.ist.psu.edu/viewdoc/download?doi=10.1.1.623.3534&rep=rep1&type=pdf

Sander, R. (1999, April 8). *Compilation of Henry's Law Constants for Inorganic and Organic Species of Potential Importance in Environmental Chemistry*[PDF]. Mainz, Germany: Air Chemistry Department, Max-Planck Institute of Chemistry.

Schenk PM Thomas-Hall SR Stephens E Marx UC Mussgnug JH Posten C Kruse O Hankamer B . 2008. Second generation biofuels: High-efficiency microalgae for biodiesel production. Bioenergy Research 1: 20–43.

Seider, W. D., Lewin, D. R., Seader, J. D., Widagdo, S., Gani, R., & Ng, K. M. (2016). *Product and process design principles synthesis, analysis and evaluation*. New York: John Wiley & Sons.

Shelp, B. J., & Canvin, D. T. (1980). Photorespiration and Oxygen Inhibition of Photosynthesis in Chlorella pyrenoidosa. *Plant Physiology,65*(5), 780-784. doi:10.1104/pp.65.5.780

Sim, T., Goh, A., & Becker, E. (1988). Comparison of centrifugation, dissolved air flotation and drum filtration techniques for harvesting sewage-grown algae. *Biomass, 16*(1), 51-62. doi:10.1016/0144-4565(88)90015-7

Slade, R. , Bauen, A. Micro-algae cultivation for biofuels: Cost, energy balance, environmental impacts and future prospects, 2013. Biomass and Bioenergy, Volume 53,Pages 29-38, ISSN 0961-9534, https://doi.org/10.1016/j.biombioe.2012.12.019.

Stein, J. (ED.) Handbook of Phycological methods. Culture methods and growth measurements. Cambridge University Press. 448 pp.

Stephens E Ross IL King Z Mussgnug JH Kruse O Posten C Borowitzka MA Hankamer B . 2010. An economic and technical evaluation of microalgal biofuels. Nature Biotechnology 28: 126–128.

Talbot, P., Gortares, M. P., Lencki, R. W., & Noüe, J. D. (1991). Absorption of CO2in algal mass culture systems: A different characterization approach. *Biotechnology and Bioengineering,37*(9), 834-842. doi:10.1002/bit.260370907

Transparency Market Research, Algae Market (Application - Marine Sector, Aviation Sector, Road Transport, DHA Production (Protein Sales), DHA Production (Pharmaceutical Applications), Bioplastics; Cultivation Technology - Open Ponds Cultivation, Raceway Ponds Cultivation, Closed Photobioreactor Cultivation, Closed Fermenter Systems Cultivation) - Global Industry Analysis, Size, Share, Growth, Trends, And Forecast 2016 - 2024 (Rep. No. TMRGL14804). (2016).

Turton, R. (2003). *Analysis, synthesis, and design of chemical processes*. Upper Saddle River, NJ: Prentice Hall.

Vandamme, D., Foubert, I., Fraeye, I., Meesschaert, B., & Muylaert, K. (2012). Flocculation of Chlorella vulgaris induced by high pH: Role of magnesium and calcium and practical implications. *Bioresource Technology, 105*, 114-119. doi:10.1016/j.biortech.2011.11.105

Vandamme, D., Foubert, I., & Muylaert, K. (2013). Flocculation as a low-cost method for harvesting microalgae for bulk biomass production. *Trends in Biotechnology, 31*(4), 233-239. doi:10.1016/j.tibtech.2012.12.005

Verwey, E. J. W.; Overbeek, J. Th. G. (1948), *Theory of the stability of lyophobic colloids*, Amsterdam: Elsevier.Williamson, Phil. "Scrutinize CO2 removal methods: the viability and environmental risks of removing carbon dioxide from the air must be assessed if we are to achieve the Paris goals." Nature, vol. 530, no. 7589, 2016, p. 153+.

Wigmosta, M. S., Coleman, A. S., Skaggs, R. J., Huesemann, M. H., Lane, L. J. National Microalgae Biofuel Production Potential and Resource Demand. Water Resources, Research. Published online April 13, 2011. DOI:10.1029/2010WR009966

WorldWatch, Herro, A. (n.d.). Better Than Corn? Algae Set to Beat Out Other Biofuel Feedstocks. Retrieved from http://www.worldwatch.org/node/5391

Xu, X., Song, C., Wincek, R., Andresen, J. M., Miller, B. G., & Scaroni, A. W. (2003). Separation of CO2 from Power Plant Flue Gas Using a Novel CO2 "Molecular Basket" Adsorbent. *Fuel Chemistry Division Preprints,48*(1), 162-163.

Zhang, X., Wang, L., Sommerfeld, M., & Hu, Q. (2016). Harvesting microalgal biomass using magnesium coagulation-dissolved air flotation. *Biomass and Bioenergy, 93*, 43-49. doi:10.1016/j.biombioe.2016.06.024

Zhu, X., Rong, J., Chen, H., He, C., Hu, W., & Wang, Q. (2016). An informatics-based analysis of developments to date and prospects for the application of microalgae in the biological sequestration of industrial flue gas. Applied Microbiology and Biotechnology,100(5), 2073-2082. doi:10.1007/s00253-015-7277-7

A Appendix

A .1 Matlab Code

A .1.1 Code for Optimization

GradDescent.m

```
%Script that runs the optimization procedure.

global ObjFuncTrack
ObjFuncTrack = [];
%Guesses: (Guess are for Daytime reactor)
L = 304;
A = 0.02315;
X = 1.689;

%Should include T_bubbler because the cooling will affect costs
x = [L A X];
diffs = [0.1, 0.00005, 0.01];
N = length(x);
xold = 999999*(1:N);
maxit = 1000;
iter = 0;
dx = inf*(1:N); %Just to get loop started
xTrack = [x,ObjFunc(x)];
alphaTrack = [];
while sum((abs(x-xold)./(x+xold))>0.000000001)>0 && iter<maxit %adjust these conditions
    iter = iter + 1;
    dx = -1*Grad(x,diffs);
    alpha = lineSearch(x,dx,@(x)ObjFunc(x));
    xold = x;
    x = x + alpha*dx;
    xTrack = [xTrack;x,ObjFunc(x)];
    alphaTrack = [alphaTrack,alpha];
end
if iter==maxit
    disp('Loop did not converge before reaching maxit')
    return
end
```

lineSearch.m

```
function alpha = lineSearch(x,dx,func)

%Function that returns the number alpha that minimizes func(x-alpha*dx)
%func is a function handle for the objective function

alpha = 0.1/norm(dx);
alphaIncr = 2; %Factor by which alpha gets increased
vOld = func(x);

if vOld==inf
    abc=123;
end

vNew = func(x + alpha*dx);
steps = 0;
if vNew < vOld
```

```
    Case = 1;
    while vNew < vOld
        steps = steps + 1;
        alpha = alpha*alphaIncr;
        vOld = vNew;
        vNew = func(x + alpha*dx);
    end
else
    Case = 2;
    while vNew > vOld
        steps = steps + 1;
        alpha = alpha/alphaIncr;
        vNew = func(x + alpha*dx);
        if alpha < 0.00000000000000001
            alpha = 0;
            return
        end
    end
end

phiInv = 0.61803398875;
if Case==1
    aH = alpha;
    if steps >= 2 %Just incase 0 should be lower bound
        aL = alpha/alphaIncr^2;
    else
        aL = 0;
    end
elseif Case==2
    aL = 0;
    aH = alpha*alphaIncr;
end
amH = aL + (aH - aL)*phiInv;
amL = aH - (aH - aL)*phiInv;
vH = func(x + aH*dx);
vL = func(x + aL*dx);
vmH = func(x + amH*dx);
vmL = func(x + amL*dx);
if Case==2 && min([vL,vmL,vmH,vH])>vOld
    epsilon = 10e-7;
else
    epsilon = 10e-5;
end

while abs((vmH-vmL)/(vmH+vmL))>epsilon || vmH==inf || vmL==inf
    if vmH > vmL
        aH = amH;
        vH = vmH;
        amH = amL;
        vmH = vmL;
        amL = aH - (aH - aL)*phiInv;
        vmL = func(x + amL*dx);
    elseif vmH <= vmL
        aL = amL;
        vL = vmL;
        amL = amH;
        vmL = vmH;
```

```
        amH = aL + (aH - aL)*phiInv;
        vmH = func(x + amH*dx);
    elseif vmH==inf && vmL==inf %Both are past the barrier stops
        aH = amL;
        amH = aL + (aH - aL)*phiInv;
        amL = aH - (aH - aL)*phiInv;
        vmH = func(x + amH*dx);
        vmL = func(x + amL*dx);
    end
end

alpha = (amL + amH)/2;
```

Grad.m

```
function dx = Grad(x,diffs)

%returns scaled-gradient of ObjFunc at point x

N = length(x);
dx = 1:N;
I = eye(N);
v0 = ObjFunc(x);
for i = 1:N
    dx_i = diffs.*I(i,:); %selects ith component of diffs
    v1 = ObjFunc(x+dx_i);
    dx(i) = (v1 - v0)/diffs(i);
end
dx = dx.*(x.*x);

if sum(isfinite(dx)) < N
    bads = ~isfinite(dx);
    dx = 0*(1:N);
    for i = 1:N
        if bads(i)
            dx(i) = 10;
        end
    end
end
```

A .1.2 Code for Photobioreactor Process Simulation and Optimization

mainModelFunc.m

```
function [Prod,TotalPdrop,Qout,Ecool,deltaT,seqFrac,LDR] = ...
            mainModelFunc(Ltest,Atest,Xtest,Qgas)

%Function that runs Photobioreactor process simulation, as a function of L,
%A X, and F_2

global Yco2 Yo2 I A L Tbubbler Tair diameter Ks Ke H_O2 umax Nu ...
    HeatCond dPdx density

%Define Constants
H_CO2 = 34; %(mol/m3*atm)
H_O2 = 1.3; %(mol/m3*atm)
H_NO = 34; %(mol/m3*atm)
```

```
H_NO2 = 1.3; %(mol/m3*atm)
H_SO2 = 1.3; %(mol/m3*atm)
kla_CO2 = 0.26; %(m/s) * (m2/m3)
%kla_CO2 = 0.11; %(m/s) * (m2/m3)
kla_O2 = 0.26; %(m/s) * (m2/m3)
kla_NO = 0.26; %(m/s) * (m2/m3)
kla_NO2 = 0.26; %(m/s) * (m2/m3)
kla_SO2 = 0.26; %(m/s) * (m2/m3)
R = 0.000082057; %m3*atm/mol*K
Ks = 0.000167; %mol/m3,
Ke = 18.7;
umax = 0.27/3600; %1/s
density = 1000; %kg/m3

Yco2 = 41.63; %mol CO2 sequestered per kg algae grown
Yo2 = 41.63; %mol O2 released per kg algae grown

%Define system parameters
L = Ltest; %tube length (m)
A = Atest; %tube cross sectional area (m2)
Qout = .3*A; %m3/s
P = 1; %atm
y_in = 0.1; %mol fraction CO2 in input flue gas, dimensionless
gamma_in = 0.1; %mol fraction O2 in input flue gas, dimensionless
NO_in = .1;
NO2_in = .1;
SO2_in = .1;
I = 825; %Intensity W/m2
Tbubbler = 303; %K , Bubbler temp held fixed by HX
h = 3; %Bubbler height (m)
Radius = 0.001; %Bubble radius (m)
rhoDiff = 998; %density difference between bubble and liquid (kg/m3)
mu = 0.00089; %Dynamic Viscosity of liquid (kg/m*2)
%Qgas = .1; %Flow rate of flue gas through bubbler per reactor tube (m3/s)
Tair = 290; %Ambient air temperature in (K)
Vwind = 3.3; % Wind speed around tubes (m/s)

%Calculated parameters
K1_CO2 = H_CO2*kla_CO2*R*Tbubbler;
K1_O2 = R*Tbubbler*H_O2*kla_O2;
K1_NO = H_NO*kla_NO*R*Tbubbler;
K1_NO2 = H_NO2*kla_NO2*R*Tbubbler;
K1_SO2 = H_SO2*kla_SO2*R*Tbubbler;
texit = h*9*mu/(2*rhoDiff*Radius^2); % (s) residence time of bubbles in bubbler
diameter = 2*sqrt(A/3.14159);
velocity = Qout/A;

%Parameters for P drop and heat transfer calculations
Pr = 0.786-0.000397*Tair+0.000000448*Tair^2; %Pr of ambient air
KinVisc = -0.00000318+0.0000000335*Tair+9.82E-11*Tair^2; % Kinematic viscosity of ambient air
Re = Vwind*diameter/KinVisc;
Nu = 0.3+0.62*Re^0.5*Pr^0.333*(1+(Re/282000)^0.625)^0.8 ...
    /(1+(0.4/Pr)^0.667)^0.25; %Incropera Eqn 7.54
HeatCond = 0.0000727*Tair+0.00454;
ReD = velocity*diameter/0.8e-6;
fdfind = @(fd) 1/sqrt(fd)+1.93*log10(1.9/(ReD*sqrt(fd)));
```

```
if ~(-999999<fdfind(0.03) && fdfind(0.03)<999999) && imag(fdfind(0.03))~=0
    abc = 1;
end
try
    fd = fzero(fdfind,0.03);
catch
    fd=0.03;
end
if isnan(fd)
    fd = 0.03;
end
dPdx = fd*density*velocity^2/(2*diameter);
TotalPdrop = dPdx*L; %Pa, pressure drop through tubes

%Set desired Xout
Xout = Xtest; %kg/m3

%Guess values of calculated parameters (using Henry's law)
CO2out = H_CO2*P*y_in; %Concentration of CO2 in Bubbler, mol/m3
O2out = H_O2*P*gamma_in; %Concentration of O2 in Bubbler, mol/m3

CO2out_old = inf;
O2out_old = inf;
iterations = 0;
expelledO2 = 0;
maxit = 200; %maximum number of iterations
while abs(CO2out_old-CO2out)>0.01 && abs(O2out_old-O2out)>0.01 && iterations<maxit
    %'here'
    CO2out_old = CO2out;
    O2out_old = CO2out;
    iterations = iterations + 1;

    %Run horizTubeModel to get tube outputs (the ins) given guesses
    [Xin,CO2in,O2in,Tin,uTrack,LDRTrack] = horizTubeModel(O2out,CO2out,Xout,Qout);
    if O2in > H_O2*P
        expelledO2 = expelledO2 + O2in-H_O2*P;
        O2in =H_O2*P;
    end
    %Determine Harvest rate and rate of liquid into bubbler
    Qharvest = (Xin*Qout-Xout*Qout)/Xin;
    Qin = Qout - Qharvest; %Qin is flow into bubbler from tube. It's not fresh feed!

    %Use mass transfer equations to update guesses
    CO2out = (y_in*(exp(-K1_CO2*texit)-1)-CO2in*Qin*R*Tbubbler/(P*Qgas))/ ...
        (exp(-K1_CO2*texit)/(P*H_CO2)-1/(P*H_CO2)-R*Tbubbler*Qout/(P*Qgas));
    O2out = (Qin*O2in*R*Tbubbler/(P*Qgas)+gamma_in-gamma_in*exp(-K1_O2*texit)) / ...
        (Qout*R*Tbubbler/(P*Qgas)-exp(-K1_O2*texit)/(P*H_O2)+1/(P*H_O2));
end

if iterations==maxit
    disp(strcat('Error: balances did not converge in',{' '},string(maxit), ...
        ' iterations. Consider increasing maxit.') )
    Prod = 0;
    TotalPdrop = 10000;
    Ecool = 1;
    deltaT = 25;
    seqFrac = .4;
```

```
    LDR = .04;
    return %Exit script
end

%Cooling required
Cp = 4185.5; %Heat capacity of liquid (assume it's independent of X), J/kg*K
Ecool = Qin*Cp*(Tin-Tbubbler);

%Determine NOx and SOx for pH calcs
NO = NO_in*(exp(-K1_NO*texit)-1)/ ...
    (exp(-K1_NO*texit)/(P*H_NO)-1/(P*H_NO)-R*Tbubbler*Qout/(P*Qgas));
NO2 = NO2_in*(exp(-K1_NO2*texit)-1)/ ...
    (exp(-K1_NO2*texit)/(P*H_NO2)-1/(P*H_NO2)-R*Tbubbler*Qout/(P*Qgas));
SO2 = NO_in*(exp(-K1_SO2*texit)-1)/ ...
    (exp(-K1_SO2*texit)/(P*H_SO2)-1/(P*H_SO2)-R*Tbubbler*Qout/(P*Qgas));
Qout*(NO+NO2+SO2);

%Back to horizTubeModel and repeat
biomassPerSecondPerTube = (Xin-Xout)*Qout;
CO2PerSecondPerTube = biomassPerSecondPerTube*Yco2; %mol/s per tube
CO2total = 170.415/3600; %required uptake per second
NumTubes = CO2total/CO2PerSecondPerTube;
FlueGasReq = CO2PerSecondPerTube/y_in;
Prod = Qharvest*Xin;

deltaT = abs(Tin-Tbubbler);

removed = (CO2out-CO2in)*Qout;
entering = Qgas*y_in/(R*Tbubbler);
seqFrac = removed/entering;
LDR = mean(LDRTrack(1:99));
```

horizTubeModel.m

```
function [Xin,CO2in,O2in,Tin,uTrack,LDRTrack] = horizTubeModel(O2out,CO2out,Xout,Q)

%Function that integrates petal tube mass and energy balances


%out (in) means out of (in to) bubbler, not tubes!!!

global Yco2 Yo2 I A L Tbubbler Tair diameter Nu HeatCond dPdx density

T = Tbubbler;
O2 = O2out;
CO2 = CO2out;
X = Xout;
Cp = 4185.5; %Heat capacity of liquid (assume it's independent of X), J/kg*K
Halg = 15000000; %Enthalphy of burning algae (J/kg)
velocity = Q/A;

if CO2 < 0
    CO2=0;
end

steps = 100;
tau = A*L/Q;
```

```
dt = tau/steps;
dx = dt*velocity; %m, Distance traveled in time step
dVol = dx*A; %m3, volume of differential plug
stepnum = 0;
uTrack = 1:steps;
LDRTrack = 1:steps;
for step=linspace(0,tau,steps)
    %Mass bal
    [u,LDR] = mu1(I,CO2,O2,X);
    dX = X*u*dt;
    X = X + dX;
    O2 = O2 + dX*Yo2;
    CO2 = CO2 - dX*Yco2;
    if CO2 < 0
        CO2 = 0;
    end

    %E Bal
    dQconv = Nu*HeatCond*3.14159*(Tair-T)*dx*diameter*dt; %J, Convective heat
            %transfer to differential piece of reactor
    dQlight = dx*diameter*I*dt; %Total light energy onto plug
    dQgrowth = dX*dVol*Halg; %Amount of energy CONSUMED by algae to produce
            %biomass. Note the sign in the delta T line.
    dQfric = dPdx*dx*dVol;
    T = T + (dQconv+dQlight-dQgrowth+dQfric)/(dVol*density*Cp);
    stepnum = stepnum + 1;
    uTrack(stepnum) = u;
    LDRTrack(stepnum) = LDR;
end
Xin = X;
CO2in = CO2;
O2in = O2;
Tin = T;
```

mu1.m

```
function [u,LightDarkRatio] = mu1(I0,CO2,O2,X)

%This function gives the specific growth rate as a function of light
%intensity, CO2 concentration, O2 concentration, and algae concentration

global Ks Ke H_O2 umax diameter A
if CO2<0
    disp('Warning: mu.m was passed a negative value for O2 or CO2')
end
Po2 = 100*O2/H_O2; %Percent O2
if Po2>100
    Po2=100;
end
PInhib = -0.0011*Po2^2+.3988*Po2-5.2934; %Percent inhibition by O2
B = 187; %from umax and Beers law paper

KA = umax*I0*CO2*(100-PInhib)/100;
KB = B*X;
KC = Ke*(Ks+CO2);
KD = I0*(Ks+CO2);
u = 0;
```

```
steps = 10;
dy = diameter/(2*steps);
for y = linspace(0,diameter/2,steps) %Numerical integral of mu_y over horizontal
        %cross sections
    pathLen = 2*sqrt(diameter^2/4-y^2); %length of path of light
    mu_y = (KA*KB*pathLen-A*log(KC*exp(KB*pathLen)+KD))/(KB*KD); %Integral of
        % mu from 0 to pathlength
    u = u + mu_y*dy;
end
u = 2*u/A; %Average mu

%Light/Dark ratio calculation
LightDef = 0.01; %Fraction of umax required to be considered "in light"
a = -log(LightDef)/(2*B*X);
b = diameter/2;
alpha = sqrt(b^2 - a^2);
C = b^2*atan(alpha/a)-alpha*a;
LightDarkRatio = A/(2*C) - 1;
```

QgasSelect

```
function [Prod,TotalPdrop,Qout,Ecool,deltaT,seqFrac,LDR] = QgasSelect(x)

%Function that determines F_2 requirement to meet 50% CO2 sequestration

Qgas = fminbnd(@(Q)Er2(Q,x),0.000001,0.01);
[Prod,TotalPdrop,Qout,Ecool,deltaT,seqFrac,LDR] = mainModelFunc(x(1),x(2),x(3),Qgas);
end

function E = Er2(Q,x)

%Function that returns error which reflects deviation from sequestration
%goal.

Qdim = size(Q);
if Qdim(2)>1
    abc = 123;
end
if Q<=0
    E = inf;
    return
end
[~,~,~,~,~,a,~] = mainModelFunc(x(1),x(2),x(3),Q);
E = (a-0.52)^2;
end
```

ObjFunc.m

```
function loss = ObjFunc(x)

% Function f_1 in described in Optimization section. Reflects -1*(profits
% per tube) + Constraint barriers

%loss is -1*profits per tube
global ObjFuncTrack

%Barriers on x (L,A,X, and Qgas):
```

```
low_barrier_starts = [1,5e-5,0.01];
low_barrier_stops = [5e-6,5e-6,5e-6];
loss = 0;
N = length(x);
for i = 1:N
    if x(i) <= low_barrier_stops(i)
        loss = Inf;
        return
    elseif x(i)< low_barrier_starts(i)
        E = (x(i) - low_barrier_stops(i))/(low_barrier_starts(i)-low_barrier_stops(i));
        loss = loss + E - log(E) - 1;
    end
end

%Run simulation
[Prod,TotalPdrop,Qout,Ecool,deltaT,seqFrac,LDR] = QgasSelect(x);


%Additional Barriers:
deltaTstart = 18;
deltaTstop = 20;
if deltaT >= deltaTstop
    loss = inf;
    return
elseif deltaT >= deltaTstart
    E = (deltaTstop-deltaT)/(deltaTstop-deltaTstart);
    loss = loss + E - log(E) - 1;
end

seqFracstart = .51;
seqFracstop = .5;
if seqFrac <= seqFracstop
    loss = inf;
    return
elseif seqFrac <= seqFracstart
    E = (seqFrac-seqFracstop)/(seqFracstart-seqFracstop);
    loss = loss + E - log(E) - 1;
end

LDRstart = .12;
LDRstop = .10;
if LDR <= LDRstop
    loss = inf;
    return
elseif LDR <= LDRstart
    E = (seqFrac-LDRstop)/(LDRstart-LDRstop);
    loss = loss + E - log(E) - 1;
end

%Calculating Costs and Revenue:

%Biomass selling cost = $1.2/kg
%Acrylic cost = $1/kg
radius = sqrt(x(2)/3.14159);
thickness = 0.005;
AcrylCost = x(1)*(3.14159*(radius+thickness)^2-x(2))*1*1180/(3600*24*365*10);
        %The 10 at the end is lifetime in years
```

```
LandCost = x(1)*4*radius*(3036.39/10000)*.04/(3600*24*365);
        %Change 1234 to su'm that makes sense...
NutCost = 0.0001*x(1)*x(2)*Prod; %using Mikaela's formula
CoolingCost = Ecool*(1/3.4+1)*.17/(1000*3600); %0.01 is cost of cooling 1 m3/s of flue gas
PumpingCost = TotalPdrop*Qout*(1/.7)*.17/(1000*3600);

Revenue = Prod*1.2;

loss = loss + AcrylCost + LandCost + NutCost + CoolingCost + PumpingCost - Revenue;
ObjFuncTrack = [ObjFuncTrack;[x loss]];
```

KlaCalcs.m

```
%Script that estimates of k_La (mass transfer coefficients) in bubbler

P = 1;
R = 0.08201;
T = 303;
MW = (.1*44 + .1*32 * .8*14)/1000;
do = 0.001;
holes = 1200;
Qgas = 0.0053;
QperHole = Qgas*11.9206/holes;
rhog = P*MW/(R*T); %bubble density
mug = 1.81e-5; % water viscosity, from wikipedia
db = .19*do^.48*(4*QperHole*rhog/(3.14159*do*mug))^.32;
size = sqrt(holes); %cm, side length of square to fit all the holes, with 1cm spacing
kl = 5.32e-4;
kla = kl*6/db;
```

flueGasTemp.m

```
%Script that estimates the temperature of flue gas entering the bubbler,
%after flowing through stream 2 from power plant.

%Required heat removal in bubbler
m = 1320/8/3600; %kg/s
dT = 3; %Needs to be low!!
Cp = 1; %kJ/kg*K
Qflue = m*Cp*dT; %kW
V = 1129/8/3600; %m3/s flue gas
Vwater = 9.43e-5; %m3/s
Cpwater = 4.1855;
Qwater = Vwater*1000*Cpwater*dT; %kW

diameter = .1;
L = 100;
tau = L*(diameter/2)^2*3.14159/V;
velocity = (L/tau);
Tair = 300;
Vwind = 1;
Pr = 0.786-0.000397*Tair+0.000000448*Tair^2; %Pr of ambient air
KinVisc = -0.00000318+0.0000000335*Tair+9.82E-11*Tair^2; % Kinematic
        %viscosity of ambient air
Re = Vwind*diameter/KinVisc;
Nu = 0.3+0.62*Re^0.5*Pr^0.333*(1+(Re/282000)^0.625)^0.8 ...
```

```
    /(1+(0.4/Pr)^0.667)^0.25; %Incropera Eqn 7.54
HeatCond = 0.0000727*Tair+0.00454;
ReD = velocity*diameter/0.8e-6;
fdfind = @(fd) 1/sqrt(fd)+1.93*log10(1.9/(ReD*sqrt(fd)));
fd = fzero(fdfind,0.03);

L = 100;
tau = L*(diameter/2)^2*3.14159/V;
steps = 5000;
dt = tau/steps;
T = 200+273;
rho = m/V;
dx = L/steps;
dM = ((L/steps)*(diameter/2)^2*3.14159)*rho;
TTrack = [];
for i = linspace(0,tau,steps)
    dQconv = Nu*HeatCond*3.14159*(Tair-T)*dx*diameter*dt;
    T = T + dQconv/(dM*Cp);
    TTrack = [TTrack,T];
end
plot(TTrack)

velocity = (L/tau);
dPdx = fd*rho*velocity^2/(2*diameter);
TotalPdrop = dPdx*L;
Tdiff = T - Tair;
```

A .1.3 Code for Nighttime Tank Lighting Optimization

muSet.m

```
function LPT = muSet(r0,d)

%Function that finds minimum number of lights per tube that meets intensity
        %requirements

LPT = fminbnd(@(L)Er(r0,d,L),1,10000);

end

function Error = Er(r0,d,L)

%Function that returns a value indicating deviation from minimum intensity
        %requirement

N = 24; %Choose even N
CO2 = 2.1034;
O2 = 0.1624;
P_LED = L*.95; % 1 W per mount, assume 95% efficiency
I0 = P_LED/(2*pi()*r0*2.45);

muTrack = [];
muCheck = 0;
ITrack = [];
xstep = 0;
totstep = 0;
I = 1;
position = r0;
```

```
while I>.19
    position = position + r0/50;
    I = intensity(N/2+position/d,N/2,N,r0,d,I0);
end
LightArea = (position^2-r0^2)*3.14159/6;
TotalArea = (d/2)*(d/2)*cos(3.14159/6)*.5-r0^2*3.14159/6;

Error = (LightArea/TotalArea-0.12)^2;
end

function I = intensity(rx,ry,N,r0,d,I0)

%Function that returns intensity in the tank at a given position

B = 187; %Beers law constant
X = 1.663;
I = 0;
for Rx = 1:N
    for Ry = 1:N
        rel = d*sqrt((Rx - rx)^2+0.75*(Ry-ry)^2);
        I = I + I0*exp(X*B*(r0-rel))*r0/rel;
    end
end
end

function u = mu(I,CO2,O2)

%Function that returns specific growth rate, given intensity, CO2
%concentration, and O2 concentration.

umax = 0.27/3600;
Ke = 18.7;
Ks = 0.000167;
H_O2 = 1.3;
Po2 = 100*O2/H_O2; %Percent O2
PInhib = -0.0011*Po2^2+.3988*Po2-5.2934;
u = umax*I*CO2./((Ke+I)*(Ks+CO2))*(100-PInhib)/100;
end
```

ObjFunc.m

```
function loss = ObjFunc(x)
global ObjFuncTrack

LPT = muSet(x(1),x(2));

%Barriers on x (r0,d,LPT):
low_barrier_starts = [0.01,x(1)*2.2,1];
low_barrier_stops = [0.007,x(1)*2.1,0];
loss = 0;
N = length(x);
for i = 1:N
    if x(i) <= low_barrier_stops(i)
        loss = Inf;
        return
    elseif x(i)< low_barrier_starts(i)
        E = (x(i) - low_barrier_stops(i))/(low_barrier_starts(i)-low_barrier_stops(i));
```

```
        loss = loss + E - log(E) - 1;
    end
end

%Additional Barriers:
%Mounts are 3.45mm x 3.45mm
LED_fitstop = .85*pi()*(x(1)-0.002)^2 / 0.00345^2;
LED_fitstart = LED_fitstop*0.95;
if LPT >= LED_fitstop
    loss = inf;
    return
elseif LPT >= LED_fitstart
    E = (LED_fitstop-LPT)/(LED_fitstop-LED_fitstart);
    loss = loss + E - log(E) - 1;
end

%max radius
r0stop = .06;
r0start = 0.05;
if x(1) >= r0stop
    loss = inf;
    return
elseif x(1) >= r0start
    E = (r0stop-x(1))/(r0stop-r0start);
    loss = loss + E - log(E) - 1;
end

%From Mikaela:
h = 2.45-.85*4*x(1)^2*2.45/x(2)^2;
numTubes = .85*4*91/(x(2)^2*pi()*h);

% %Old Method (using pipes and film)
% thickness = 0.003;
% AcrylCost = numTubes*2.45*3.14159*(x(2)^2-(x(2)-thickness)^2)*1*1180/10;
% FilmCost = (numTubes*x(1)*2*pi()*2.45*138.44)/10;
% LightCost = numTubes*LPT*.16/5;
% ElectricityCost = numTubes*LPT*.00016*16*365;
% loss = loss + FilmCost + LightCost + AcrylCost + ElectricityCost;

innerV = pi()*(x(1)-0.002)^2*2.45;
outerV = pi()*x(1)^2*2.45;
PTFECost = numTubes*(outerV-innerV)*2200*0.6/20;
MACost = numTubes*innerV*950*.35/20;
LightCost = numTubes*LPT*.16/8;
ElectricityCost = numTubes*LPT*.00016*16*365;
TankCost = (numTubes*outerV+91)*30/10; %should be 78, but it's not working for some reason...
ManufCost = numTubes*2.45*3/8;
%All costs are per year
loss = loss + PTFECost + MACost + LightCost + ElectricityCost+TankCost+ManufCost;
ObjFuncTrack = [ObjFuncTrack;[x loss]];
```

A .2 Estimation of Bare Module Costs

Most of the fabricated equipment for this process will require some level of customization, as it is unique to the design. This made finding accurate costs and Bare Module Factors (BMF) difficult. Most of the equipment costs were estimated by searching B2B-provided listings. Furthermore, many of the purchased machinery, such as pumps, would be purchased at a smaller scale than would normally be used for a full scale chemical production plant. This means that many of the reported Bare Module Factors from sources such as Seider et al overestimate the indirect costs associated with things like installation. Finally, this pilot plant can be considered part of a start-up business scenario, where much of the custom fabrication could be done cheaply on-site by start-up business owners. The following sections list the BMF for each equipment item, accompanied by an explanation of how or where the Bare Module Factors were estimated or sourced from. Smaller or very simple pieces of equipment like plastic holding tanks were assigned smaller BMFs, while more complex equipment such as pressure vessels were assigned BMFs more consistent with those assigned to similar equipment in larger scale facilities. Refer to Section 10 for equipment specification sheets and Section 11 for the full table of costs. Note that the final profitability analysis (Section 11) was performed using contingency factors ranging from 15 to 50 percent of the direct permanent investment to further account for unexpected costs.

Plastic Gas Exchange Tank (E-2): 2.1 This is a small plastic tank with a maximum volume of 3000L. The listed B2B price is $100 including accessories such as a mesh exhaust cover and input/output pipes. One provider lists an additional $100 fee to cover installation, which was therefore included in the BMF.

Acrylic Tubing (A): 1.1 The listed price is $1/kg for custom made acrylic tubes of the size that is desired for this design. Installation would involve piecing together individual lengths of tubing (lengths do not exceed 13 meters, so handling can be performed easily by one person) and arranging them in the layout described in Section 4. Cost of installation was determined by estimating the cost of paying someone at a rate consistent with engineering hourly pay in Ceara, Brazil, for the time required to piece together each length of tubing with a pipe elbow fitting. Time per connecting two lengths was conservatively estimated at approximately twenty minutes, resulting in 4% of total costs. The cost for elbow fittings is 1% of the total acrylic cost and was also included in the BMF. The final BMF was raised to 1.1 to include any other small indirect costs.

Multi-stage Blower (E-1): 2.15 This is the bare module cost given for gas compressors in Chapter 16 of *Product and Process Design Principles* (Seider et. al, 2016).

Water Chiller (E-3): 1.1 This is a small $380 water chiller that is listed as involving "easy installation". It can be installed as-is into the plastic water tank by a single person in little time. A BMF of

1.1 includes any added costs associated with piping and tubing.

Centrifugal Pump (E-4): 1.1 This a small pump, costing less than $3000. It is listed as a simple structure involving convenient operation. The pump is small and can be set up by one or two people in little time, resulting in low installation fees. This cost and other direct and indirect costs should not exceed $300.

Night Tank (E-11): 3 The listed B2B price for the large 100m3 night tank was $5000. The provider manufactures individual siding plates that are then custom-configured to reflect the customers desired tank height. For the volume required for this design, the total listed cost would be approximately $50/m3. Other providers listed similar costs for similar scales and manufacturing methods. Installation costs at a rate of pay consistent with engineering pay in Ceara, Brazil were lumped into a BMF of 3, which includes other indirect and direct costs as well. This is a conservative estimate, compared to the methods outlined in Chemical process equipment: Selection and design(2nd ed.), Couper, J. R. (2005). Amsterdam: Elsevier. (http://kkft.bme.hu/htms/kornykozp/Cost.of.Equipments.pdf)

LEDs (B): 1.05 The cost per LED is $0.16. Installation involves soldering the LED mount onto a light guide base. This should be able to be easily accomplished in under 5 hours given the small size and simple procedure.

PTFE Granules (D), PMMA Granules (C): 2 PTFE granules will be melted down and formed into tubes in a mold, after which the roughening procedure (described in Section 7) will take place. PMMA granules will be then melted down and poured into the PTFE hollow tubes, forming the core of the light guide. The BMF accounts for low-cost materials required to perform this manufacturing, as well as costs associated with pay consistent with engineer pay in Ceara, Brazil, for performing the manufacturing and installation.

Chemical Storage Containers: 1.05 These are small storage containers requiring almost no added costs, and no installation.

Peristaltic Pumps: 1.05 These are very small pumps requiring only a small amount of added (and very cheap) tubing, and short set-up time by one person.

Rotary Steam Dryer (E-10): 1.3 The BMF was found in Figure A.7 of Analysis, synthesis, and design of chemical processes (Turton, 2003) as a conservative estimate for a rotary dryer.

Gas Blower (E-7): 2.15 This is the bare module cost given for gas compressors in Chapter 16 of *Product and Process Design Principles* (Seider et. al, 2016).

Pressure Vessel (E-8): 4.16 This is the bare module cost given for gas compressors in Chapter 16 of *Product and Process Design Principles* (Seider et. al, 2016).

Flotation Tank (E-6): 1.2 This is a small tank consisting of 14 panels of 1mx0.5m that are easily configured into a tank of volume 1.5m3. Installation is included at a rate of pay consistent with engineer

pay in Ceara, Brazil.

Holding Tank (E-5): 1.05 This is a small plastic tank solely for the purpose of holding harvested algae. It will require very little installation or other indirect costs.

A .3 Aspen Plus Rotary Steam Tube Dryer Simulation

```
 + + + + + + + + + + + + + + + + + + + + + + + + + + + + + + + + + + + + + + + + + + + + + + + + + + + +
 + + + + + + + + + + + + + + + + + + + + + + + + + + + + + + + + + + + + + + + + + + + + + + + + + + + + +
 + +                                                                                                 + +
 + +                        ASPEN PLUS CALCULATION REPORT                                            + +
 + +                                                                                                 + +
 + + + + + + + + + + + + + + + + + + + + + + + + + + + + + + + + + + + + + + + + + + + + + + + + + + + + +
 + + + + + + + + + + + + + + + + + + + + + + + + + + + + + + + + + + + + + + + + + + + + + + + + + + + + + +

 ASPEN PLUS IS A TRADEMARK OF           HOTLINE:
 ASPEN TECHNOLOGY, INC.                 U.S.A. 888/996-7100
 781/221-6400                           EUROPE (44) 1189-226555

 PLATFORM: WINDOWS                                      APRIL 10, 2018
 VERSION: 36.0   Build 249                              TUESDAY
 INSTALLATION:                                          6:02:58 A.M.

ASPEN PLUS   PLAT: WINDOWS   VER: 36.0                  04/10/2018  PAGE    I
```

```
      ASPEN PLUS (R) IS A PROPRIETARY PRODUCT OF ASPEN TECHNOLOGY, INC.
      (ASPENTECH), AND MAY BE USED ONLY UNDER AGREEMENT WITH ASPENTECH.
      RESTRICTED RIGHTS LEGEND:  USE, REPRODUCTION, OR DISCLOSURE BY THE
      U.S. GOVERNMENT IS SUBJECT TO RESTRICTIONS SET FORTH IN
      (i) FAR 52.227-14, Alt. III, (ii) FAR 52.227-19, (iii) DFARS
      252.227-7013(c)(1)(ii), or (iv) THE ACCOMPANYING LICENSE AGREEMENT,
      AS APPLICABLE. FOR PURPOSES OF THE FAR, THIS SOFTWARE SHALL BE DEEMED
      TO BE "UNPUBLISHED" AND LICENSED WITH DISCLOSURE PROHIBITIONS.
      CONTRACTOR/SUBCONTRACTOR: ASPEN TECHNOLOGY, INC. 20 CROSBY DRIVE,
      BEDFORD, MA 01730.
                              TABLE OF CONTENTS


           RUN CONTROL SECTION.....................................  1
                RUN CONTROL INFORMATION............................  1

           FLOWSHEET SECTION.......................................  2
                FLOWSHEET CONNECTIVITY BY STREAMS..................  2
                FLOWSHEET CONNECTIVITY BY BLOCKS...................  2
                CONVERGENCE STATUS SUMMARY.........................  2
                DESIGN-SPEC:  DS-1.................................  2
                CONVERGENCE BLOCK:  $OLVER10.......................  2
                COMPUTATIONAL SEQUENCE.............................  3
                OVERALL FLOWSHEET BALANCE..........................  3
```

RUN CONTROL SECTION

RUN CONTROL INFORMATION

THIS COPY OF ASPEN PLUS LICENSED TO UNIVERSITY OF PENNSYLVAN

TYPE OF RUN: EDIT

INPUT FILE NAME: _1810itd.inm

INPUT PROBLEM DATA FILE NAME : _1810itd
OUTPUT PROBLEM DATA FILE NAME: _0253xrf
LOCATED IN:

PDF SIZE USED FOR INPUT TRANSLATION:
NUMBER OF FILE RECORDS (PSIZE) = 0
NUMBER OF IN-CORE RECORDS = 256
PSIZE NEEDED FOR SIMULATION = 1

CALLING PROGRAM NAME: apmain
LOCATED IN: C:\Program Files (x86)\AspenTech\Aspen Plus V10.0\Engine\\xeq

SIMULATION REQUESTED FOR ENTIRE FLOWSHEET

FLOWSHEET SECTION

FLOWSHEET CONNECTIVITY BY STREAMS

STREAM	SOURCE	DEST	STREAM	SOURCE	DEST
1	----	HX	2	----	HX
4	HX	----	3	HX	----

FLOWSHEET CONNECTIVITY BY BLOCKS

BLOCK	INLETS	OUTLETS
HX	2 1	4 3

```
 CONVERGENCE STATUS SUMMARY
 --------------------------

   DESIGN-SPEC SUMMARY
   ===================


   DESIGN                                                          CONV
   SPEC      ERROR        TOLERANCE    ERR/TOL      VARIABLE   STAT  BLOCK
   ------    -----        ---------    -------      --------   ----  -----
   DS-1     -0.39065E-03  0.10000E-02 -0.39065       44.483     #    $OLVER10

   #  = CONVERGED
   *  = NOT CONVERGED
   LB = AT LOWER BOUNDS
   UB = AT UPPER BOUNDS

 DESIGN-SPEC:  DS-1
 ------------------

   SAMPLED VARIABLES:
     VFRAC    : VAPOR FRACTION IN STREAM 4 SUBSTREAM MIXED

   SPECIFICATION:
     MAKE VFRAC APPROACH 0.100000
     WITHIN          0.00100000

   MANIPULATED VARIABLES:
     VARY     : TOTAL MASSFLOW IN STREAM 2 SUBSTREAM MIXED
     LOWER LIMIT =          15.0000                   KG/HR
     UPPER LIMIT =          50.0000                   KG/HR
     FINAL VALUE =          44.4831                   KG/HR

   VALUES OF ACCESSED FORTRAN VARIABLES:
     VARIABLE      VALUE AT START      FINAL VALUE     UNITS
                      OF LOOP
     --------      --------------      -----------     -----
     VFRAC          0.203542           0.996094E-01

 CONVERGENCE BLOCK:  $OLVER10
 ----------------------------
     SPECS: DS-1
ASPEN PLUS   PLAT: WINDOWS   VER: 36.0                   04/10/2018  PAGE 3

                               FLOWSHEET SECTION

 CONVERGENCE BLOCK:  $OLVER10 (CONTINUED)
     MAXIT=   30 STEP-SIZE=    1.0000    % OF RANGE
                 MAX-STEP=       10.0    % OF RANGE
                 XTOL=       1.000000E-08
     THE NEW ALGORITHM WAS USED WITH BRACKETING=NO
     METHOD: SECANT        STATUS: CONVERGED
     TOTAL NUMBER OF ITERATIONS:     4
     NUMBER OF ITERATIONS ON LAST OUTER LOOP:     0

                          *** FINAL VALUES ***
```

```
VAR#  MANIPUL/TEAR-VAR VARIABLE DESCRIPTION
----  ---------------- ------------------------
   1  TOTAL MASSFLOW   2.MIXED.TOTAL.MASSFLOW


 UNIT         VALUE       PREV VALUE       ERR/TOL
---------- ------------   ------------   ------------
KG/HR          44.4831        46.1500        -0.3906


                         *** ITERATION HISTORY ***

     DESIGN-SPEC ID: DS-1
     ITERATED:  TOTAL MASSFLOW IN STREAM 2 SUBSTREAM MIXED

     ITERATION  VARIABLE         ERROR          ERR/TOL
     ---------  --------         -----          -------
          1      50.00     UB    0.1035          103.5
          2      49.65           0.9763E-01      97.63
          3      46.15           0.3363E-01      33.63
          4      44.48          -0.3906E-03     -0.3906

 COMPUTATIONAL SEQUENCE
 ----------------------

 SEQUENCE USED WAS:
    $OLVER10 HX
    (RETURN $OLVER10)

 OVERALL FLOWSHEET BALANCE
 -------------------------

                     ***  MASS AND ENERGY BALANCE  ***
                                     IN              OUT        RELATIVE DIFF.
    CONVENTIONAL COMPONENTS (KMOL/HR )
       H2O                        4.49580         4.49580         0.00000
    SUBTOTAL(KMOL/HR )            4.49580         4.49580         0.00000
            (KG/HR   )            80.9931         80.9931         0.00000
ASPEN PLUS   PLAT: WINDOWS   VER: 36.0                   04/10/2018  PAGE 4

                               FLOWSHEET SECTION

 OVERALL FLOWSHEET BALANCE (CONTINUED)
    NON-CONVENTIONAL COMPONENTS (KG/HR   )
       COAL                       2.49500         2.49500         0.00000
    SUBTOTAL(KG/HR   )            2.49500         2.49500         0.00000
    TOTAL BALANCE
       MASS(KG/HR   )             83.4881         83.4881         0.00000
       ENTHALPY(CAL/SEC )        -77759.1        -77759.1        0.120635E-08

                     ***  CO2 EQUIVALENT SUMMARY ***
    FEED STREAMS CO2E             0.00000      KG/HR
    PRODUCT STREAMS CO2E          0.00000      KG/HR
    NET STREAMS CO2E PRODUCTION   0.00000      KG/HR
    UTILITIES CO2E PRODUCTION     0.00000      KG/HR
```

```
   TOTAL CO2E PRODUCTION         0.00000      KG/HR
ASPEN PLUS   PLAT: WINDOWS   VER: 36.0                  04/10/2018  PAGE 5

                          PHYSICAL PROPERTIES SECTION

 COMPONENTS
 ----------

  ID       TYPE  ALIAS          NAME
   COAL     NC                   MISSING
   H2O      C     H2O            WATER

  ID             ATTRIBUTE TYPES
   COAL           PROXANAL ULTANAL SULFANAL
ASPEN PLUS   PLAT: WINDOWS   VER: 36.0                  04/10/2018  PAGE 6

                             U-O-S BLOCK SECTION

 BLOCK:  HX       MODEL: HEATX
 ------------------------------
   HOT SIDE:
   ---------
   INLET STREAM:             2
   OUTLET STREAM:            4
   PROPERTY OPTION SET:   IDEAL     IDEAL LIQUID / IDEAL GAS
   COLD SIDE:
   ----------
   INLET STREAM:             1
   OUTLET STREAM:            3
   PROPERTY OPTION SET:   IDEAL     IDEAL LIQUID / IDEAL GAS

                     ***  MASS AND ENERGY BALANCE  ***
                                    IN              OUT        RELATIVE DIFF.
      CONV. COMP.(KMOL/HR )     4.49580         4.49580         0.00000
                 (KG/HR   )     80.9931         80.9931         0.00000
      NONCONV. COMP(KG/HR   )   2.49500         2.49500         0.00000
    TOTAL BALANCE
      MASS(KG/HR   )            83.4881         83.4881         0.00000
      ENTHALPY(CAL/SEC )       -77759.1        -77759.1        0.120635E-08

                     ***  CO2 EQUIVALENT SUMMARY ***
    FEED STREAMS CO2E             0.00000      KG/HR
    PRODUCT STREAMS CO2E          0.00000      KG/HR
    NET STREAMS CO2E PRODUCTION   0.00000      KG/HR
    UTILITIES CO2E PRODUCTION     0.00000      KG/HR
    TOTAL CO2E PRODUCTION         0.00000      KG/HR

                          ***  INPUT DATA  ***

   FLASH SPECS FOR HOT SIDE:
   TWO    PHASE      FLASH
   MAXIMUM NO. ITERATIONS                                  30
   CONVERGENCE TOLERANCE                                    0.000100000

   FLASH SPECS FOR COLD SIDE:
   TWO    PHASE      FLASH
   MAXIMUM NO. ITERATIONS                                  30
```

```
   CONVERGENCE TOLERANCE                                    0.000100000

   FLOW DIRECTION AND SPECIFICATION:
     COUNTERCURRENT   HEAT EXCHANGER
     SPECIFIED COLD VAPOR FRACTION
     SPECIFIED VALUE                                        0.9925
     LMTD CORRECTION FACTOR                                 1.00000
ASPEN PLUS   PLAT: WINDOWS   VER: 36.0                  04/10/2018  PAGE 7

                              U-O-S BLOCK SECTION

 BLOCK:  HX       MODEL: HEATX (CONTINUED)

   PRESSURE SPECIFICATION:
     HOT  SIDE PRESSURE DROP        BAR                     0.0000
     COLD SIDE PRESSURE DROP        BAR                     0.0000

   HEAT TRANSFER COEFFICIENT SPECIFICATION:
     HOT LIQUID    COLD LIQUID      CAL/SEC-SQCM-K          0.0203
     HOT 2-PHASE   COLD LIQUID      CAL/SEC-SQCM-K          0.0203
     HOT VAPOR     COLD LIQUID      CAL/SEC-SQCM-K          0.0203
     HOT LIQUID    COLD 2-PHASE     CAL/SEC-SQCM-K          0.0203
     HOT 2-PHASE   COLD 2-PHASE     CAL/SEC-SQCM-K          0.0203
     HOT VAPOR     COLD 2-PHASE     CAL/SEC-SQCM-K          0.0203
     HOT LIQUID    COLD VAPOR       CAL/SEC-SQCM-K          0.0203
     HOT 2-PHASE   COLD VAPOR       CAL/SEC-SQCM-K          0.0203
     HOT VAPOR     COLD VAPOR       CAL/SEC-SQCM-K          0.0203

                          ***  OVERALL RESULTS  ***

   STREAMS:
                    ---------------------------------------
                    |                                     |
   2         ----->|                HOT                  |-----> 4
   T=  1.6000D+02   |                                     |       T=  1.1140D+02
   P=  1.5000D+00   |                                     |       P=  1.5000D+00
   V=  1.0000D+00   |                                     |       V=  9.9609D-02
                    |                                     |
   3         <-----|                COLD                 |<----- 1
   T=  1.0002D+02   |                                     |       T=  2.7000D+01
   P=  1.0132D+00   |                                     |       P=  1.0132D+00
   V=  9.9250D-01   |                                     |       V=  0.0000D+00
                    ---------------------------------------

   DUTY AND AREA:
     CALCULATED HEAT DUTY           CAL/SEC              6193.4815
     CALCULATED (REQUIRED) AREA     SQM                     2.3802
     ACTUAL EXCHANGER AREA          SQM                     2.3802
     PER CENT OVER-DESIGN                                   0.0000

   HEAT TRANSFER COEFFICIENT:
     AVERAGE COEFFICIENT (DIRTY)    CAL/SEC-SQCM-K          0.0203
     UA (DIRTY)                     CAL/SEC-K             483.2238

   LOG-MEAN TEMPERATURE DIFFERENCE:
     LMTD CORRECTION FACTOR                                 1.0000
     LMTD (CORRECTED)               C                      12.8170
```

NUMBER OF SHELLS IN SERIES 1

PRESSURE DROP:
HOTSIDE, TOTAL BAR 0.0000
COLDSIDE, TOTAL BAR 0.0000

U-O-S BLOCK SECTION

BLOCK: HX MODEL: HEATX (CONTINUED)

*** ZONE RESULTS ***

TEMPERATURE LEAVING EACH ZONE:

HOT

HOT IN ------> 160.0	VAP 111.4	COND 111.4	COND	HOT OUT ------> 111.4
COLDOUT <------ 100.0	BOIL 100.0	BOIL 100.0	LIQ	COLDIN <------ 27.0

COLD

ZONE HEAT TRANSFER AND AREA:

ZONE	HEAT DUTY CAL/SEC	AREA SQM	LMTD C	AVERAGE U CAL/SEC-SQCM-K	UA CAL/SEC-K
1	273.286	0.0460	29.2453	0.0203	9.3446
2	5157.151	2.2310	11.3858	0.0203	452.9451
3	763.045	0.1031	36.4498	0.0203	20.9341

U-O-S BLOCK SECTION

HEATX COLD-TQCU HX TQCURV INLET

PRESSURE PROFILE: CONSTANT2
PRESSURE DROP: 0.0 BAR
PROPERTY OPTION SET: IDEAL IDEAL LIQUID / IDEAL GAS

DUTY	PRES	TEMP	VFRAC
CAL/SEC	BAR	C	
0.0	1.0133	100.0178	0.9925
294.9277	1.0133	100.0178	0.9386
589.8554	1.0133	100.0178	0.9386

```
 !   884.7831 !     1.0133 !   100.0178 !     0.8847 !
 !  1179.7108 !     1.0133 !   100.0178 !     0.8308 !
 !------------+------------+------------+------------!
 !  1474.6385 !     1.0133 !   100.0178 !     0.7769 !
 !  1769.5661 !     1.0133 !   100.0178 !     0.7230 !
 !  2064.4938 !     1.0133 !   100.0178 !     0.6691 !
 !  2359.4215 !     1.0133 !   100.0178 !     0.6152 !
 !  2654.3492 !     1.0133 !   100.0178 !     0.5613 !
 !------------+------------+------------+------------!
 !  2949.2769 !     1.0133 !   100.0178 !     0.5074 !
 !  3244.2046 !     1.0133 !   100.0178 !     0.4535 !
 !  3539.1323 !     1.0133 !   100.0178 !     0.3996 !
 !  3834.0600 !     1.0133 !   100.0178 !     0.3457 !
 !  4128.9877 !     1.0133 !   100.0178 !     0.2918 !
 !------------+------------+------------+------------!
 !  4423.9154 !     1.0133 !   100.0178 !     0.2379 !
 !  4718.8430 !     1.0133 !   100.0178 !     0.1840 !
 !  5013.7707 !     1.0133 !   100.0178 !     0.1301 !
 !  5308.6984 !     1.0133 !   100.0178 !  7.6152-02 !
 !  5430.4367 !     1.0133 !   100.0178 !  2.2250-02 !
 !------------+------------+------------+------------!
 !  5603.6261 !     1.0133 !   100.0178 ! BUB>0.0    !
 !  5898.5538 !     1.0133 !    84.1071 !     0.0    !
 !  6193.4815 !     1.0133 !    56.0661 !     0.0    !
 ------------------------------------------------------
ASPEN PLUS   PLAT: WINDOWS   VER: 36.0                    04/10/2018  PAGE 10

                              U-O-S BLOCK SECTION

 HEATX HOT-TQCUR HX       TQCURV INLET
 -------------------------------------
   PRESSURE PROFILE:      CONSTANT2
   PRESSURE DROP:         0.0         BAR
   PROPERTY OPTION SET:   IDEAL     IDEAL LIQUID / IDEAL GAS

 ------------------------------------------------------
 !  DUTY      !  PRES      !  TEMP      !  VFRAC     !
 !            !            !            !            !
 !            !            !            !            !
 !            !            !            !            !
 !  CAL/SEC   !  BAR       !  C         !            !
 !            !            !            !            !
 !============!============!============!============!
 !     0.0    !     1.5000 !   160.0000 !     1.0000 !
 !   294.9277 !     1.5000 !   111.4037 !     0.9967 !
 !   589.8554 !     1.5000 !   111.4037 !     0.9519 !
 !   884.7831 !     1.5000 !   111.4037 !     0.9070 !
 !  1179.7108 !     1.5000 !   111.4037 !     0.8621 !
 !------------+------------+------------+------------!
 !  1474.6385 !     1.5000 !   111.4037 !     0.8173 !
 !  1769.5661 !     1.5000 !   111.4037 !     0.7724 !
 !  2064.4938 !     1.5000 !   111.4037 !     0.7276 !
 !  2359.4215 !     1.5000 !   111.4037 !     0.6827 !
 !  2654.3492 !     1.5000 !   111.4037 !     0.6379 !
 !------------+------------+------------+------------!
 !  2949.2769 !     1.5000 !   111.4037 !     0.5930 !
 !  3244.2046 !     1.5000 !   111.4037 !     0.5482 !
```

```
 !  3539.1323 !     1.5000 !   111.4037 !     0.5033 !
 !  3834.0600 !     1.5000 !   111.4037 !     0.4584 !
 !  4128.9877 !     1.5000 !   111.4037 !     0.4136 !
 !------------+------------+------------+------------!
 !  4423.9154 !     1.5000 !   111.4037 !     0.3687 !
 !  4718.8430 !     1.5000 !   111.4037 !     0.3239 !
 !  5013.7707 !     1.5000 !   111.4037 !     0.2790 !
 !  5308.6984 !     1.5000 !   111.4037 !     0.2342 !
 !  5430.4367 !     1.5000 !   111.4037 !     0.2157 !
 !------------+------------+------------+------------!
 !  5603.6261 !     1.5000 !   111.4037 !     0.1893 !
 !  5898.5538 !     1.5000 !   111.4037 !     0.1445 !
 !  6193.4815 !     1.5000 !   111.4037 !  9.9609-02 !
 ------------------------------------------------------
ASPEN PLUS   PLAT: WINDOWS   VER: 36.0                  04/10/2018  PAGE 11

                                STREAM SECTION

 SUBSTREAM ATTR PSD TYPE: PSD
 ----------------------------

 INTERVAL     LOWER LIMIT           UPPER LIMIT
     1          0.0     METER      2.0000-05  METER
     2       2.0000-05  METER      4.0000-05  METER
     3       4.0000-05  METER      6.0000-05  METER
     4       6.0000-05  METER      8.0000-05  METER
     5       8.0000-05  METER      1.0000-04  METER
     6       1.0000-04  METER      1.2000-04  METER
     7       1.2000-04  METER      1.4000-04  METER
     8       1.4000-04  METER      1.6000-04  METER
     9       1.6000-04  METER      1.8000-04  METER
    10       1.8000-04  METER      2.0000-04  METER

ASPEN PLUS   PLAT: WINDOWS   VER: 36.0                  04/10/2018  PAGE 12

                                STREAM SECTION

 1 2 3 4
 -------

 STREAM ID              1          2          3          4
 FROM :                 ----       ----       HX         HX
 TO   :                 HX         HX         ----       ----
 CLASS:                 MCINCPSD   MCINCPSD   MCINCPSD   MCINCPSD
 TOTAL STREAM:
   KG/HR                39.0050    44.4831    39.0050    44.4831
   CAL/SEC           -3.8896+04 -3.8863+04 -3.2703+04 -4.5056+04
 SUBSTREAM: MIXED
 PHASE:                 LIQUID     VAPOR      MIXED      MIXED
 COMPONENTS: KMOL/HR
   H2O                   2.0266     2.4692     2.0266     2.4692
 TOTAL FLOW:
   KMOL/HR               2.0266     2.4692     2.0266     2.4692
   KG/HR                36.5100    44.4831    36.5100    44.4831
   L/MIN                 0.6134   988.0468  1026.5191    88.1135
 STATE VARIABLES:
   TEMP   C             27.0000   160.0000   100.0178   111.4037
```

PRES	BAR	1.0133	1.5000	1.0133	1.5000
VFRAC		0.0	1.0000	0.9925	9.9609-02
LFRAC		1.0000	0.0	7.5000-03	0.9004
SFRAC		0.0	0.0	0.0	0.0
ENTHALPY:					
CAL/MOL		-6.8227+04	-5.6661+04	-5.7225+04	-6.5691+04
CAL/GM		-3787.1580	-3145.1548	-3176.4614	-3646.3903
CAL/SEC		-3.8408+04	-3.8863+04	-3.2215+04	-4.5056+04
ENTROPY:					
CAL/MOL-K		-38.8471	-8.3598	-8.9962	-31.7807
CAL/GM-K		-2.1563	-0.4640	-0.4994	-1.7641
DENSITY:					
MOL/CC		5.5066-02	4.1651-05	3.2904-05	4.6705-04
GM/CC		0.9920	7.5035-04	5.9278-04	8.4140-03
AVG MW		18.0153	18.0153	18.0153	18.0153
SUBSTREAM: NCPSD		STRUCTURE: NON CONVENTIONAL			
COMPONENTS: KG/HR					
COAL		2.4950	0.0	2.4950	0.0
TOTAL FLOW:					
KG/HR		2.4950	0.0	2.4950	0.0
STATE VARIABLES:					
TEMP	C	35.0000	MISSING	100.0178	MISSING
PRES	BAR	1.0133	1.5000	1.0133	1.5000
VFRAC		0.0	MISSING	0.0	MISSING
LFRAC		0.0	MISSING	0.0	MISSING
SFRAC		1.0000	MISSING	1.0000	MISSING
ENTHALPY:					
CAL/GM		-704.2956	MISSING	-704.2956	MISSING
CAL/SEC		-488.1160	MISSING	-488.1160	MISSING
DENSITY:					
GM/CC		1.1020	MISSING	1.1020	MISSING
AVG MW		1.0000	1.0000	1.0000	1.0000
COMPONENT ATTRIBUTES:					
COAL	PROXANAL				

STREAM SECTION

1 2 3 4 (CONTINUED)

STREAM ID		1	2	3	4
	MOISTURE	0.0	MISSING	0.0	MISSING
	FC	0.0	MISSING	0.0	MISSING
	VM	0.0	MISSING	0.0	MISSING
	ASH	0.0	MISSING	0.0	MISSING
ULTANAL					
	ASH	0.0	MISSING	0.0	MISSING
	CARBON	62.6000	MISSING	62.6000	MISSING
	HYDROGEN	8.5900	MISSING	8.5900	MISSING
	NITROGEN	7.0200	MISSING	7.0200	MISSING
	CHLORINE	0.0	MISSING	0.0	MISSING
	SULFUR	0.0	MISSING	0.0	MISSING
	OXYGEN	20.2500	MISSING	20.2500	MISSING
SULFANAL					
	PYRITIC	0.0	MISSING	0.0	MISSING

```
           SULFATE       0.0       MISSING     0.0       MISSING
           ORGANIC       0.0       MISSING     0.0       MISSING
 SUBSTREAM ATTRIBUTES:
 PSD
   FRAC1                 1.0000    MISSING     1.0000    MISSING
   FRAC2                 0.0       MISSING     0.0       MISSING
   FRAC3                 0.0       MISSING     0.0       MISSING
   FRAC4                 0.0       MISSING     0.0       MISSING
   FRAC5                 0.0       MISSING     0.0       MISSING
   FRAC6                 0.0       MISSING     0.0       MISSING
   FRAC7                 0.0       MISSING     0.0       MISSING
   FRAC8                 0.0       MISSING     0.0       MISSING
   FRAC9                 0.0       MISSING     0.0       MISSING
   FRAC10                0.0       MISSING     0.0       MISSING
ASPEN PLUS   PLAT: WINDOWS   VER: 36.0                  04/10/2018  PAGE 14

                            PROBLEM STATUS SECTION

 BLOCK STATUS
 ------------

 ********************************************************************************
 *                                                                              *
 * Calculations were completed normally                                         *
 *                                                                              *
 * All Unit Operation blocks were completed normally                            *
 *                                                                              *
 * All streams were flashed normally                                            *
 *                                                                              *
 * All Convergence blocks were completed normally                               *
 *                                                                              *
 ********************************************************************************
```

A .4 Nutrient Formula

As recommended by the Canadian Phycological Culture Center, the BBM formula from the Handbook of Phycological Methods (Stein, 2013) was chosen, as it has been shown to support high levels of Chlorella growth. The formula was then modified to support the biomass productivity goals of the design in the most economic manner possible. The following table tabulates the formula components and preparation amounts. Stock solutions should be made manually every two days, and then stock solution is injected continuously into the freshwater stream that is delivered to the reactor.

Table A .1: Nutrient formula and preparation amounts for stock solution and broth.

Component	g/L of stock	L stock/ L of broth
KH2PO4	17.5	0.0193
CaCL2.2H2O	25	0.0001
MgSO4.7H2O	75	0.0001
NaNO3	250	0.001
K2HPO4	75	0.0001
NaCl	25	0.0001
Na2EDTA.2H2O	10	0.0001
KOH	6.2	0.0062
FeSO4.7H2O	4.98	0.0001
H2SO4(in ml)	1	0.001
H3BO3	11.5	0.00007
Trace metal sol'n	below	0.0001
H3BO3	2.86	
MnCl2.4H20	1.81	
ZnSO4.7H20	0.222	
NaMoO4.2H20	0.39	
CuSO4.5H20	0.079	
Co(NO3)2.6H20	0.049	

A .5 List of Acronyms and Short-forms

- AC - Annualized cost
- BBM - Bold's Basal Medium
- BFD - Block flow diagram
- BMF - Bare Module Factor
- B2B - Business to business

- CO2 - Carbon dioxide
- DAF - Dissolved air flotation
- DPI (CDPI) - Direct permanent investment
- EMC - Equilibrium moisture content
- GEC - Gas exchange column
- LED - Light emitting diode
- NOx - Nitrogen oxide based gases
- OJT - Objective time chart
- O2 - Oxygen
- PBP - Payback period
- PBR - Photobioreactor
- PFD - Process flow diagram
- ROI - Return on investment
- SOx - Sulfur oxide based gases
- TBM (CTBM) - Total bare module cost
- TCI (CTCI) - Total capital investment
- TDC (CTDC) - Total depreciable costs
- TPI (CTPI) - Total permanent investment
- TRL - Technology readiness level
- VP - Venture profit
- v/v - Volume-by-volume fraction
- w.b. - Wet basis